UNIVERSITY OF SOUTHAMPTON

FACULTY OF ENGINEERING, SCIENCE
AND MATHEMATICS
School of Ocean and Earth Science

Development of proxy seawater records from gorgonian coral skeletons

Zoë Ann Bond

Thesis submitted for the degree of

Doctor of Philosophy

September 2005

Graduate School of the
Southampton Oceanography Centre

This PhD dissertation by

Zoë Ann Bond

has been produced under the supervision of the following persons

Supervisor/s
Dr. William J. Jenkins
Dr. Paul A. Wilson
Dr. Anne L. Cohen

Chair of Advisory Panel
Dr. Peter J. Statham

Member/s of Advisory Panel
Prof. Paul A. Tyler

UNIVERSITY OF SOUTHAMPTON

ABSTRACT

FACULTY OF ENGINEERING, SCIENCE AND MATHEMATICS

SCHOOL OF OCEAN AND EARTH SCIENCE

Doctor of Philosophy

DEVELOPMENT OF PROXY SEAWATER RECORDS FROM GORGONIAN CORAL SKELETONS

Zoë Ann Bond

Information about the history of Earth's climate system is largely derived from the chemical composition of biogenic skeletons preserved in the geologic record. The isotope and elemental composition of scleractinian corals have proven to be useful tools for palaeoceanographic reconstruction, providing information about the surface and deep oceans on time scales of decades to millennia.

The potential of gorgonian corals (Cnidaria: Octocorallia) as archives of past oceanic conditions is less well explored. Gorgonians are widely distributed throughout the world's oceans from the shallows to great depths, and with banded skeletons formed of organic gorgonin and calcite, the possibility exists to measure previously unobtainable proxy records. This Ph.D. focuses on the development of new methods for extracting proxy information from gorgonian coral skeletons and investigating the potential of gorgonians to record the conditions of the seawater in which they grew.

Bermudian shallow water gorgonian colonies (*Pseudoplexaura porosa*, *Plexaurella dichotoma* and *Plexaurella nutans*) were sampled and their axial skeleton structure examined. The periodicity of skeletal banding was investigated using a series of staining and isotopic marking experiments, as well as the measurement of a radiocarbon time series.

Mg/Ca and Sr/Ca ratios were measured in skeletal calcite using SIMS ion microprobe. Mg/Ca ratios show an overall, positive correlation with annual sea surface temperatures (SSTs) that is strongest in the autumn months (October–December). Interannual variability in Sr/Ca does not follow SST and may be influenced primarily by growth rate.

A technique was developed to measure Tritium (^{3}H) in skeletal gorgonin. Tritium, produced by nuclear weapons testing in the 1950s and 1960s, is a valuable diagnostic tool for ocean circulation models because it was produced in a spike-like fashion and has a strong north-south hemispheric contrast. A significant limitation to the utility of tritium observations in ocean circulation models is our imperfect knowledge of the time history of surface water concentrations. The technique developed here proves that gorgonian corals have the potential to provide a detailed time history of surface water tritium concentrations at a variety of locations.

This thesis has successfully combined a wide range of techniques, some newly developed, to illustrate the potential of gorgonian corals as recorders of seawater conditions in the recent past. Because of their wide geographic and depth distribution, as well as their organic and inorganic skeletal components, gorgonian corals, although largely over looked thus far, should prove important archives of past oceanic conditions in the future.

TABLE OF CONTENTS

LIST OF FIGURES

LIST OF TABLES

DECLARATION OF AUTHORSHIP

I, *Zoë Ann Bond*, declare that the thesis entitled

Development of proxy seawater records from gorgonian coral skeletons

and the work presented in it are my own. I confirm that:

- this work was done wholly or mainly while in candidature for a research degree at the University;
- where any part of this thesis has previously been submitted for a degree or any other qualification at this University or any other institution, this has been clearly stated;
- where I have consulted the published work of others, this is always clearly attributed;
- where I have quoted from the work of others, the source is always given. With the exception of such quotations, this thesis is entirely my own work;
- I have acknowledged all main sources of help;
- where the thesis is based on work done by myself or jointly with others, I have made clear exactly what was done and what I have contributed myself;
- parts of this work have been published as:

Bond, Z. A., A. L. Cohen, S. R. Smith, and W. J. Jenkins (2005), Growth and composition of high-Mg calcite in the skeleton of a Bermudian gorgonian (Plexaurella dichotoma): Potential for paleothermometry, Geochem. Geophys. Geosyst., 6, Q08010, doi:10.1029/2005GC000911.

Signed: ……

Date: ……

ACKNOWLEDGEMENTS

I am grateful to the many people who have made completing this research so enjoyable.

Thanks to my supervisors. To Bill Jenkins for proposing such an interesting Ph.D. project and for his cheerful attitude to work, his wisdom and guidance. I am indebted to Anne Cohen for her enthusiasm for this project and her invaluable help and advice. Paul Wilson has welcomed me into his research group and I am thankful for his support and encouragement.

Thank you to my thesis panel, to Peter Statham and Paul Tyler, for their support and many helpful discussions.

To everyone at BBSR who made my fieldwork trips both fruitful and fun! To Robbie Smith for welcoming me into the BERP lab team and his many useful suggestions. To Graham Webster for being so helpful and sharing his expertise on working with corals in the field, without the help of Graham and Jo Pitt, I would never have found 'Zoë's reef'! To Sam De Putron for providing the SST data and many helpful discussions about gorgonians. To my field assistants and dive buddies: Anne, Caro and Jim – thanks so much, it was a hard job but somebody had to do it!

I am very grateful to Dempsey Lott for his patience and immense talent at finding a perfect solution for any laboratory problem! Also to Clare Postlethwaite for her encouragement and patience especially while I was sealing samples!

Thank you to Barry Marsh for his help and recommendations with the photomicroscope work and to Ian Croudace for his advice with the x-ray work. A big thanks to Bob Jones and John Ford for thin section preparation and Glenn Gaetani for the use of his laboratory facilities.

I am very grateful to Graham Layne and Nobu Shimizu for their advice and expertise with the ion microprobe measurements and would like to thank Stan Hart for providing the ^{84}Sr spike and for sharing his expert knowledge during helpful discussions.

I have been very lucky to work within some great research groups. Thanks to Clare, Rachel, Sheila and Caro at SOC and to Rachel S., Dempsey, Josh, Kevin, Jim and Burkard at WHOI for providing such a friendly and productive working atmosphere.

I am grateful to my friends and office mates over the years. To Clare, Ago, Angela, Phil, Rachel S, Joyce and Fiona, anyone for a cuppa?

Thanks to my family for being so encouraging and relaxed with regards to the thesis!

Finally, a huge thanks to my best mate Alice. After 8 years in Oceanography, do you think we've reached orange fish status yet?

I would like to dedicate this thesis to my mum, the first Dr. Bond, for providing some sound footsteps to follow in and also, to my Jim, who accompanied me across the ocean in pursuit of this Ph.D.!

Chapter 1: Introduction

Information about the history of Earth's climate system is largely derived from the chemical composition of biogenic skeletons preserved in the geologic record. The isotope and elemental composition of scleractinian corals, including massive reef corals and deep-sea species, have proven to be useful tools for palaeoceanographic reconstruction, providing information about the surface and deep oceans on time scales of decades to millennia [e.g., *Dunbar and Cole*, 1999].

The potential of gorgonian corals (Cnidaria: Octocorallia) as archives of past oceanic conditions is less well explored. This Ph.D. has focused on developing methods of extracting proxy information from gorgonian coral skeletons.

1.1 Gorgonian corals

Gorgonian octocorals (Figure 1.1) are widely distributed throughout the world's oceans and are found in shallow surface waters and at great depths [*Sterrer*, 1986]. Gorgonians have internal axial skeletons formed primarily of a proteinaceous material 'gorgonin', which provide them with structure and form. Gorgonians are sedentary and are usually cemented to a hard surface. In most species it is the supporting axis, which spreads out over the substrate to form a holdfast anchoring the coral body to the seabed. This central skeletal structure is encased in the coenenchyme comprising the colonial polyps and gastro vascular canals [e.g., *Esford and Lewis*, 1990]. Within the coenenchymal tissue, gorgonians possess calcareous particles called sclerites or spicules. The shape, ornamentation and size of sclerites are species specific and thus are used for species identification.

This thesis focuses on gorgonian corals in the family Plexauridae within the suborder Holaxonia. In the Holaxonia, gorgonians have an arborescent growth form. Their axis or axial skeleton has a narrow, hollow, cross-chambered central core formed primarily of proteinaceous gorgonin and permeated with non-scleritic calcareous material. The particular species studied here are *Pseudoplexaura porosa*, *Plexaurella dichotoma* and *Plexaurella nutans*.

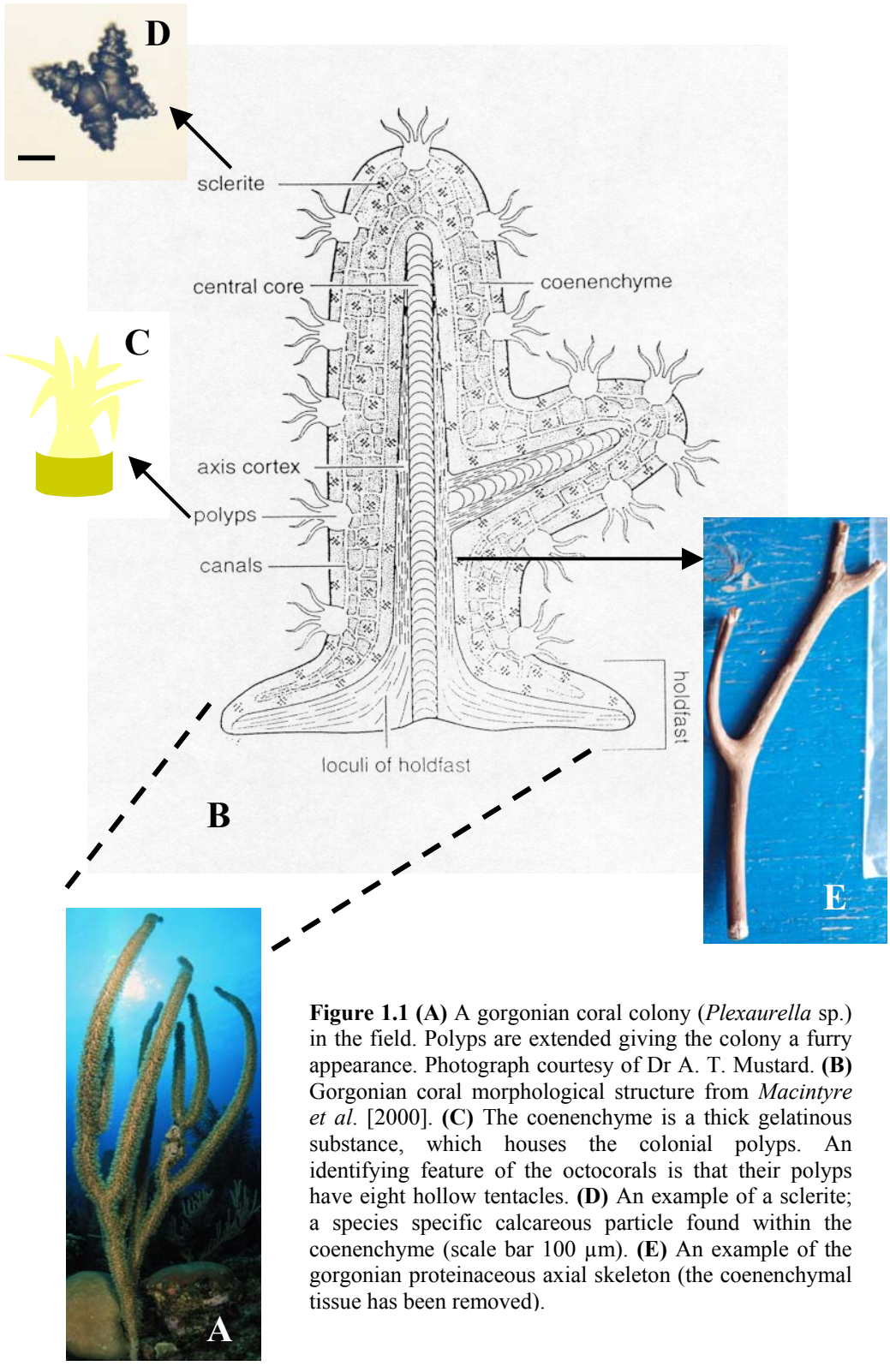

Figure 1.1 (A) A gorgonian coral colony (*Plexaurella* sp.) in the field. Polyps are extended giving the colony a furry appearance. Photograph courtesy of Dr A. T. Mustard. **(B)** Gorgonian coral morphological structure from *Macintyre et al*. [2000]. **(C)** The coenenchyme is a thick gelatinous substance, which houses the colonial polyps. An identifying feature of the octocorals is that their polyps have eight hollow tentacles. **(D)** An example of a sclerite; a species specific calcareous particle found within the coenenchyme (scale bar 100 µm). **(E)** An example of the gorgonian proteinaceous axial skeleton (the coenenchymal tissue has been removed).

1.1.1 Biology

1.1.1.1 Reproduction

Gorgonian corals undergo both asexual and sexual reproduction. An example of asexual reproduction is fragmentation when fragments of a parent colony break off and then continue to grow as independent colonies. Some gorgonian species exhibit morphologies that aid fragmentation. In the Pacific sea whip *Junceella fragilis*, the coenenchyme is absorbed near the tip of the colony, weakening the branch, which breaks off to form a daughter colony [*Walker and Bull*, 1983]. For the Caribbean gorgonian *Plexaura kuna*, constrictions in the brittle axial skeleton promote fragmentation and thus colony propagation [*Lasker*, 1984, as *Plexaura* A].

Regarding sexual reproduction, most gorgonians studied to date are gonochoric [e.g., *Zeevi Ben-Yosef and Benayahu*, 1999; *De Putron*, 2002], meaning they produce single-sex colonies; all of the polyps in one colony produce only sperm and all of the polyps in another colony produce only eggs. Those in the family Plexauridae studied thus far are either gonochoric brooders [*Theodor*, 1967; *Grigg*, 1977; *Coma et al*., 1995] or gonochoric broadcasters [*Goldberg and Hamilton*, 1974; *Brazeau and Lasker*, 1989; *Lasker et al*., 1996; *Coma and Lasker*, 1997; *Coffroth and Lasker*, 1998; *Beiring and Lasker*, 2000; *De Putron*, 2002]. Broadcasting involves the release of gametes into the water column where fertilisation occurs and the time of spawning is normally related to seawater temperature and lunar cycles [e.g., *Fabricius and Alderslade*, 2001]. Brooding involves internal fertilisation and the planulae (coral larvae) develop inside the parental polyps before release into the water column. Once a larva settles it metamorphoses into a founder polyp and develops through budding to a colonial stage. Gorgonian broadcasting and brooding species delay reproduction for several years in order to reach suitable size for the optimum production of gametes [e.g., *Kapela and Lasker*, 1999].

In relevance to this thesis, the reproductive cycle of *Pseudoplexaura porosa* has been studied on Bermuda [*De Putron*, 2002], colonies are gonochoric, broadcast spawners. Spawning occurs in July and August, with the reproductive season extending into September and October following warmer weather [*De Putron*, 2002].

1.1.1.2 Feeding

Octocorals derive nourishment using a range of mechanisms and sources [e.g., *Sterrer*, 1986]. Gorgonians have a heterogeneous diet; they are opportunistic feeders

and exploit a wide range of resources that are variable in both space and time [*Ribes et al*., 1999b]. Gorgonians have been observed feeding on zooplankton [e.g., *Coma et al*., 1994], suspended particulate matter [e.g., *Lasker*, 1981], dissolved organic matter [e.g., *Murdock*, 1978], and microplankton [e.g., *Ribes et al*., 1998a].

Many gorgonians are passive suspension feeders and depend on ambient currents to provide food sources to the colony [e.g., *Sponaugle*, 1991; *Sponaugle and LaBarbera*, 1991]. Gorgonians have been noted to adapt morphologically to current flows and location to maximise feeding rates [*Leversee*, 1976; *Sponaugle and LaBarbera*, 1991]. For example, in uni or bi-directional currents colonies adopt a planar morphology with the plane perpendicular to the flow direction, whereas in turbulent current flow, bushy morphologies enable interception of food from any direction. *Lewis* [1982] investigated the mechanics of octocoral feeding on particulate matter and zooplankton and found a common strategy; individual polyp tentacles captured fine particulate matter, whereas coordinated movement of the tentacles enabled the seizure of larger particles.

Several gorgonians, especially those found in shallow, tropical waters, have the ability to use photoautotrophic as well as heterotrophic food sources through a symbiotic relationship [e.g., *Lasker et al*., 1983]. These species host zooxanthellae (dinoflagellate microalgae) within the body wall of their polyps enabling them to utilise photosynthetic products.

1.1.2 Skeletal structure

Gorgonian coral skeletons are composed of one of the most resilient and chemically resistant proteinaceous materials known [*Goldberg*, 1978]. The skeleton's task is to act as a support system; the axis must be rigid enough to hold the fragile polyps away from the seabed, and be able to withstand the total water velocities encountered [*Muzik and Wainwright*, 1977]. *Esford and Lewis* [1990] found a relationship between the stiffness of different gorgonian species' axial skeletons and water movement based zonation. The stiffest axial skeletons were found in deep water sites and the moderately stiff axes were located in the high-energy zones. Species of the family Plexauridae inhabit the surge zone where they are subjected to both current and wave generated water movements that produce high forces in storm conditions [*Lewis et al*., 1992].

1.1.2.1 Chemical characterisation of the gorgonian axial skeleton

Many studies have investigated the composition of the gorgonian internal supporting skeleton. *Marks et al.* [1949], using x-ray diffraction evidence, first identified collagen as a component of gorgonin, which is the primary constituent of the gorgonian axial skeleton. *Goldberg* [1974] confirmed and developed the information on collagen as a major structural element of gorgonin. *Szmant-Froelich* [1974] studied the skeletal components of two gorgonian species *Muricea Californica* and *Muricea Fruticosa*. The results indicated the presence of a collagen-like protein, also present, at approximately 1% by weight, were the saccharides, glucose and galactose. *Goldberg* [1976] chemically characterised the skeletons of five gorgonian species. The five species studied were morphologically diverse, but their skeletal chemistry, specifically the amino acid composition, was remarkably similar; all skeletons contained collagen-like amounts of glycine, proline, hydroxyproline and hydroxylysine.

Collagen is composed of three polypeptide chains assembled together and intertwined to form a triple helix, wherein the individual helices are linked by hydrogen bonds. This configuration provides a compact molecule with great tensile strength [*Istin*, 1975]. Collagen has a distinctive amino acid composition, nearly one third of its residues are glycine and another 15-30% are proline and 4-hydroxyproline [e.g., *Voet and Voet*, 1990] (Figure 1.2).

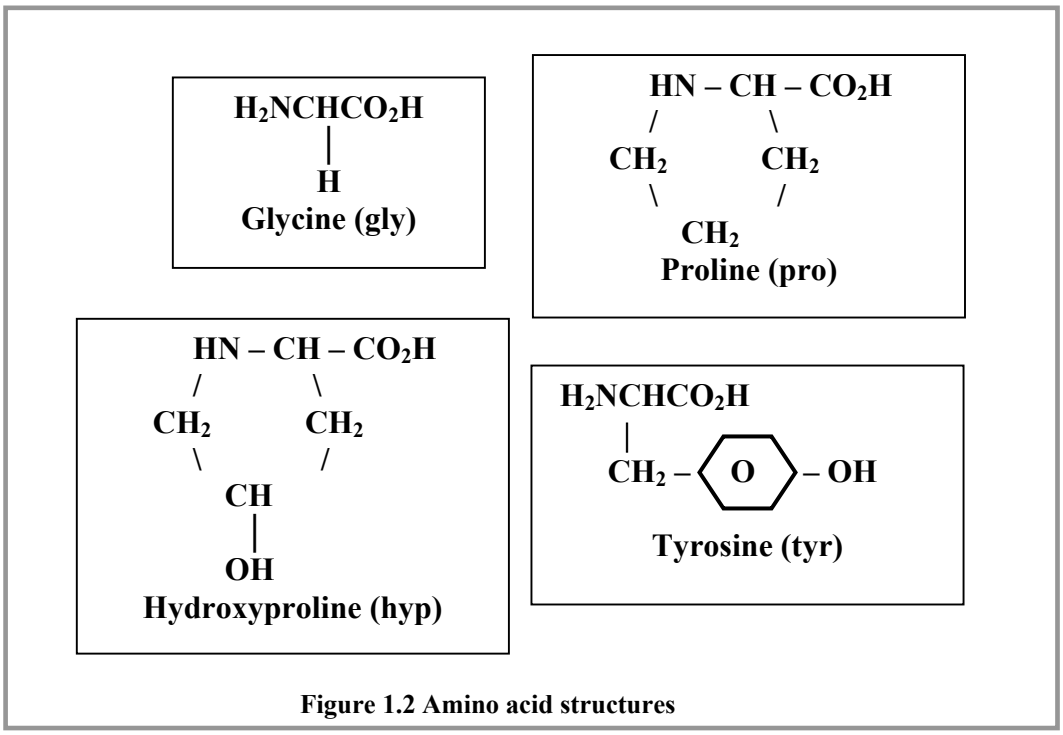

Figure 1.2 Amino acid structures

Jeyasuria and Lewis [1987] studied the Young's Modulus (as a measure of stiffness) of the axial skeleton of thirteen gorgonian species (spanning a wide range of Genera). The Young's Modulus measured for the gorgonian samples was higher than that for tendon and suggests that axial skeleton is made from a stiffer form of collagen. The difference is of functional significance since axial skeletons of gorgonian corals, unlike tendons and ligaments of vertebrates, are the primary support structures that maintain both the elevation and separation of the branches of the colony. Even with the support provided by water, a material with the stiffness of most ordinary collagens would be too flexible to maintain separation of the colony branches and keep the fragile polyps away from the abrasive seabed. Another unusual feature of the collagen-like material in axial skeletons is that it is high in tyrosine content [*Goldberg*, 1976]. Tyrosine (Figure 1.2) concentrations are thought to reflect the degree of tyrosine-derived cross-linkage [*Tidball*, 1985]. A cross-linked form of collagen would also explain the increase in stiffness of the collagen as recognised by *Jeyasuria and Lewis* [1987]. Structural materials so linked almost always develop a brown colour and are referred to as tanned or sclerotised. The reactive agent in sclerotising cross-links is almost always a phenol derived from the oxidation of tyrosine [*Goldberg*, 1974]. If tyrosine content were proportional to the degree of cross-linking/sclerotisation, then species containing less tyrosine should be less cross-linked and therefore less tanned. When *Goldberg* [1976] studied the chemical composition and structure of five species of gorgonian coral he noted that the colour developed by the species with supposed less cross-linking (i.e. less tyrosine content) was less dark than the others.

The gorgonian axial skeleton is synthesised and tanned within the axial epithelium [*Szmant-Froelich*, 1974]. The axial epithelium completely encases the axial skeleton and so lies between it and the gorgonian tissue. The fastest growing parts of the colony soon become separated from the axial epithelium by new deposits, whereas the slower growing parts remain in contact with the epithelium for longer and have more time to become tanned (cross-linked) [*Szmant-Froelich*, 1974].

In gorgonian axial skeletons the proteinaceous gorgonin is, for many species, permeated with non-scleritic calcareous material. *Lewis et al.* [1992] examined the structure of thirteen species of gorgonians and found the axes examined to be diverse. Gorgonin varied from brown and fibrous to almost glassy black. Some axes had no apparent mineralisation, whereas others contained white, calcified aggregates encased in gorgonin and some axes were white and heavily calcified. Thus both the degree of

sclerotisation and the inorganic portion of the skeleton vary in importance between species. *Cook* [1904] estimated the inorganic fraction of thirteen gorgonian axes by weighing ash left after incineration of the gorgonian skeleton. *Leptogorgia virgulata* was found to contain a higher inorganic proportion (41% weight as ash) than any of the other twelve gorgonian species skeletons tested. *Muricea* and *Gorgonia* species contained <10% ash and *Plexaura* species contained <13% ash. *Goldberg* [1978] chemically analysed the skeletal composition of three different gorgonian species. Protein values ranged from 70.1 to 91.4%; ash from 9.6 to 19.4%; lipid from 0 to 8.4%; carbohydrate from 1.24 to 3.48% and halogens from 4.2 to 12.04% of the dry skeletal weight.

Investigations of the skeletal inorganic components using x-ray diffraction have identified calcite as the principal form of carbonate occurring in these gorgonian axes [*Lewis et al.*, 1992]. Further study by *Macintyre et al.* [2000] of the Plexauridae family found that when present, the skeletal mineral of holdfasts and axes was either Mg-calcite (6.3-15.7 mol% $MgCO_3$) or aragonite. Most authors agree that both increased sclerotisation and deposition of inorganic inclusions contribute to increased axis strength.

The axial skeleton structure is investigated for *Pseudoplexaura porosa*, *Plexaurella dichotoma* and *Plexaurella nutans* in Chapter 2 of this thesis.

1.1.3 Growth banding

Variations in the density of collagenous fibres in the cortex of the axial skeleton produce alternating light and dark layers; low- and high-density bands. *Szmant-Froelich* [1974] suggested that many new layers are added to the skeleton in rapid succession during the times of the year more favourable to growth. These gorgonin layers are rapidly separated from the axial epithelium and its' tanning action, resulting in the formation of a lighter band. During the remainder of the year the deposition rate of new gorgonin layers is slower and so more tanned, darker layers are formed. Could the high- and low-density bands when grouped together represent a year of skeletal growth?

1.1.3.1 Growth banding periodicity

Grigg [1974] used a range of techniques to conclude that the growth rings present in the gorgonians *Muricea Californica* and *Muricea Fruticosa* were annual in

periodicity. Two techniques *Grigg* [1974] employed were firstly, counting bands in basal cross sections of colonies of various sizes and comparing these to estimates of colony age based on growth rate data, and secondly, band counts were also performed on basal sections of large colonies sampled from substrate of a known age.

Marschal et al. [2004] investigated the periodicity of banding in the red coral *Corallium rubrum* from the Mediterranean using calcein labelling and band counts in colonies of known age. They concluded that each annual growth ring was formed of one light and one dark calcite band, the darker band containing a higher proportion of organics than the light. Periodic calcein labelling indicated secretion of the darker band took place in the autumn/winter time.

Annual banding in the deep-sea gorgonian *Primnoa resedaeformis* was validated using growth rates determined from the decay of ^{210}Pb [*Andrews et al*., 2002] and radiocarbon dating [*Risk et al*., 2002]. *Sherwood et al*. [2005] used radiocarbon measurements of individual bands isolated from the skeleton of *Primnoa resedaeformis* compared to ages of those bands determined from band counting to prove that skeletal growth banding was annual in periodicity.

To date no work has been conducted on the periodicity of growth banding in *Plexaurella dichotoma*, *Plexaurella nutans* and *Pseudoplexaura porosa*, the species studied here. This investigation is important to this thesis as it provides information on the growth rate and longevity of these surface dwelling gorgonian corals. Furthermore, skeletal growth banding will provide a chronology for the material to be sampled for the proxy measurements to be carried out in this thesis.

In this thesis the periodicity of skeletal growth banding is investigated in *Pseudoplexaura porosa*, *Plexaurella dichotoma* and *Plexaurella nutans* using staining and isotopic marking of the skeleton (Chapter 3), and through measurements of radiocarbon in gorgonin growth bands (Chapter 6).

1.2 Gorgonian corals as proxies

There have been relatively few studies on the potential of obtaining records of past seawater conditions from gorgonian coral skeletons.

Ward-Paige et al. [2005], measured δ^{15}N and δ^{13}C from skeletal gorgonin in a number of colonies from the species *Plexaura homomalla* and *Plexaura flexuosa*. The data obtained enabled an analysis of water quality in the Florida Keys over a 30 year

period. Thus gorgonians have the ability to provide information about past oceanographic nutrient conditions.

Griffin and Druffel [1989] used radiocarbon measurements to investigate carbon sources to the organic and calcareous portions of deep-sea gorgonian corals. They discovered that skeletal calcite was formed from dissolved inorganic carbon (DIC) from the surrounding seawater at the depth of colony growth whereas the carbon source for the organic matter (polyps and gorgonin) was derived from particulate organic matter (POM) rained down from the surface and consumed by the corals at depth. These findings have recently been confirmed by *Roark et al*. [2005] who measured radiocarbon in deep-sea bamboo corals from the Gulf of Alaska. Therefore, deep-sea gorgonians are valuable dual archives; within their skeletal calcite past deep-sea conditions are recorded whilst the gorgonin portion of the skeleton documents surface productivity.

Heikoop et al. [2002] have investigated potential climate signals from the deep-sea gorgonian *Primnoa resedaeformis*. For the calcite fraction of the coral skeleton, *Heikoop et al*. [2002] concluded that the use of $\delta^{18}O$ to obtain past seawater temperatures would be difficult but palaeothermometry using Sr/Ca ratios showed potential. In the same study, *Heikoop et al*. [2002] noted $\delta^{15}N$ measurements of the coral polyps were highly correlated ($r^2 = 0.94$) with $\delta^{15}N$ of the skeletal gorgonin, indicating that gorgonin records the nitrogen isotope composition of the polyps through time and could prove to be a useful archive of information on surface productivity variations through time. *Sherwood et al*. [2005] further investigated the potential of deep-sea gorgonians (*Primnoa* spp.) to record surface productivity over time. They discovered that $\delta^{13}C$ in skeletal gorgonin was able to track variations in surface processes.

There have been studies undertaken to investigate the composition of the calcified regions in the gorgonian skeleton, including measurements of sclerites embedded within the coenenchymal tissue. Analysis of Mg/Ca in gorgonian sclerites showed a direct positive relationship between Mg/Ca and seawater temperature [*Chave*, 1954; *Weinbauer and Velimirov*, 1995]. *Weinbauer and Velimirov* [1995] also measured Sr/Ca in gorgonian sclerites. They found no correlation between Sr/Ca and seawater temperature but suggested growth rate as a potential influence on sclerite Sr/Ca concentrations. The calcified axis of the red coral *Corallium rubrum* has been demonstrated to be of importance as an ecological indicator [*Weinbauer et al*., 2000].

Weinbauer et al. [2000] note that an increase in seawater temperature promotes the incorporation of magnesium into *Corallium rubrum* calcite whereas incorporation of strontium appears to be inversely related to growth rate.

The above studies indicate that gorgonian calcite elemental chemistry, especially the Mg/Ca content, may be a valuable proxy for ocean temperature. Indeed, *Thresher et al*. [2004] used measurements of Mg/Ca in calcite as a proxy for seawater temperature from two deep-sea gorgonians (*Keratoisis* spp.) to investigate climate change in southern Australia over the past 300 years.

The potential of Mg/Ca and Sr/Ca in *Plexaurella dichotoma* calcite to record past seawater conditions are examined in Chapter 4.

1.3 Tritium

Tritium (^{3}H) a radioactive isotope of hydrogen, decays with a half-life 12.43 years to its stable, daughter product helium 3. Tritium combines with oxygen to form tritiated water (HTO) [e.g., *Michel and Suess*, 1975] and this is its most common form in the environment, although some fraction does exist as molecular hydrogen (HT). The tritium content of natural waters is expressed in tritium units (TU). 1TU equals 1 tritium atom per $1x10^{18}$ hydrogen atoms.

1.3.1 Tritium production

Natural tritium on the surface of the Earth is produced by cosmic ray spallation reactions of nuclear species present in the atmosphere. The production rate of natural tritium is estimated at 0.25 atomscm^{-2}s [*Jouzel et al*., 1982]. Most of the tritium in the world today was produced by atmospheric nuclear weapons testing in the late 1950s and early 1960s. The amount of naturally produced tritium in the oceans is negligible compared to the quantity of bomb produced tritium. The early thermonuclear weapons tests of 1952 resulted in the first major injection of artificial tritium into the atmosphere. Very few pre-bomb seawater measurements for tritium exist, but the best estimates are thought to be in the range of 0.2-0.5TU [*Begemann and Libby*, 1957; *Dreisigacker and Roether*, 1978]. In 1962 and 1963, a large series of H bomb tests were exploded, these tests produced three times more tritium than all previous tests combined [*Eriksson*, 1965]. The artificial tritium produced by these explosions increased the total tritium concentrations on the Earth's surface by about two orders of magnitude. Measurements of tritium in precipitation, in the northern hemisphere, in 1963-1964 when they reached

their maximum, were occasionally as high as 10,000TU [*Michel and Suess*, 1975]. Thereafter, values fell steadily until 1968 as a result of the moratorium on atmospheric bomb testing and relatively little artificial tritium has been produced since the Nuclear Test Ban Treaty in 1963 [*Michel and Suess*, 1975].

The radioactive debris produced by the atmospheric weapons testing was injected into the stratosphere and troposphere of the higher latitudes of the northern hemisphere [*Fine and Östlund*, 1977] where the tritium was oxidised to HTO and thus acts as a valuable label for water. Residence times of tritium in the stratosphere range from a few weeks just above the tropopause and are extended to a few years at higher altitudes [*Fine and Östlund*, 1977]. The residence time of tritium in the troposphere, whether injected directly by the bomb blast or indirectly from the stratosphere, is 30-60 days [*Michel and Suess*, 1975]. The rate at which bomb-injected tritium mixes down from the stratosphere to the troposphere depends on the time, place and size of the bomb exploded [*Fine and Östlund*, 1977]. Exchange between the stratosphere and the troposphere occurs mainly during the 'spring leaks' at the higher latitudes and along the jet stream belts [*Fine and Östlund*, 1977]; half of the stratosphere inventory is transferred to the troposphere in the spring and summer months of the year.

1.3.2 The distribution of tritium in the world's oceans

The distribution of tritium is asymmetric between the two hemispheres and reflects the predominantly northern hemisphere locations for the weapons testing; there was only minor atmospheric weapons testing in the southern hemisphere and none before 1968 [*Weiss and Roether*, 1980]. As most tritium was produced by tests conducted in the northern hemisphere, the tritium was initially carried to this hemisphere's stratosphere. Additionally, as the transfer of stratospheric air to the troposphere occurs largely at latitudes greater than 35ºN, and as the residence time of water in the troposphere is not long enough to allow transport to the tropics, the major amount of the tritium reached the Earth's surface north of 15ºN [*Weiss and Roether*, 1980].

In 1958, a programme to monitor tritium in monthly precipitation started, run by the International Atomic Energy Agency (IAEA). The purpose of the programme was to monitor the deposition and distribution of tritium on the surface of the Earth as a basis for hydrological investigation [*Michel and Suess*, 1975]. The first systematic survey of the distribution of bomb tritium in the world's oceans was carried out by the

GEOSECS (Geochemical Ocean Sections) survey (1972-1978). The next large scale programme was undertaken in the early 1980s; the Transient Tracers in the Ocean (TTO) programme provided more information on tritium and its evolution through time. Examples of smaller scale programmes carried out are the North Pacific Experiment (NORPAC) in 1977 and 1979-1980, and the Equatorial Pacific Ocean Climate Studies (EPOCS) from 1979 to 1980. From 1959-1973 the La Jolla tritium laboratory monitored bomb produced tritium in the surface waters at 15 stations in the Pacific Ocean [*Michel and Suess*, 1975]. The results obtained showed that even as early as 1959 nearly all oceanic tritium concentrations were above pre-bomb levels. Only near Samoa, at 13ºS, did tritium concentrations remain close to natural levels until the 1963 weapons tests. In the sub Arctic and central Pacific Oceans, tritium concentrations hit peak values in 1964-1965 and have since been decreasing.

Broecker et al. [1986] used data from the GEOSECS and NORPAC expeditions to examine the lateral distribution of tritium in the oceans. The most prominent feature that *Broecker et al*. [1986] noted was the large contrast in tritium distribution north and south of 15ºN, both in the Pacific and Atlantic Oceans. Water column properties (nutrients, salinity, and density) reveal that strong fronts extend across the Atlantic [*Broecker and Östlund*, 1979] and Pacific Oceans at about 15ºN. As these fronts prevent lateral mixing, tritium is trapped in the northern zones.

Broecker et al. [1986] also studied the distribution of tritium inventories in the southern hemisphere. In the southern hemisphere the maximum tritium concentration is seen in the south temperate zone of the Pacific, Atlantic and Indian Oceans. Waters between 20ºS and 40ºS have tritium concentrations greater than those in the tropics or those in the Antarctic. According to *Broecker et al*. [1986] comparisons of water column inventories of bomb tritium clearly show that tritium is being transported at important rates from one region of the oceans to another, depletions being noted in the tropics and at high southern latitudes. Therefore, the evolution of the tritium inventory offers strong constraints on oceanic transport models.

It is important to note that in the ocean, tritium concentration changes are independent of biological and chemical processes. Apart from radioactive decay, there is no in situ consumption or production of tritium. Below the ocean surface, the only factors that influence the tritium concentration are diffusion, flow of water and radioactive decay. There are several ways in which tritium can be used to examine oceanographic processes. For example, from changes in concentration of tritium in the

mixed layer of the ocean, a mean residence time of the water there can be calculated. Furthermore, because the deposition of bomb produced tritium into the oceans has been latitudinally asymmetric, its distribution should allow the flow of ocean currents to be determined. Tritium data examined so far have been used to evaluate box models [*Weiss and Roether*, 1980]. As *Broecker et al*. [1986] noted, if the tritium data are to be used to constrain ocean models effectively, a complete global distribution of tritium must be measured and a better knowledge of the delivery of tritium to the ocean will be also required.

To improve knowledge of the tritium input to the oceans, *Stark* [2003] developed a technique to measure tritium concentrations in annual tree rings as a reflection of ambient precipitation. Tritium time series measurements were made on cellulose, the primary constituent of wood, from an Irish tree and compared to precipitation tritium data from the Valentia weather station [*Stark*, 2003; *Stark et al*., 2005]. The study demonstrated the clear potential to improve the time history of tritium delivery to the oceans by measuring historical precipitation concentrations in ocean island tree rings.

Gorgonian corals have the potential to provide a detailed time history of surface water tritium concentrations at a variety of locations as their skeletons are formed of proteinaceous gorgonin where tritium should be sequestered during growth. Tritium has never previously been measured in gorgonian corals. Chapter 5 describes the techniques that have been developed throughout the course of this thesis to reconstruct surface ocean tritium measurements using gorgonian coral skeletons.

1.4 Thesis aims

The broad aim of this thesis is to explore the potential of gorgonian corals as archives of past oceanic conditions by investigating and testing methods of extracting proxy information from gorgonian coral skeletons.

The detailed thesis aims can be summarised as follows:

- To examine and describe the skeletal structure of three Bermudian gorgonians *Pseudoplexaura porosa*, *Plexaurella dichotoma* and *Plexaurella nutans* (Chapter 2).

- To investigate the periodicity of skeletal growth banding in three Bermudian gorgonians using staining experiments and newly developed isotopic marking techniques (Chapter 3).

- To explore the potential of calcite contained within the gorgonian skeleton of *Plexaurella dichotoma* to record environmental proxy information (Chapter 4).

- To develop a technique to measure bomb tritium in the gorgonian coral skeleton and to investigate whether tritium concentrations measured within the gorgonin of the coral skeleton reflect the surface water tritium concentrations over the time period this skeleton was accreted (Chapter 5).

- To further study the periodicity of growth banding through measurement of a radiocarbon time series within the axial skeleton gorgonin of *Pseudoplexaura porosa* (Chapter 6).

Chapter 2: Sampling and structural characterisation for three Bermudian gorgonians

2.1 Outline

This chapter first outlines the sampling and identification of three gorgonians from Bermuda: *Pseudoplexaura porosa*, *Plexaurella dichotoma* and *Plexaurella nutans*. Following this, the skeletal structure of these gorgonians is investigated and described.

2.2 Methods - Sample collection and identification

Live gorgonian colonies were collected on SCUBA during three sampling trips (2000, 2001, 2002) from inner lagoon reef sites on Bermuda (Figure 2.1).

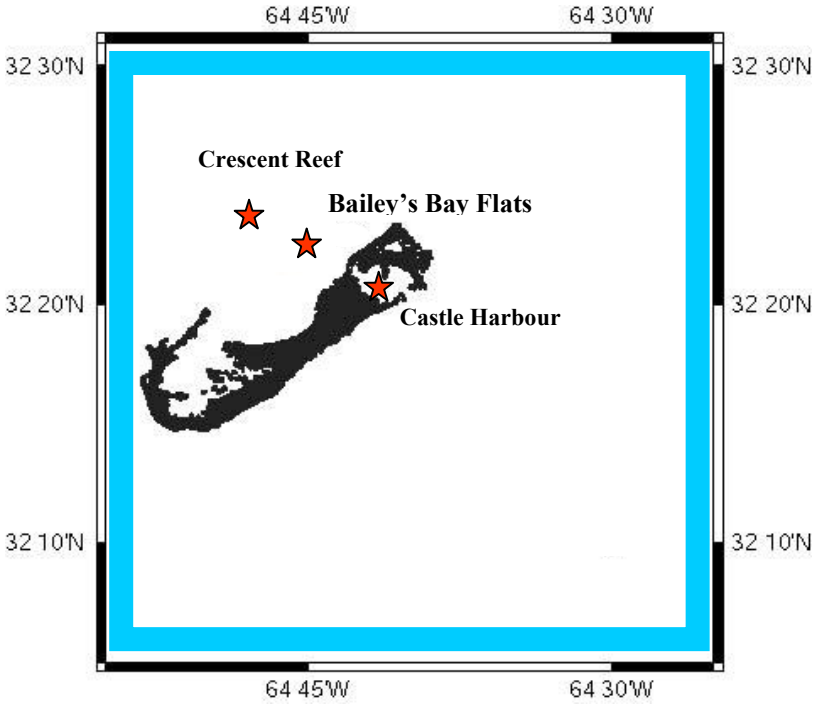

Figure 2.1 Map to show locations of gorgonian sample sites on Bermuda.

The details of all colonies collected are shown in Table 2.1.

Sample	Species	Trip	Location	Latitude and Longitude	Date	Depth (m)	Notes
2	*Pseudoplexaura porosa*	1st	Crescent Reef	N32°24.05 W064°47.95	7/12/2000	5	Tritium TS3
3A	*Plexaurella dichotoma*	1st	Crescent Reef	N32°24.05 W064°47.95	7/12/2000	5	Structural investigation
3B	*Plexaurella dichotoma*	1st	Crescent Reef	N32°24.05 W064°47.95	7/12/2000	5	Structural investigation
3C	*Plexaurella dichotoma*	1st	Crescent Reef	N32°24.05 W064°47.95	7/12/2000	5	Structural investigation
4	*Pseudoplexaura porosa*	1st	Castle Harbour	N32°20.40 W64°41.90	8/12/2000	2	Structural investigation
1	*Pseudoplexaura porosa*	2nd	Bailey's Bay Flats	N32°21.73 W064°44.84	26/09/2001	6	Skeleton degraded
2	*Pseudoplexaura porosa*	2nd	Bailey's Bay Flats	N32°21.73 W064°44.84	27/09/2001	6	Tritium TS2
3	*Plexaurella dichotoma*	2nd	Bailey's Bay Flats	N32°21.73 W064°44.84	27/09/2001	6	Ion probe work and Tritium TS4
4	*Pseudoplexaura porosa*	2nd	Bailey's Bay Flats	N32°21.73 W064°44.84	30/09/2001	7	Basal section degraded
1	*Pseudoplexaura porosa*	3rd	Bailey's Bay Flats	N32°21.73 W064°44.84	11/10/2002	4	Tritium TS1
2	*Plexaurella nutans*	3rd	Crescent Reef	N32°24.05 W064°47.95	15/10/2002	6	Staining and marking experiments
3	*Pseudoplexaura porosa*	3rd	Bailey's Bay Flats	N32°21.73 W064°44.84	16/10/2002	6	Radiocarbon
4	*Pseudoplexaura porosa*	3rd	Bailey's Bay Flats	N32°21.73 W064°44.84	18/10/2002	7	Tritium TS5

Table 2.1 Details of all samples collected during this project.

2.2.1 Identifying a suitable colony

Potential samples were identified on SCUBA and the width and length of the basal section (defined here as the section of the colony before branching, not including the holdfast) measured using callipers.

During the 2001 (2nd) sampling trip I sampled some of the largest colonies on the reef. However, after examination, the skeletons of some of these colonies (samples 1-2nd and 4-2nd) were found to be degraded and portions were in-filled with secondary calcium carbonate. This skeletal degradation is probably due to overgrowth by sponges and tunicates competing for space with the corals. These encrusting organisms can bore into and destroy the gorgonian skeleton [*Humann and Deloach*, 2002]. For example, when collecting sample 1-2nd a chicken liver sponge, *Chondrilla nucula*, was removed from the gorgonian base. Later, skeletal sectioning and examination revealed the base to be almost completely degraded with only the innermost bands intact (see Figure 2.2).

Following this sampling trip, any colonies with organisms attached to the base or having evidence of skeletal degradation were avoided.

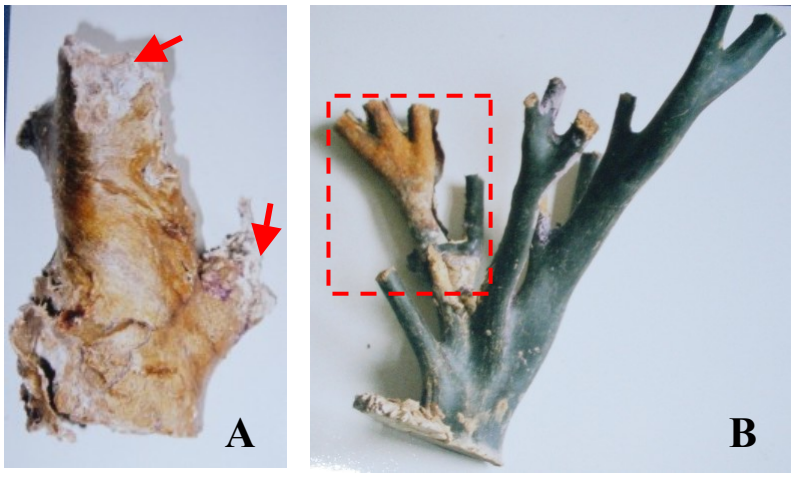

Figure 2.2 Degradation of gorgonian axial skeleton.
(A) Sample 1-2nd. Complete degradation of skeleton caused by encrusting sponge. Red arrows indicate secondary $CaCO_3$.
(B) Sample 2-2nd. Healthy portion of skeleton compared to degraded section of skeleton (outlined in red).

2.2.2 Sampling in the field

When a suitable colony had been identified, its branches were replanted so that the entire colony is not destroyed when a sample is collected. Suitable holes were first located on the reef, then the upper branches of the colony removed using wire cutters and the bottom ~2 cm of tissue peeled away from the branch section. The branch was placed into the cavity on the reef and secured using underwater cement. A batch of underwater cement (7 parts Portland type 2 cement to 1 part plaster of Paris, contained premixed in doses in a water tight plastic bag) was mixed with seawater in situ and when the required consistency was achieved, the cement was placed all around the base of the branch. The base of the colony was then sampled using a hammer and chisel to prise the gorgonian holdfast from the reef. The coenenchyme was peeled away from the colony base to reveal the organic rich axial skeleton. Samples of this tissue were retained in order to confirm species identification using the sclerites contained within (section 2.2.3). The holdfast was cut away from the basal skeleton using a band saw and the base width and length measured, dried at 40°C for 48 hours and weighed.

2.2.3 Species identification

Species are identified in the field using a range of indicators: the colour and size of the colony, its branching pattern and the polyp aperture shape and size. Sclerites or spicules (calcareous particles) contained in the coenenchyme are species specific and thus are routinely used, once a sample has been collected, to confirm species identification. Tissue samples are placed in labelled beakers and submerged in a dilute sodium hypochlorite solution (household bleach, concentration ~5%). After 2-4 hours the tissue has dissolved and the exposed sclerites are rinsed several times with distilled water and dried at 70°C overnight. Sclerites were examined under a microscope,

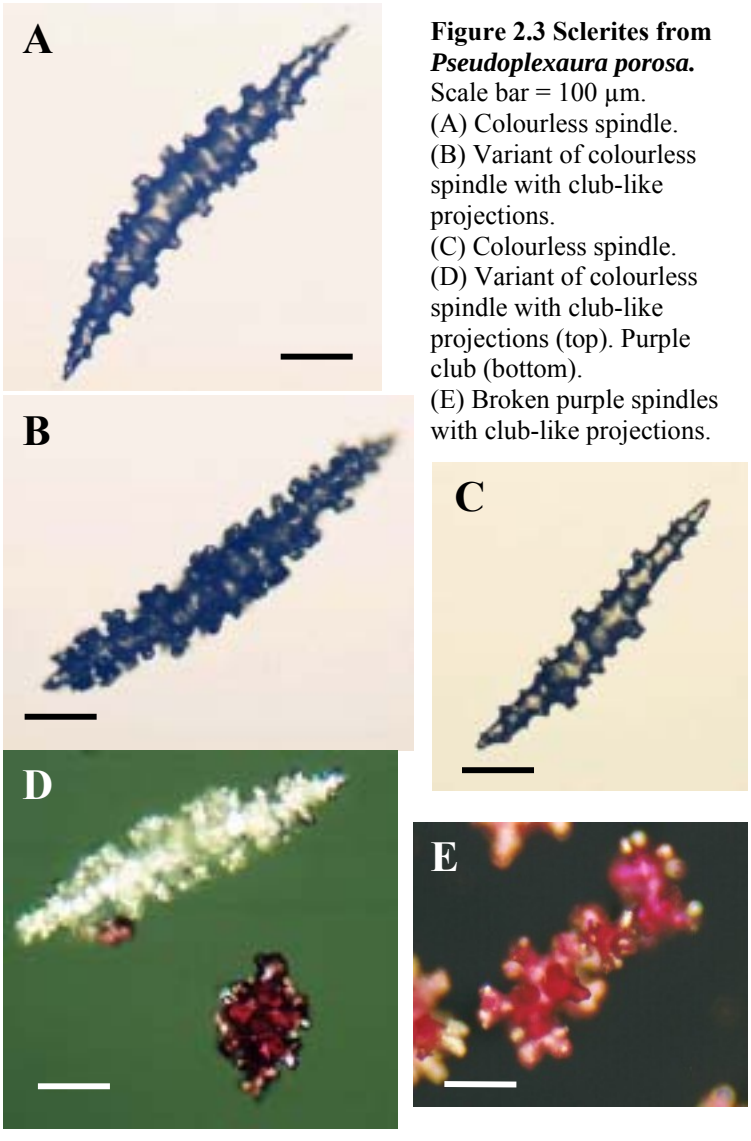

Figure 2.3 Sclerites from *Pseudoplexaura porosa.* Scale bar = 100 µm. (A) Colourless spindle. (B) Variant of colourless spindle with club-like projections. (C) Colourless spindle. (D) Variant of colourless spindle with club-like projections (top). Purple club (bottom). (E) Broken purple spindles with club-like projections.

photographed and the species identified using *Bayer* [1956], *Sterrer* [1986] and *De Putron* [2002]. Sclerites for *Pseudoplexaura porosa*, *Plexaurella dichotoma* and *Plexaurella nutans* are shown in Figures 2.3, 2.4 and 2.5 respectively.

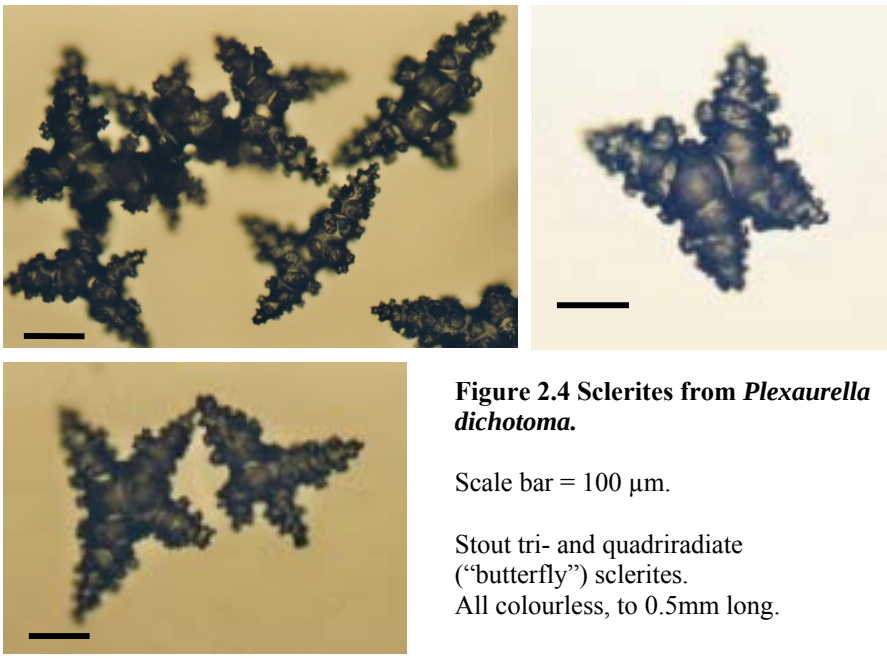

Figure 2.4 Sclerites from *Plexaurella dichotoma.*

Scale bar = 100 µm.

Stout tri- and quadriradiate ("butterfly") sclerites.
All colourless, to 0.5mm long.

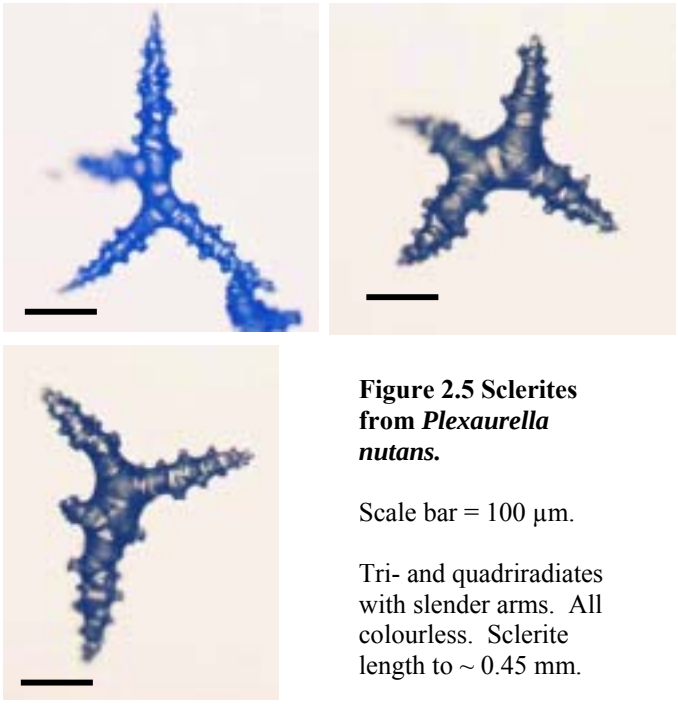

Figure 2.5 Sclerites from *Plexaurella nutans.*

Scale bar = 100 µm.

Tri- and quadriradiates with slender arms. All colourless. Sclerite length to ~ 0.45 mm.

2.3 Methods - Structural characterisation of the gorgonian skeleton

Investigation of the axial skeleton structural elements was completed using a variety of techniques.

2.3.1 X-ray imaging

High-density (dark) and low-density (light) bands are present in gorgonian skeletons [*Szmant-Froelich*, 1974]. These bands are also present in stony corals and are revealed by x-ray [*Knutson et al*., 1972].

Basal sections from *Pseudoplexaura porosa* and *Plexaurella nutans* (~0.5 cm thick) were cut using a band saw for image (x-radiograph) analysis. Optimum results were achieved using exposure times of 40 minutes at 29 kV for *Pseudoplexaura porosa* and 20 minutes at 29 kV for *Plexaurella nutans*. The difference in exposure time indicates that the skeleton of *Pseudoplexaura porosa* is denser than that of *Plexaurella nutans*. The x-radiographs reveal alternating light and dark growth bands in both species. It was not possible to do individual band counts from these images.

2.3.2 Chemical examination of skeletal composition

Gorgonian axial skeletons are formed of a proteinaceous material termed gorgonin and calcium carbonate in the form of calcite. The ratio of these two components varies depending on species [e.g., *Cook*, 1904; *Lewis et al*., 1992]. In order to investigate these skeletal ratios for *Pseudoplexaura porosa* and *Plexaurella nutans*, I adapted methods described in *Goldberg* [1976], *Lewis et al*. [1992] and *Macintyre et al*. [2000]. Two sections, with dimensions ~0.5 cm thick, ~2 cm diameter *(Pseudoplexaura poros*a) and ~1.5 cm thick, ~1 cm diameter *(Plexaurella nutans)* were cut from each colony using a band saw. All sections were dried to constant weight at 50°C. One of the sections from each colony was decalcified in 12% trichloroacetic acid for 24 hours. Once removed from the acid, the samples were rinsed in distilled water and dried to constant weight. The organic material was removed from the second section of each colony. Sections were submerged in 10% sodium hypochlorite solution. Complete dissolution of gorgonin occurred after 3 days for *Plexaurella nutans* and 6 days for *Pseudoplexaura porosa*. The remaining calcite was rinsed in distilled water and dried to constant weight. The axial skeleton of *Plexaurella nutans* is heavily calcified, containing up to 30% calcite by weight. No calcite was recovered from *Pseudoplexaura porosa*; however, following optical examination of the skeleton some

calcite is clearly present (see section 2.4.1). *Esford and Lewis* [1990] characterised the axial skeleton of *Pseudoplexaura porosa* as containing low (1%) calcium and magnesium content. It may be that any calcite present in this section was broken down along with the organics due to the length of time the sample was immersed in the bleach solution.

2.3.3 Optical examination of skeletal composition

Petrographic thin sections from the base, lower and upper (where applicable) branches were prepared for each colony for micro structural examination. Slabs were cut using a band saw and mounted (using Epotek 301 glue) onto slides. These sections were set in epoxy resin, vacuum impregnated and sectioned further using a Buehler petrothin sectioning system. The mounted sections were ground and highly polished to thicknesses between 90 μm and 110 μm. Petrographic thin sections were viewed under microscope at objectives between 1.5 and 20 in transmitted and reflected light. Examination of the thin sections under microscope revealed further structural details.

2.4 Results and Discussion

2.4.1 Pseudoplexaura porosa

In *Pseudoplexaura porosa* banding is clearly evident. Under transmitted light the skeleton appears to be composed entirely of gorgonin, however when examined under reflected light, calcite deposits are revealed (Figure 2.6). Calcite is abundant in the lighter sections of the skeleton normally adjacent to the core. Furthermore, it appears for *Pseudoplexaura porosa*, that the lighter band in each growth band couplet is not only due to less cross-linking or tanning [*Szmant-Froelich*, 1974] but also to a greater proportion of calcite as noted in the deep-sea gorgonian *Primnoa resedaeformis* [*Risk et al*., 2002].

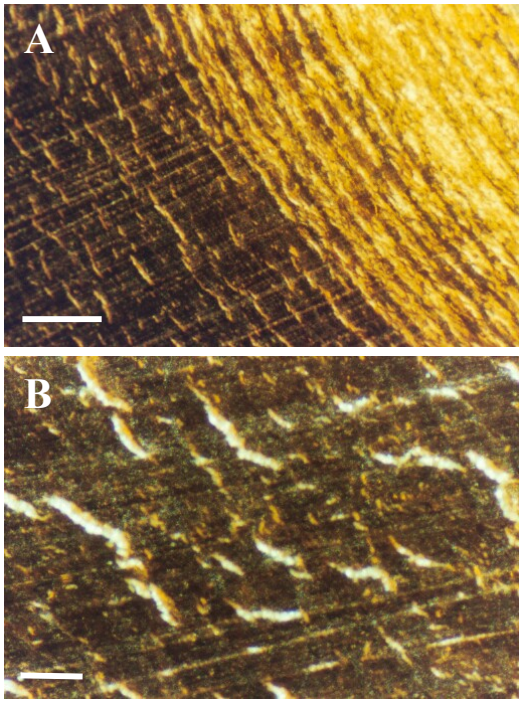

Figure 2.6 Calcite secretions in the *Pseudoplexaura porosa* axial skeleton.

(A) Scale bar = 500 µm. Thin section of base viewed in reflected light. Calcite is clearly visible and is more abundant towards the central core (top right of picture).

(B) Scale bar = 100 µm. Close up of calcite secretions. They are smaller than the loculi found in *Plexaurella* spp.

The banding in *Pseudoplexaura porosa* is mainly concentric or oval in shape. At the centre of the base of the skeleton (oldest material), banding is concentric whereas in the outermost areas banding follows the shape of the outer skeleton, which is usually oval. The gorgonin is identical throughout the whole skeleton, there appears to be no difference in structure between branch sections and basal sections or younger/older portions of the colony (Figure 2.7). This indicates that once a gorgonin band is laid down it remains unmodified throughout the life of the colony and additionally, on longer timescales. *Szmant-Froelich* [1974] states that the gorgonian skeletal material is inert and persists long after the death of a colony.

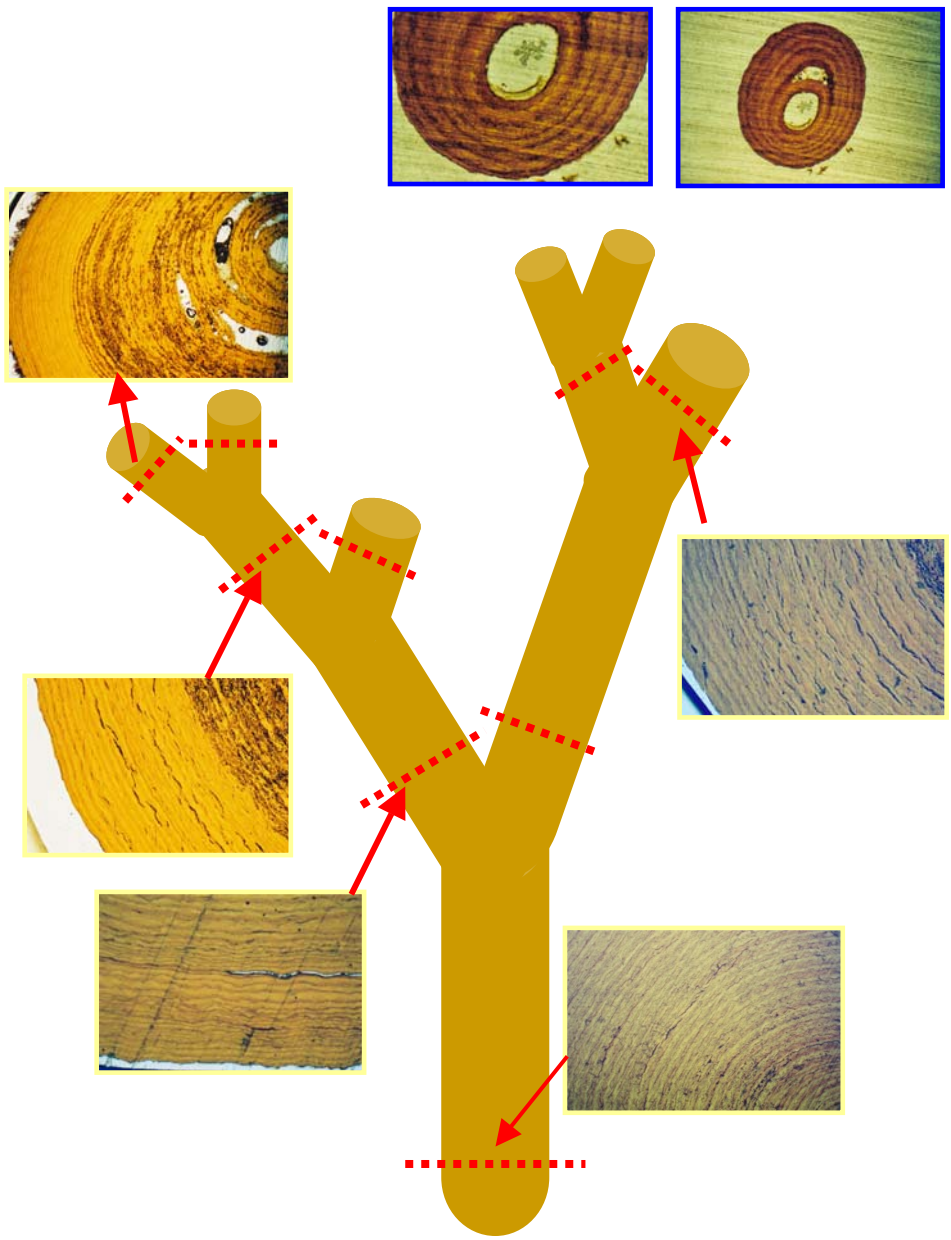

Figure 2.7 Photographs of skeletal structure and banding throughout a *Pseudoplexaura porosa* colony.
The red dashed lines show where thin sections were made throughout the colony's lower branches and base. Blue-bordered photographs are from upper branches. The banding patterns and gorgonin are the same throughout the whole colony.

2.4.2 Plexaurella spp.

In *Plexaurella dichotoma* and *Plexaurella nutan*s, the calcite loculi, embedded within the organic gorgonin layers, are clearly visible and are distributed throughout the entire skeleton. This indicates that the carbonate fraction is laid down sequentially and probably at the same time as the organic fraction. Concentrations of gorgonin are greater in the older portions of the colony i.e. the outer layers of the basal section.

Lewis et al. [1992] provide an in depth description of calcification in the *Plexaurella nutans* skeleton so I have concentrated here on *Plexaurella dichotoma's* skeletal structure.

2.4.3 Plexaurella dichotoma

Calcification of the *Plexaurella dichotoma* skeleton is concentrated in the younger sections of the colony; the branches are heavily calcified. The central portions of the base also have a high concentration of calcite (Figure 2.8) and this material would have been laid down when the colony was first established. This implies that calcification provides strength preferentially to the thinnest, weakest portions of the colony and the calcification effort of the colony is concentrated in these regions.

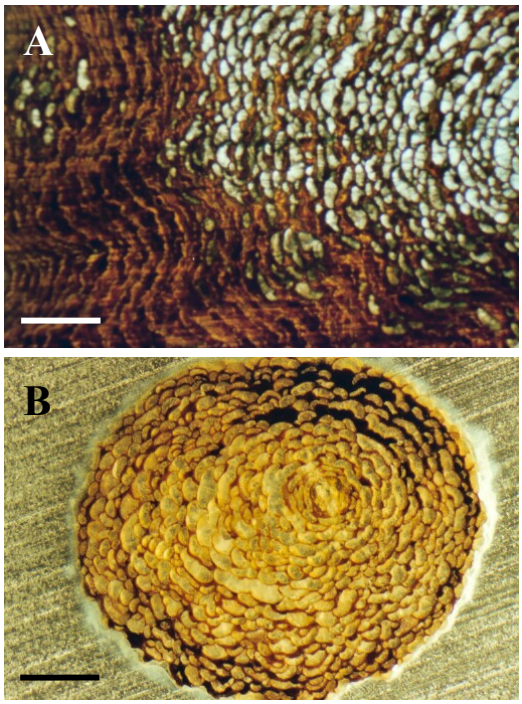

Figure 2.8 Calcite loculi distribution in the *Plexaurella dichotoma* axial skeleton.
(A) Scale bar = 0.5 mm. Basal section, calcite loculi are most abundant in the central portion of the colony around the core. In the outer layers calcification is less common.
Note banding changes from concentric near the core (right) to undulating in the outer layers (left).

(B) Scale bar = 0.5 mm. Branch section, the entire skeleton is calcified. Note that banding is concentric throughout.

Banding in *Plexaurella dichotoma* appears to be controlled by the gorgonin layers, bands are concentric in the central portions of the base and in the branch sections (Figure 2.8). However in the outer layers of the base, bands undulate (Figure 2.8) and this wavy pattern is reflected in the perimeter of the base. This undulation may be caused by the location at the axis surface of longitudinal channels containing gastrodermal canals as noted in the red coral *Corallium rubrum* [*Marschal et al*., 2004]. In the basal outer layers where these undulating bands are found loculi are less numerous. Various patterns of calcification are observed (see Figure 2.9A and B). Loculi distribution can be restricted to the troughs of each wave giving the appearance of spokes on a wheel radiating outwards from the heavily calcified core region (Figure 2.9B). In Figure 2.9A, the calcification in the basal, outer skeleton is restricted to one area, perhaps implying that within this plane the skeleton requires strength. *Wainwright et al*. [1982] observed that calcite deposition in *Plexaurella nutans* correlated with directional stiffness. Thus, this colony was most likely situated in an area of the reef subject to unidirectional water currents.

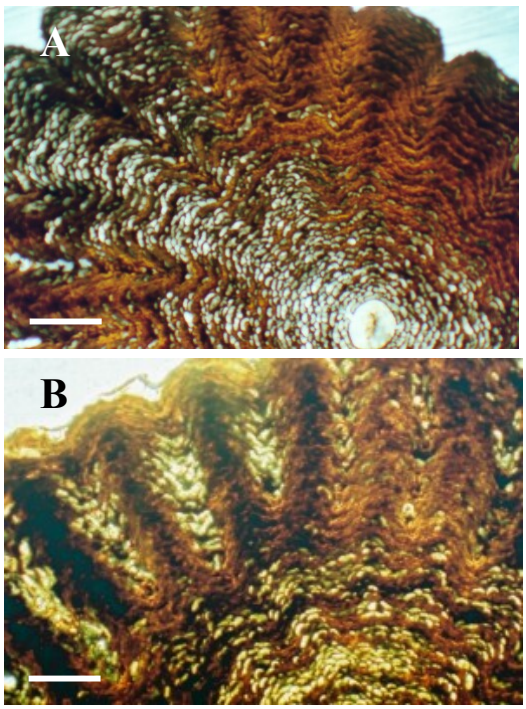

Figure 2.9 Calcification patterns in *Plexaurella dichotoma*.

Scale bars = 1 mm.

(A) Calcification in one area of the skeleton provides strength in that plane.

(B) Deposition of calcite loculi in the troughs of each undulating band forming a "spokes on a wheel" pattern.

2.4.4 Structure and growth of loculi in Plexaurella dichotoma

The calcified loculi within the axial skeleton of *Plexaurella dichotoma* appear to be composed of radiating arrays of fine needle-shaped crystals that emerge from a common centre. The spherulitic morphology of the calcite crystals in *Plexaurella dichotoma* are rarely observed in inorganic calcites [*Tracy et al*., 1998] but have been described in other calcitic biominerals including scleractinian corals and avian eggshells [e.g., *Lowenstam and Weiner*, 1989]. Spherulitic morphologies in general are considered indicative of rapid crystal growth rates [e.g., *Bryan and Hill*, 1941; *Lofgren*, 1974; *Lowenstam and Weiner*, 1989].

In *Plexaurella dichotoma* loculi grow both radially (i.e. thickening) and longitudinally (i.e. lengthening) (Figure 2.10) resulting in rod-shaped structures ~10 μm to 140 μm in width and 3 mm to 5 mm in length. This observation is in agreement with those of *Lewis et al*. [1992] for other *Plexaurella* species. In cross section, loculi display a range of shapes and appear to grow initially as small crescents that later sometimes fuse with adjacent loculi (Figure 2.10A). This implies that lateral growth of the calcite needles could continue for several months after their initial accretion, a

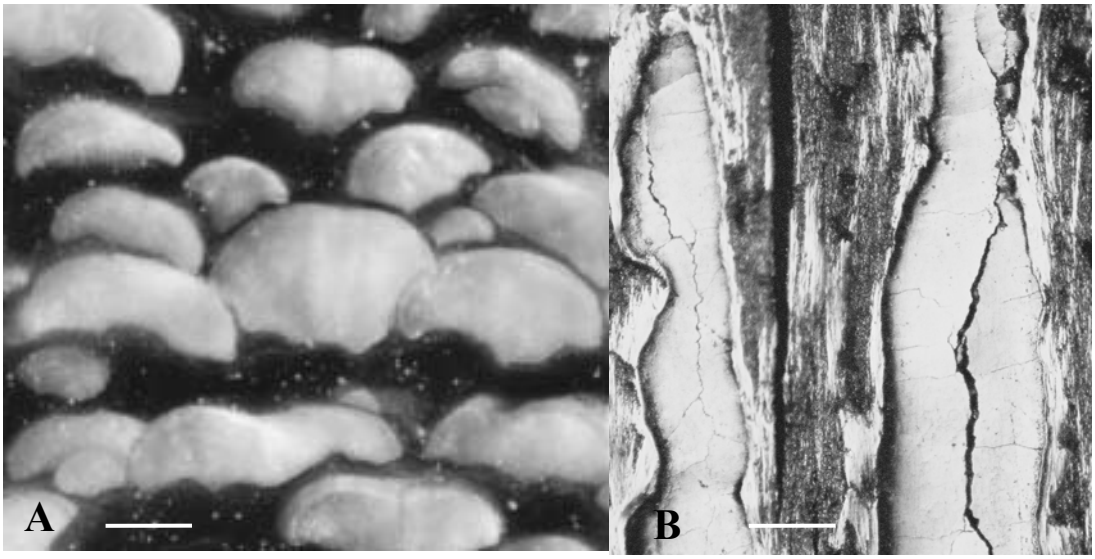

Figure 2.10 Microscope images of *Plexaurella dichotoma* calcite loculi (scale bar 100 μm).
(A) Fan shaped loculi (white) embedded in bands of gorgonin (black) viewed in cross section. Needle-shaped crystals of high-Mg calcite emerge from a common nucleation point at the base of the loculus, fanning out as they extend to form a crescent shape. Discrete loculi may continue to grow laterally and sometimes fuse with adjacent loculi.
(B) Longitudinal view of loculi showing variation in width due to gorgonin fibres restricting growth (cracks developed along loculi during sample preparation).

phenomenon also observed in the aragonitic needles of coral sclerodermites [*Barnes and Lough*, 1993; *Cohen et al*., 2004]. Fine bands, approximately 2 μm wide are visible within the loculi of *Plexaurella dichotoma*. They are oriented perpendicular to the growth axis, similar to those described by *Lewis et al*. [1992] in *Plexaurella nutans*, *P. grisea* and *P. fusifera*.

2.4.5 Growth model for Plexaurella dichotoma calcite loculi

After examining the calcification patterns in several colonies and many calcite loculi, I will attempt to describe briefly the formation process for calcite loculi in *Plexaurella dichotoma*.

It appears that nucleation sites occur along the gorgonin proteinaceous fibres. From these calcification centres spherulitic crystal growth would initially occur in all directions but as interference is encountered in most directions (e.g. from the previous gorgonin band and from the formation of neighbouring calcite loculi) growth is restricted. Furthermore, the organic matrix appears to constrain outward growth of the needle crystals, generating loculi with a finite selection of shapes.

Individual loculi grow to 5 mm in length and longitudinally, loculi appear to be formed by the fusing of calcite needles from adjacent calcification centres (Figure 2.11). The width of these loculi is not uniform along their length and this is why in cross section loculi have a range of widths. Similarly, in cross section within a band, there is some lateral fusing of loculi (Figure 2.12). Organic bands are thicker in some areas of the skeleton and this ultimately halts the locular growth both horizontally and longitudinally.

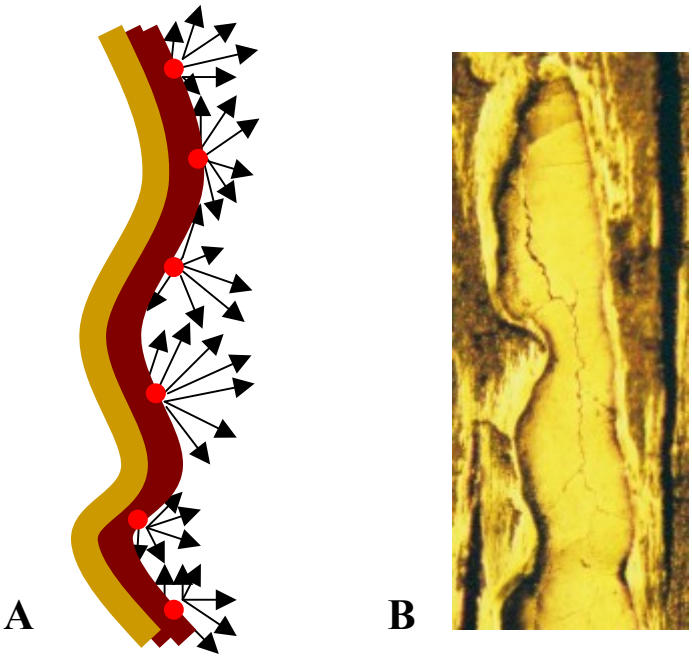

Figure 2.11 Longitudinal growth model for calcite loculi.
(A) Cartoon showing organic gorgonin band (brown) upon which calcification centres (red) are located. Spherulitic crystal growth occurs in all directions (black arrows). As interference is encountered in most directions, loculi form initially as crescents but then fuse to form the calcite rods, which grow to 5 mm long.
(B) Photograph of a calcite loculus illustrating the width of a loculus is not uniform along its length. Organic fibres restrict calcite growth in some areas.

Figure 2.12 Cross sectional growth model for calcite loculi.
Calcification centres (red circles) occur along the gorgonin band (brown). Needle growth occurs outwards (black arrows) to form crescent shaped loculi. Lateral growth can sometimes cause fusing of adjacent loculi (red dashed line).

2.5 Conclusions

2.5.1 Sampling

A method was developed to enable the sampling of gorgonian basal and lower branch sections without destroying the entire colony. This was done through the re-planting of the upper branches as "miniature colonies" on the reef.

To avoid the collection of samples with skeleton degradation it is important to avoid any colonies overgrown by encrusting organisms.

2.5.2 Skeletal structure

The variety of methods used provided an insight into the skeletal structure of *Pseudoplexaura porosa*, *Plexaurella dichotoma* and *Plexaurella nutans*.

Axial skeleton gorgonin is more cross-linked in *Pseudoplexaura porosa* than in *Plexaurella* spp. This was evident from bleach dissolution experiments and microscopic optical examination. Even to the naked eye it is noticeable that the *Pseudoplexaura porosa* organic skeleton is harder, more brittle and glassy black in colouration compared to *Plexaurella* spp. gorgonin, which is fibrous and lighter in colour.

Calcite is present in all species studied although to a lesser extent in *Pseudoplexaura porosa*. For this species, from optical examination, calcite is distributed throughout the skeleton but less so in the outer layers. The calcitic deposits in *P. porosa* are thin and sheet like. It appears *P. porosa* strengthens its skeleton in two ways. Primarily through extensive cross-linking of gorgonin and also by secreting cement-like deposits of calcium carbonate between these organic layers.

Plexaurella spp. strengthens its skeleton through calcite deposition. Lenticular, calcitic loculi, which grow both radially and longitudinally, are distributed in specific areas to provide structural support. Calcification aids the survival of the thinnest, weakest portions of the colony and provides strength against the force of directional water currents. The formation of calcite loculi within *P. dichotoma* has been briefly described, with a growth model proposed. The timing of locular formation is considered in more detail in Chapters 3 and 4.

Chapter 3: An investigation of growth banding periodicity in three Bermudian gorgonians

3.1 Introduction

The periodicity of growth banding has been investigated for only a few species of gorgonians. After a series of growth monitoring experiments the banding in *Muricea californica* and *Muricea fruticosa* both from Californian waters was found to be annual [*Grigg*, 1974]. Annual banding in the deep-sea gorgonian *Primnoa resedaeformis* was validated using growth rates determined from the decay of ^{210}Pb [*Andrews et al*., 2002] and radiocarbon dating [*Risk et al*., 2002; *Sherwood et al*., 2005]. *Marschal et al*. [2004] investigated banding periodicity in the red coral *Corallium rubrum* from the Mediterranean using calcein labelling and band counts in colonies of known age. They concluded that each annual growth ring was formed of one light and one dark calcite band, the darker band containing a higher proportion of organics than the light. Periodic calcein labelling indicated secretion of the darker band took place in the autumn/winter.

To date no work has been conducted on the periodicity of growth banding in *Plexaurella* spp. and *Pseudoplexaura porosa*, the species studied here. This investigation is important to this thesis as it provides information on growth rate and longevity of gorgonian colonies. Furthermore, the banding will provide a chronology for proxy measurements (Chapters 4 and 5). I report here on staining and isotopic marking experiments carried out to investigate the periodicity of banding for three Bermudian gorgonians *Pseudoplexaura porosa*, *Plexaurella dichotoma* and *Plexaurella nutans*.

3.2 Optical examination of growth bands

Thin sections were prepared as described in Chapter 2, section 2.3.3 and growth bands were examined under microscope. A growth band is defined here as one high- and low-density couplet of organic gorgonin, including any embedded calcitic loculi. For *Pseudoplexaura porosa* growth band widths ranged from ~50 μm to ~200 μm. Growth band widths for *Plexaurella dichotoma* spanned 60 μm to 240 μm, with an average width of 120 μm. The growth bands in *Pseudoplexaura porosa* were clearly visible in thin section, but were more difficult to identify in thicker sections, especially

in the outer layers. In the *Plexaurella dichotoma* skeleton it was more difficult to identify banding where the skeleton was heavily calcified.

3.3 Determining the periodicity of growth banding: Staining experiments

As the periodicity of banding in *Pseudoplexaura porosa* and *Plexaurella* spp. was unknown, a series of staining and marking experiments on live colonies of these species were carried out on Bermuda over a period of three years. The premise was to mark the outermost growth band and harvest the marked coral a year later, examination of these samples would, in theory, enable the amount of growth since staining to be determined. If the observed annual growth were equal to an average growth band, indications would be that banding is annual in periodicity.

3.3.1 Staining techniques - Background

Sodium alizarin sulphonate [$C_6H_4COC_6HOH_2(SO_3Na)CO$] also known as alizarin red S, is a calcium carbonate stain and has been used to assess growth rates of stony corals in the field [*Barnes*, 1970; *Smith et al*., 1979; *Dodge et al*., 1984; *Cohen et al*., 2001; *Cohen et al*., 2004]. Staining techniques have only recently been applied to gorgonian corals as a means to assess growth rate and longevity [*Marschal et al*., 2004]. The red coral skeleton labelled by *Marschal et al.* [2004] is formed of a solid red magnesium calcite and so requires different labelling techniques to the species considered here with their organic rich skeletons.

Plexaurella spp. contain up to 30% weight calcite [Chapter 2, section 2.3.2; *Lewis et al*., 1992], so alizarin red S was used for these gorgonian species. Due to the low concentration of calcite in the *Pseudoplexaura porosa* skeleton, an organic stain acid fuchsin ($C_{20}H_{17}N_3O_9S_3Ca$) was used. Acid fuchsin, a collagen muscle fibre stain, should label gorgonin, a cross-linked form of collagen. The organics of the gorgonian axial skeleton are dark brown in colouration, thus should acid fuchsin be visibly undetectable, tetracycline was also used. Tetracycline hydrochloride ($C_{22}H_{24}N_2O_8{\cdot}HCl$) is a fluorescent antibiotic used extensively for fish otolith labelling [e.g., *Hernaman et al*., 2000] and investigating crystal growth [e.g., *Bevelander*, 1963].

3.3.2 Methods - Staining procedure

3.3.2.1 Staining set up

Branch sections from *Pseudoplexaura porosa* and *Plexaurella* spp. colonies were collected live, transported from the reef in cool boxes filled with seawater, and placed in outdoor aquaria at the Bermuda Biological Station for Research (BBSR). Each branch was housed separately in a transparent tube sealed at the base, with fresh seawater and air supplies (Figure 3.1). Branches were regularly monitored and left to adapt to the experimental conditions for 48 hours. The samples adjusted quickly to their new environment; on many branches after a few hours the polyps were extended indicating feeding (Figure 3.2A).

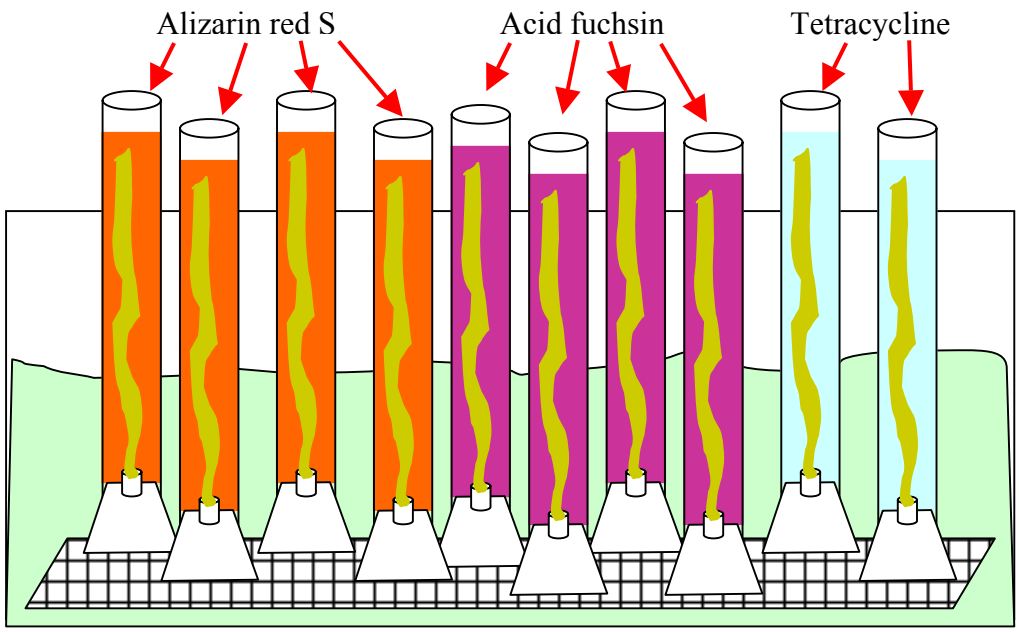

Figure 3.1 Cartoon of 2001 staining apparatus.
Individual gorgonian branches are housed in transparent tubes inside an aquarium. This allows multiple stains to be used at the same time. Each individual set up has a seawater source and aquarium pump (not shown here) to maintain mixing of the water column.

3.3.2.2 Preparation of stains

The volume of water in the experimental tubes was calculated and a solution of each stain was prepared. For alizarin red S a concentration of 10 mgl^{-1} was used as in previous studies [e.g. *Dodge et al*., 1984]. 10 mg of dark red Alizarin red S powder were added to 1 litre of distilled water to form a dark orange liquid, which turns bright purple on contact with seawater. Acid fuchsin, a green crystalline powder, turns dark pink when added to water. Experiments were conducted to determine a suitable

concentration for acid fuchsin. 10 mgl^{-1} produced a weakly coloured solution and as the gorgonian samples were unaffected (polyps remained extended on addition of the stain see Figure 3.2B), a higher concentration of 125 mgl^{-1} was used. During the 2001 field trip the availability of tetracycline was limited thus the maximum possible concentration 2.5 mgl^{-1} was used.

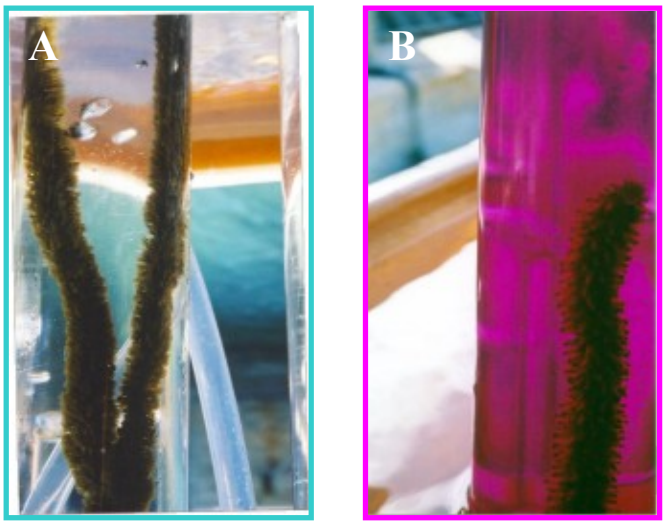

Figure 3.2 *Pseudoplexaura porosa* branches in 2001 staining set up.
(A) The sample adapting to conditions pre staining, polyps are extended indicating a healthy sample.
(B) Sample in acid fuchsin stain, again polyps are extended indicting the sample is unaffected by stain.

3.3.2.3 Staining the gorgonian samples

The stains were introduced and an aquarium pump ensured vigorous mixing of the water column within each sample housing. For gorgonian corals labelled material is incorporated in the following order: polyps, coenenchyme, gastrodermis, axis epithelium and finally axial skeleton [*Leversee*, 1980]. *Leversee* [1980] examined the incorporation of labelled proline into the gorgonian axial skeleton and concluded times of 12-24 hours were required to ensure skeletal labelling. For this experiment gorgonian samples were left for 48 hours to incorporate the stain, following this period the stained corals were sub sampled to check for stain inclusion. A comparison of stained gorgonian branches to the unstained controls indicated incorporation of stain into the coenenchyme (Figure 3.3), skeletal incorporation was harder to detect at this stage and the sub samples were retained for further analysis.

Stained samples and controls for each species were replanted (see Chapter 2 section 2.2.2 for method) at Bailey's Bay Flats, inner lagoon reef site. All replanted

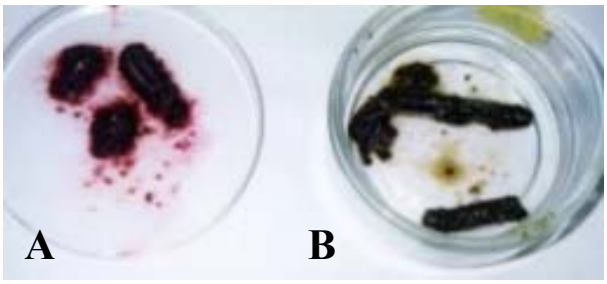

Figure 3.3 Evidence of stain incorporation in the coral coenenchyme.
(A) Sub sample of acid fuchsin stained branch.
(B) Sub sample of control branch (no staining).

branches were clearly tagged to enable identification and were monitored throughout the year by members of the Benthic Ecology Research Programme Lab (BERP lab) at BBSR. The details of all gorgonian samples stained throughout the course of this thesis are displayed in Table 3.1.

	Gorgonian samples stained	Stain used	Samples harvested after a year's growth
Field trip September 2001	4 *Pseudoplexaura porosa* branches	Acid fuchsin at 100 mgl^{-1} for 48 hours	3 recovered; alive
	2 *Pseudoplexaura porosa* branches	Tetracycline at 2.5 mgl^{-1} for 48 hours	1 recovered; alive
	4 *Plexaurella dichotoma* branches	Alizarin red S at 10 mgl^{-1} for 48 hours	2 recovered; alive
	Total stained = 10		Total recovered = 6
Field trip September 2002	6 *Pseudoplexaura porosa* colonies	Acid fuchsin at 100 mgl^{-1} for 48 hours	1 recovered; dead
	3 *Pseudoplexaura porosa* branches repeat stained	Acid fuchsin at 100 mgl^{-1} for 48 hours	/
	13 *Pseudoplexaura porosa* colonies	Tetracycline at 6 mgl^{-1} for 48 hours	2 recovered; dead
	2 *Plexaurella nutans* colonies	Tetracycline at 6 mgl^{-1} for 48 hours	/
	1 *Pseudoplexaura porosa* branches repeat stained	Tetracycline at 6 mgl^{-1} for 48 hours	/
	9 *Plexaurella* spp. colonies	Alizarin red S at 10 mgl^{-1} for 48 hours	4 recovered; alive
	2 *Plexaurella dichotoma* colonies	Alizarin red S at 10 mgl^{-1} for 48 hours	/
	Total stained = 36		Total recovered = 7
Field trip October 2003	3 *Pseudoplexaura porosa* colonies	Tetracycline at 6 mgl^{-1} for 4 days	3 recovered; alive after 6 months growth
	3 *Plexaurella dichotoma* colonies	Tetracycline at 6 mgl^{-1} for 4 days	2 recovered; alive after 6 months growth
	4 *Plexaurella nutans* colonies	Tetracycline at 6 mgl^{-1} for 4 days	3 recovered; alive after 6 months growth
	Total stained = 10		Total recovered = 8

Table 3.1 Details of staining work completed over the course of this PhD project.

3.3.2.4 Adaptations to staining experiments – Field trip 2002

Following the high loss rate of the 2001 samples (see Table 3.1), during the 2002 field trip, the staining protocol was adapted to enable entire colonies and greater numbers of samples to be stained. The adapted set up is illustrated in Figure 3.4. During the 2002 field trip the concentration of tetracycline used was increased from 2.5 mgl^{-1} to $6mgl^{-1}$.

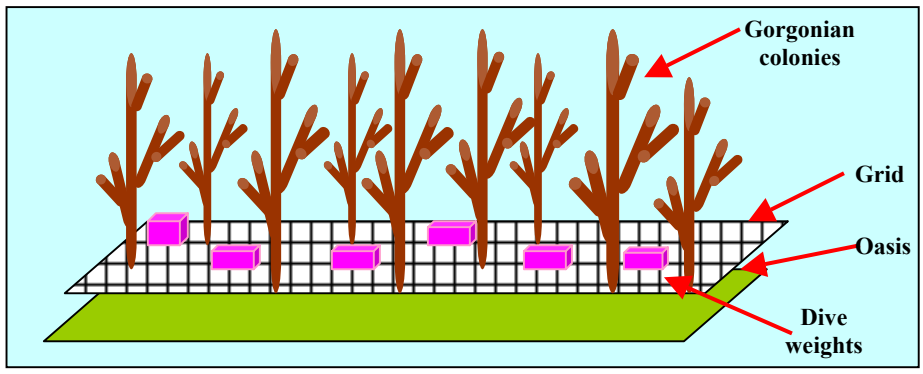

Figure 3.4 Cartoon of 2002 staining apparatus.
The set up enables whole colonies to be stained in individual aquaria. A layer of oasis (green, foam material used by florists) is weighted down with a plastic grid and dive weights. The gorgonian colony bases are pushed through the grid into the oasis, which provides good support. Aquarium pumps and seawater sources (not shown here) ensure vigorous mixing of the water mass.

3.3.2.5 Adaptations to staining experiments – Field trip 2003

On 5th September 2003 a category 3 hurricane 'Fabien' hit Bermuda. The hurricane's impact on this project was that like many gorgonians prised from Bermuda's reefs, many of the 2002 stained samples were lost (Table 3.1).

The only stain used during the 2003 field trip was tetracycline and the staining time period was extended to four days.

3.3.3 Methods – Examination of samples for evidence of stain incorporation

All sub samples taken were examined for stain incorporation using a variety of techniques. This work was completed after every field trip as the results could have implications on the methods used on subsequent trips.

Samples were first studied microscopically in thick section, following this thin sections were prepared and examined under microscope using transmitted, reflected and fluorescent light (for tetracycline samples). Acid fuchsin and alizarin red S sections

were also microscopically examined under lights with different colour filters to clarify the pink and red colours of acid fushsin and alizarin red S.

3.3.4 Results – Staining techniques

3.3.4.1 Acid fuchsin and alizarin red S

The acid fuchsin stain could not be located in the skeleton of any of the *Pseudoplexaura porosa* samples (Figure 3.5A and B). Similarly, alizarin red S was undetectable within both the calcite and the gorgonin in all the stained *Plexaurella dichotoma* and *Plexaurella nutans* sections (Figure 3.5B and C). As a consequence of these results after the 2002 field trip these stains were no longer used.

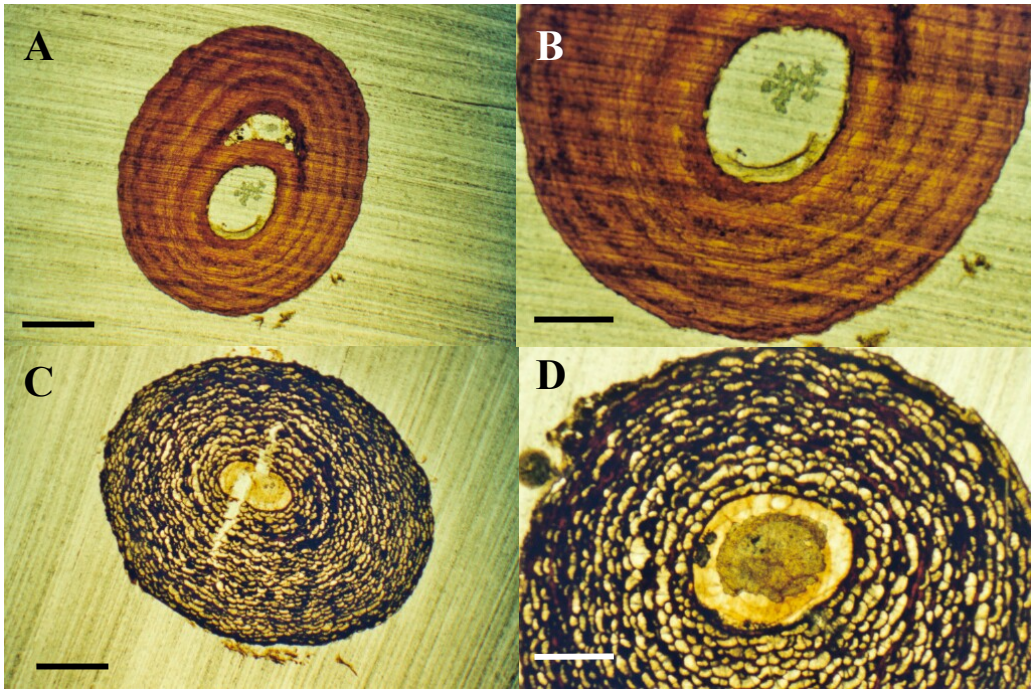

Figure 3.5 Photos to find evidence of stain line in axial skeleton after one years growth.
(A) Branch 1 *Pseudoplexaura porosa* harvested in Oct. 2002, stained once with acid fuchsin in Sept. 2001. No evidence of acid fuchsin stain is present. Scale bar = 1mm.
(B) Branch 2 *Pseudoplexaura porosa* harvested in Oct. 2002, stained once with acid fuchsin in Sept. 2001. No evidence of acid fuchsin stain is present. Scale bar = 0.5mm.
(C) Branch 3 *Plexaurella dichotoma* harvested in Oct. 2002, stained once with alizarin red S in Sept. 2001. No evidence of alizarin red S stain is present. Scale bar = 1mm.
(D) Branch 4 *Plexaurella dichotoma* harvested in Oct. 2002, stained once with alizarin red S in Sept. 2001. No evidence of alizarin red S stain is present. Scale bar = 0.5mm.

3.3.4.2 Tetracycline

Some of the gorgonian samples marked with tetracycline did fluoresce when examined under a fluorescent microscope. However it was hard to differentiate between the fluorescing sclerites immediately adjacent to the axial skeleton and the outermost layer of skeletal gorgonin. For the 2001 single branch sample harvested after one year's growth, a section about a ¼ of the total circumference did fluoresce. Furthermore, this section was one growth band away from the branch edge, indicating one year's growth since marking. As the fluorescent microscope did not have a camera set up, I was unable to document this. Samples examined from the 2003 field trip did not confirm these initial findings. The tetracycline stain was undetectable in all samples.

3.3.5 Discussion and Conclusions – Staining techniques

Neither acid fuchsin nor alizarin red S were detectable within the gorgonian coral skeleton and it is unlikely, due to the dark colour of the gorgonian skeletal material, that either stain would be visually identifiable in the future.

Regarding tetracycline it may be that a higher concentration is needed to positively mark the axial skeleton. *Hernaman et al*. [2000] used tetracycline to mark otoliths in tropical gobies, in their immersion experiments the fish were placed in aquariums containing tetracycline at a concentration of either 250 mgl^{-1} or 500 mgl^{-1} for a 12-24 hour period. However, even at these high concentrations for some species tetracycline was unsuccessful at producing a detectable mark and it is not understood why tetracycline appears to be species specific. *Hernaman et al*. [2000] note that tetracycline is labile in light and post treatment if samples are not stored in lightproof boxes the fluorescent mark can degrade. The gorgonian samples were stored in slide boxes but not having been aware that tetracycline is light labile I didn't make a concerted effort to keep the samples away from light sources. Another important point from *Hernaman et al*. [2000] is that the tetracycline immersion experiments were conducted in dark rooms to prevent light degradation of the fluorescent chemicals. My experiments were conducted in dockside aquaria, which although partially shaded from direct sunlight, are not lightproof. Therefore, degradation of tetracycline before incorporation into the coral skeleton might well have rendered the fluorescence undetectable. As the gorgonians studied here contain symbiotic zooxanthellae, growth

rates would be affected by conducting experiments in the dark and so it appears tetracycline is not an efficient way to mark gorgonian coral skeletons.

3.4 Determining the periodicity of growth banding: Isotopic marking experiments

3.4.1 Background

Strontium (Sr) is one of the major dissolved species in seawater, concentration = 7.94 ppm at salinity 35 [*Wilson*, 1975]. Natural strontium is a mixture of four isotopes; 88 (82.56%), 86 (9.86%), 87 (7.02%) and 84 (0.56%) [*Lide*, 2000]. Isotopic changes in Sr can be easily measured using the ion microprobe (see Chapter 4). ^{84}Sr was chosen as it has an extremely low concentration (0.0445 ppm) in seawater and thus a spike of ^{84}Sr should be easily detected.

3.4.2 Methods – Isotopic marking techniques

Four coral colonies (2 x *Plexaurella dichotoma* and 2 x *Plexaurella nutans*) were collected from the reef and placed in a 40 l volume aquarium using the methods illustrated in Figure 3.4. Colonies were chosen that were small enough to be completely submerged when the aquarium was half full. After a 48 hour adaptation period the seawater in the aquarium was spiked with ~2.5 times the natural seawater concentration of ^{84}Sr.

2 mg of $^{84}SrCO_3$ were dissolved in 0.5 ml 5% nitric acid. This solute was added to 1 l of seawater (which should act as a natural buffer), was well mixed and then added to 19 l of aquarium seawater (2 mg into 20 l, concentration = 0.1 mgl^{-1} or 0.1 ppm).

The gorgonian samples were left in the aquarium with the ^{84}Sr spiked seawater for 4 days. Coral samples seemed unaffected by the addition of the spike and continued to feed (polyps open). Vigorous mixing and aeration of the seawater was obtained with several aquarium pumps. After 4 days a sub sample of each colony was taken. The corals were replanted on the reef (Chapter 2, section 2.2.2) and tagged to aid identification. Due to time constraints I was unable to leave these colonies for a 12 month period and so returned to Bermuda after six months to sample each of the spiked colonies.

3.4.3 Methods - Harvesting and preparation of samples

Six months after the samples had been ^{84}Sr spiked, I returned to the replanting site Bailey's Bay Flats, Bermuda and collected in situ, a sample from each colony. Of

the four colonies spiked with ^{84}Sr, one colony was dead but the remaining three were alive and appeared healthy.

The preparation of samples for SIMS (Secondary Ionisation Mass Spectrometry) ion probe analysis is described in detail in Chapter 4, section 4.2.3.

3.4.4 Methods - Ion probe measurements

In order to ascertain control levels for ^{84}Sr in calcite, a standard (OKA calcite) was used. A series of spots were measured for OKA calcite and the $^{84}Sr/^{88}Sr$ ratio noted, these measurements were repeated at the start and end of each day on the ion probe to monitor machine drift. A control gorgonian sample (*Plexaurella dichotoma*) was probed to investigate $^{84}Sr/^{88}Sr$ ratios in an unspiked gorgonian. Then the spiked *Plexaurella* spp. samples were measured (see Table 3.2 for details). For each section I attempted to probe a semi-continuous transect from adjacent loculi starting at the outermost edge of the section and moving towards the core. This was not possible for all sections due to time restrictions on the ion probe.

Sample	Species	Transect details	# of probe spots	Distance probed (μm)
1	*Plexaurella nutans*	1A: Transect from near edge to core along narrowest growth radius of section (doesn't touch the outermost layer starts ~2 bands in)	13	448
1	*Plexaurella nutans*	1B: Incomplete transect from outermost edge along widest growth radius of section	6	252
2	*Plexaurella nutans*	2: Incomplete transect from outermost edge	8	210
3	*Plexaurella dichotoma*	3: Transect from ~1 band in to core	7	224

Table 3.2 Details of samples and sections probed for ^{84}Sr spike.

It is not easy to see the exact location of each probe spot through the ion probe eyepiece and so careful logging of probe spots is essential. After the transects were completed I used a photo microscope to identify the exact location for each ion probe spot and to measure the distance between spots and the total distance of each transect. Using the count rate raw data I identified which data points had anomalously low count rates (usually associated with probing the edge of a loculus and hence some organics). Photographs of the ion probe transects were used to confirm low count rates were due to a probe spot bordering an organic layer and as the results from these data points were unreliable, they were discounted.

The aims for the isotopic spiking work were:

1. To ascertain whether the ^{84}Sr spike had been incorporated into the calcite loculi.
2. To determine whether the ^{84}Sr spike was distributed throughout the whole skeleton or just the most recently deposited loculi.
3. To establish the amount of growth over the six month period since spiking.

3.4.5 Results

3.4.5.1 Control measurements

The OKA calcite control measurements of $^{84}Sr/^{88}Sr$ averaged 0.008 ion probe units (ipu). The gorgonian calcite control $^{84}Sr/^{88}Sr$ results were higher at 0.012 ±0.0005 ipu compared to OKA calcite (Figure 3.6).

If the strontium isotopes were incorporated into calcite at the same ratios in which they are found in seawater a $^{84}Sr/^{88}Sr$ ratio of around 0.007 would be expected. The OKA calcite value of 0.008 is close to this ratio but gorgonian calcite has further elevated levels of ^{84}Sr. This result could be a characteristic of gorgonian calcite or could be due to interference by gorgonin (organics). Further measurements of different gorgonian control calcites treated with bleach to remove organics should provide clarification.

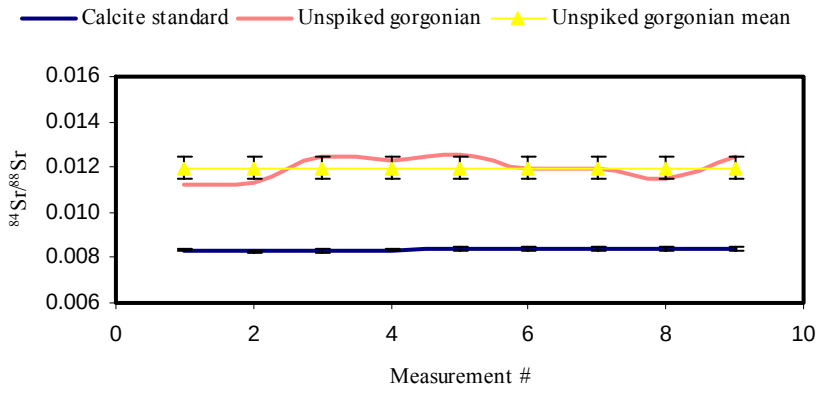

Figure 3.6 $^{84}Sr/^{88}Sr$ control values for OKA calcite and gorgonian calcite.

3.4.5.2 Section 1: transect A

Section 1 (sample 1) is from a *Plexaurella nutans* colony; this gorgonian was healthy when sampled on 11th May 2004.

Transect 1A was the first to be probed from section 1 on 3rd June 2004, it was also the longest transect probed and is shown in Figure 3.7A. I aimed to probe the entire growth history of this colony, however examination following the ion probe work illustrated that due to shadowing on the sample (caused by the slightly irregular topography of the sample surface) this transect actually started about two growth bands in from the section edge. This is unfortunate as it means the most recent growth, which should provide information on growth since spiking, remains unprobed. Results from transect 1A are displayed in Figure 3.7B. Transect 1A starts at 63 µm from the edge and continues to the core at a distance of 511 µm from the outermost edge. $^{84}Sr/^{88}Sr$ levels are elevated for the middle section of this transect; from ~200 µm to ~400 µm the ^{84}Sr spike appears detectable. The highest $^{84}Sr/^{88}Sr$ value equals 0.0151 ipu nearly twice the OKA calcite standard value. Although it can be concluded that for this sample the ^{84}Sr spike has been successfully incorporated into the calcite skeleton, there is too

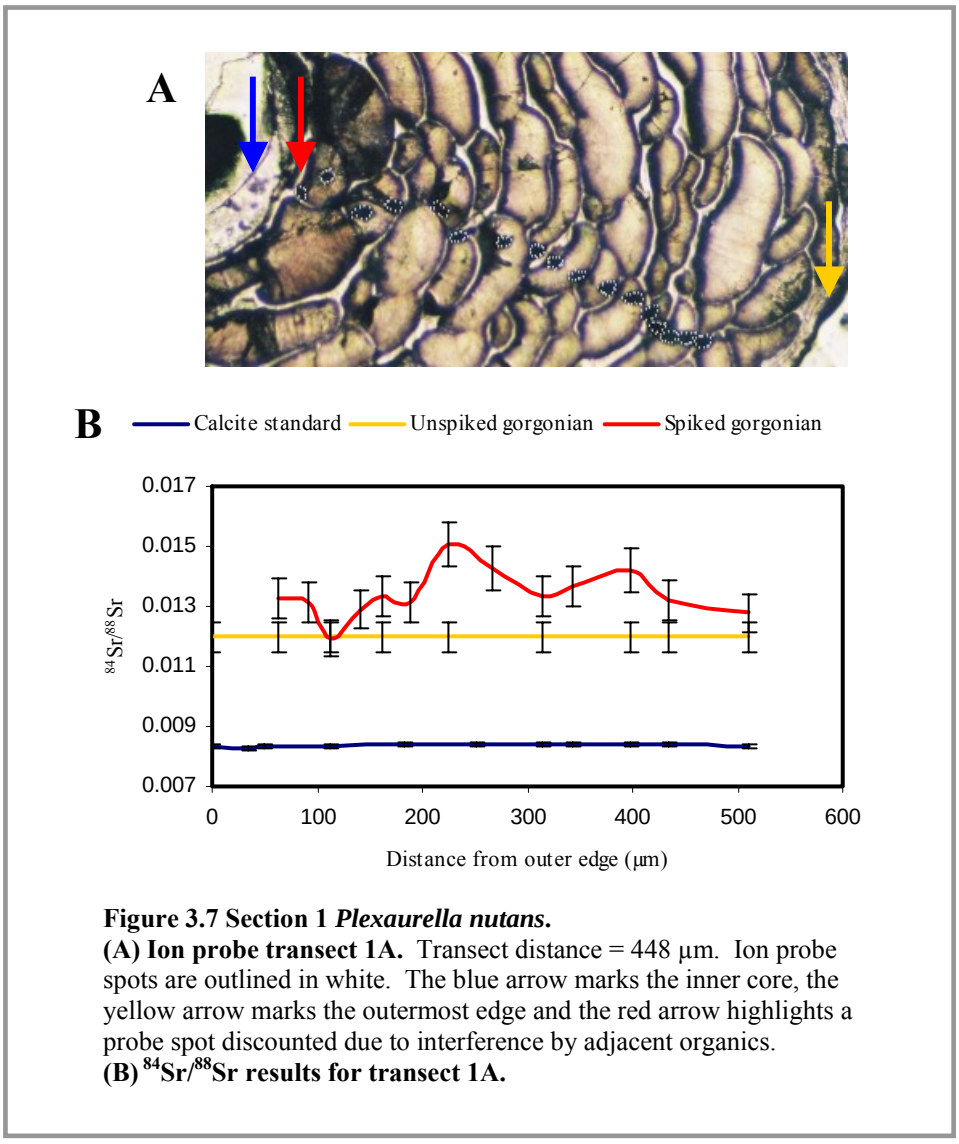

Figure 3.7 Section 1 *Plexaurella nutans*.
(A) Ion probe transect 1A. Transect distance = 448 µm. Ion probe spots are outlined in white. The blue arrow marks the inner core, the yellow arrow marks the outermost edge and the red arrow highlights a probe spot discounted due to interference by adjacent organics.
(B) $^{84}Sr/^{88}Sr$ results for transect 1A.

much variation within this transect to conclude more than this. It is also unfortunate that the measurements don't continue to the outermost layer as this could enable calculation of growth since spiking.

3.4.5.3 Section 1: transect B

Transect 1B (sample 1) is from the same *Plexaurella nutans* colony section as transect 1A and was also probed on 3rd June 2004. 1B is a shorter transect and is probed from the opposite, wider side of the section to 1A. The transect starts at the outermost edge and continues towards the core for a distance of 252 µm (Figure 3.8A). The $^{84}Sr/^{88}Sr$ results for transect 1B are displayed in Figure 3.8B plotted against the OKA calcite standard measurements and the gorgonian *Plexaurella dichotoma* unspiked data. At the outermost edge of this transect values appear to be decreasing toward control values, the spike is incorporated at around 50 µm away from the section edge. Moving

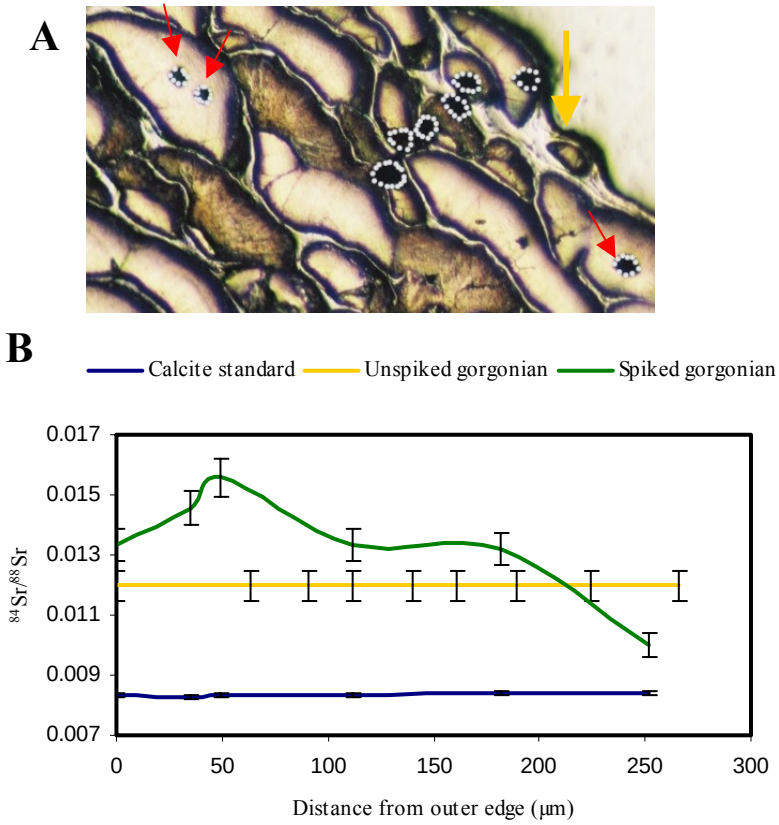

Figure 3.8 Section 1 *Plexaurella nutans*.
(A) Ion probe transect 1B. Transect distance = 252 µm. Ion probe spots are outlined in white. The yellow arrow indicates the section's edge and red arrows show trial ion probe spots not included in this transect.
(B) $^{84}Sr/^{88}Sr$ Results for transect 1B.

core-wards the $^{84}Sr/^{88}Sr$ values drop off and even decrease below the *Plexaurella dichotoma* unspiked values. This could be a species difference with *Plexaurella nutans* having lower control levels of ^{84}Sr than *Plexaurella dichotoma* or could again indicate that our gorgonian control levels were elevated through organic contamination.

3.4.5.4 Section 2

Section 2 was the first spiked section to be probed during the second ion probe session on 14th June 2004. Section 2 is from a *Plexaurella nutans* colony, which six months after spiking was still attached to the reef but was no longer alive. Although it is impossible to tell when in the six months the colony died, it will be interesting to see whether the ^{84}Sr spike was assimilated by this colony. The section 2 transect covers about half the total colony growth (Figure 3.9A) and runs for a distance of 210 µm. The section 2 transect results are displayed in Figure 3.9B. Section 2 demonstrates a clear

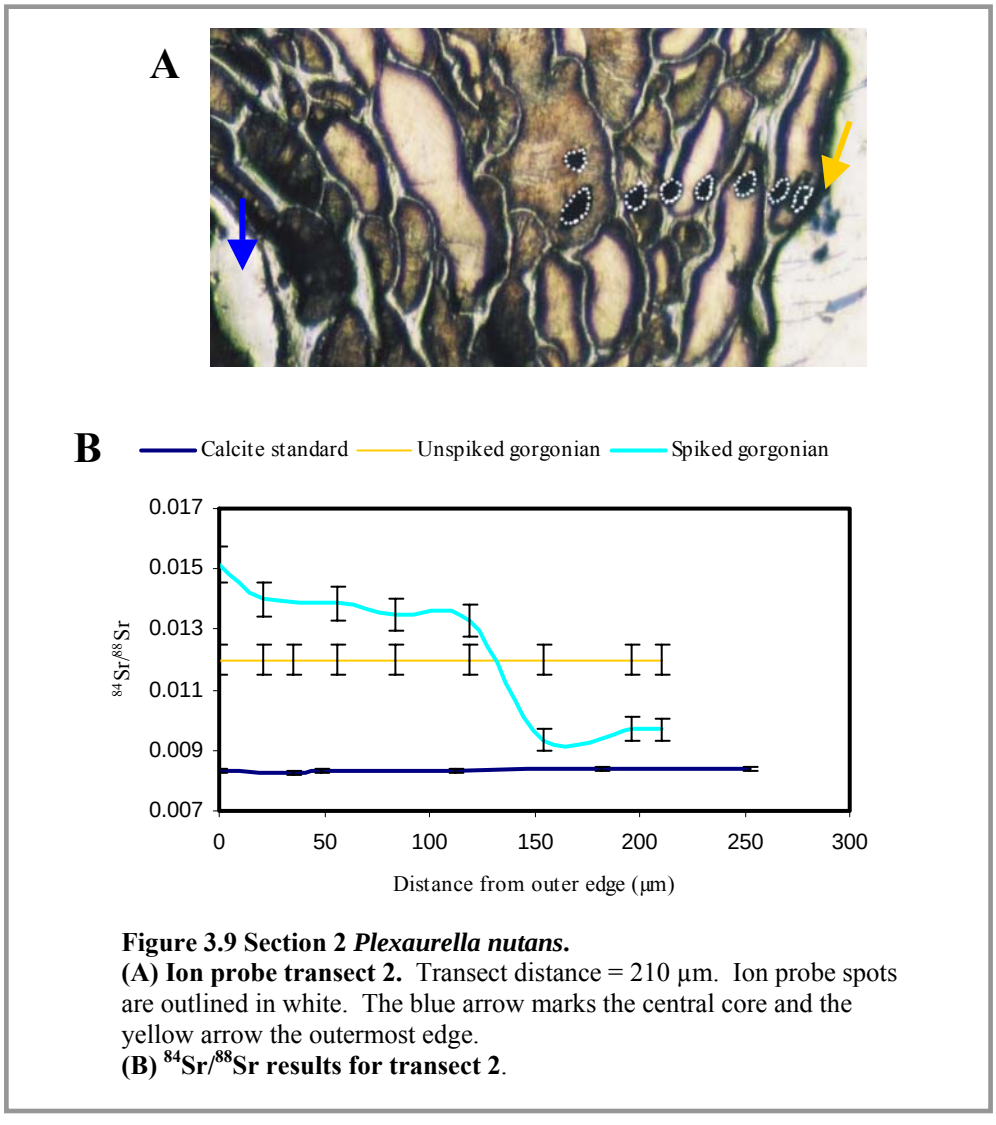

Figure 3.9 Section 2 *Plexaurella nutans*.
(A) Ion probe transect 2. Transect distance = 210 µm. Ion probe spots are outlined in white. The blue arrow marks the central core and the yellow arrow the outermost edge.
(B) $^{84}Sr/^{88}Sr$ results for transect 2.

^{84}Sr signal; the ^{84}Sr spike was obviously incorporated into the calcite skeleton before the death of the colony, although there has been no growth since. The transition from spiked to non-spiked skeleton is sharp at ~150 µm from the outermost edge; the $^{84}Sr/^{88}Sr$ values drop from ~0.014 ipu to ~0.009 ipu. Again for *Plexaurella nutans* the calcite unspiked value tends toward OKA calcite and not the *Plexaurella dichotoma* unspiked value.

3.4.5.5 Section 3

The final section to be ion probed was taken from a healthy *Plexaurella dichotoma* colony. The transect was completed on 14th June 2004. As this section was

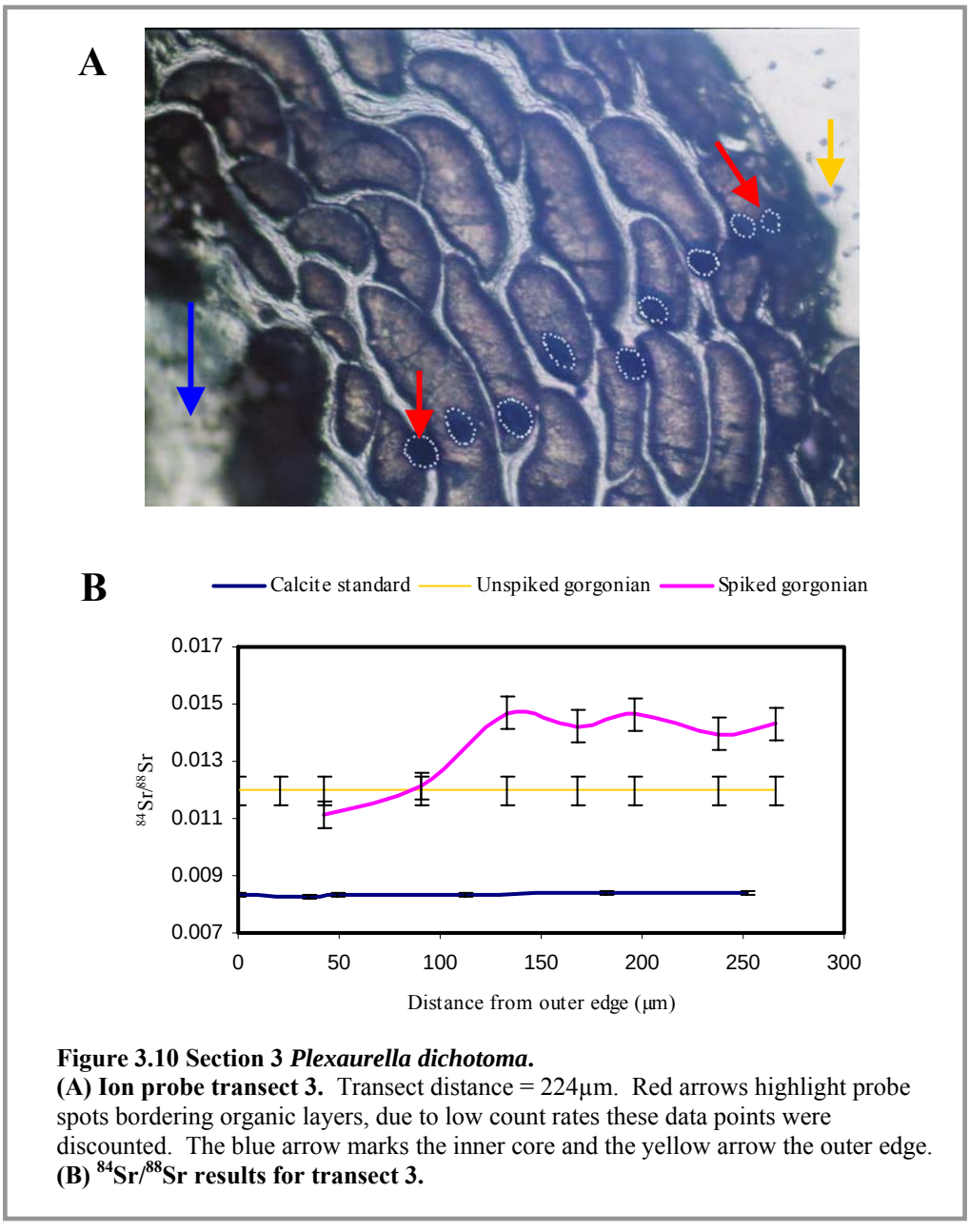

Figure 3.10 Section 3 *Plexaurella dichotoma*.
(A) Ion probe transect 3. Transect distance = 224µm. Red arrows highlight probe spots bordering organic layers, due to low count rates these data points were discounted. The blue arrow marks the inner core and the yellow arrow the outer edge.
(B) $^{84}Sr/^{88}Sr$ results for transect 3.

the smallest there was sufficient time to probe the entire growth history of the sample (Figure 3.10A). Ion probe transect results for section 3 are shown in Figure 3.10B. Unfortunately, the probe spots nearest the edge and core for this transect both had low count rates. Photo microscope examination of the ion probe transect showed that these spots were bordering organic layers and so their data were discounted.

The ^{84}Sr spike is evident in transect 3 with elevated $^{84}Sr/^{88}Sr$ values (~0.014 ipu) from 133 µm – 266 µm. The unspiked values appear to decrease to the *Plexaurella dichotoma* control line, which is interesting as this is the only *Plexaurella dichotoma* spiked sample. The spiked calcite runs almost to the inner core (~275 µm) and illustrates that for this sample at least the spike appears to have been distributed throughout the entire skeleton.

3.4.5.6 All data

Figure 3.11 displays all the spiked sections plotted with the two control calcites. The total transect distances probed are unchanged, however the individual plots have been shifted along the x-axis to allow comparison of the "spiked calcite growth distance" and growth since spiking.

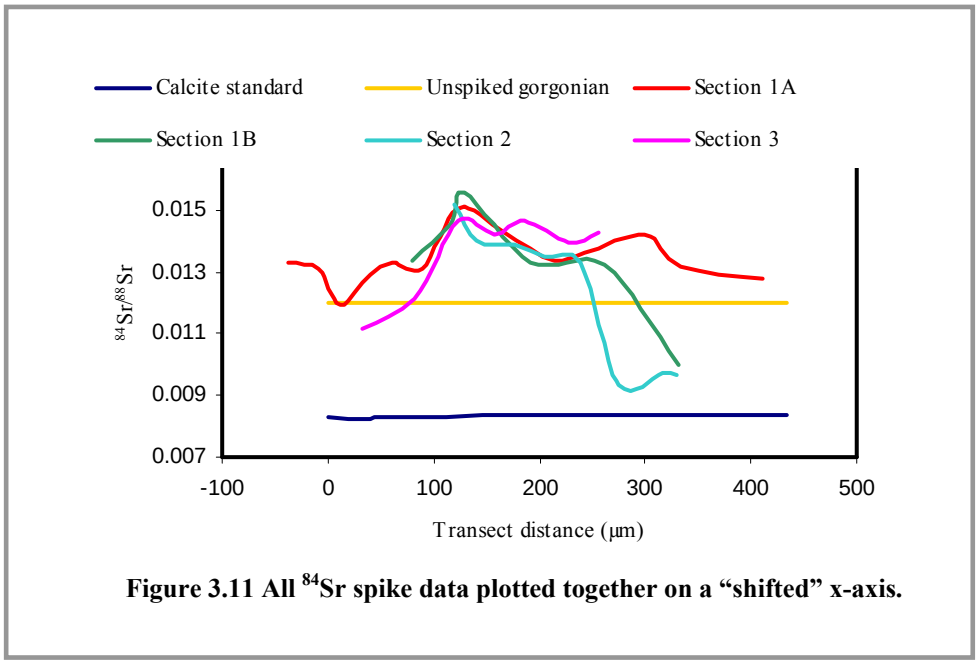

Figure 3.11 All ^{84}Sr spike data plotted together on a "shifted" x-axis.

The first observation from Figure 3.11 is how similar the distance of spiked calcite is for transects 1B, 2 and 3, in all three cases the spike is incorporated for ~125

μm of calcite growth. For transects 1B and 2 the plots are remarkably similar with sharp transitions from non-spiked to spiked calcite growth. This is important as it enables the time of spiking to be pinpointed. For all the sections that were still living when sampled (1A, 1B and 3), the transition to calcite grown "post spiking" is more gradual.

3.4.6 Discussion

The aims for this ion probe work were:

1. To ascertain whether the ^{84}Sr spike had been incorporated into the calcitic loculi.
2. To determine whether the ^{84}Sr spike was distributed throughout the whole skeleton or just the most recently deposited loculi.
3. To establish the amount of growth over the six month period since spiking.

To answer aim #1, in all four transects the ^{84}Sr spike was present. It can also be noted that in two portions of section 1 (transects 1A and 1B) the spike was detected and so it appears that the spike was incorporated within the entire circumference of the skeleton and not just in the fastest growing or highest calcification areas.

Aim #2 raises some interesting points, from transects 1B and 2 it would appear that the spike was taken up by the gorgonian and directly deposited in the calcite layers being formed at that time. However transect 1A appears to have a wider spread of the spike which continues almost to the central core indicating that in this case the spike was deposited throughout the entire skeleton, conflicting evidence is seen in transect 1B from the same section where the spike is restricted to some of the most recent growth layers. Transect 3 also has the ^{84}Sr spike distributed to the near core layers, however section 3 was the smallest sample and is noticeably smaller than any of the other samples, it is probable that section 3 has the spike distributed in these inner layers as they were still forming when the sample was spiked.

Regarding aim #3, the simplest way to determine the amount of growth over the six months since spiking is to choose the onset of the spike value and measure distance to the outermost layer:

Growth for section 1B = 182 μm.

Growth for section 2 = 119 μm.

Growth for section 3 = 266 μm.

Obviously section 2 would have less growth associated as this sample died sometime after spiking. The most interesting point is that all these values fall near to or

within the growth band width range for *Plexaurella dichotoma* of 60 μm to 240 μm (see section 3.2). Our values only represent a six month growth period but autumn/winter time has been associated with maximum growth rates for other corals. *Cohen et al*. [2004] showed that colonies of the massive reef coral *Diploria labyrinthiformis* on Bermuda exhibited maximum linear skeletal extension rates from late September through February. Higher growth rates were also observed in winter rather than summer for gorgonians from the Bay of Calvi, Mediterranean [*Weinbauer and Velimirov*, 1995; *Coma et al*., 1998].

3.4.7 Conclusions – Isotopic marking techniques

Thus far the ^{84}Sr spiking experiments have been successful, this is the first time this technique has been used for gorgonians or any corals. The results indicate that the majority of a band is formed for most sections during a six month period. This is a strong indication that for *Plexaurella dichotoma* and *Plexaurella nutans* banding is annual.

^{84}Sr spiking has the potential to provide essential information on the loculi formation process. For example, the amount of time the spike is retained within the calcifying regions of the colony could provide vital clues to loculi growth rates.

Ideally, I would like to have completed more ion probe measurements. For example, to have completed all transects in their entirety and to have measured further transects alongside one another to see if the same results are achieved for adjacent loculi. Furthermore, to probe further gorgonian control sections to investigate any species variation in ^{84}Sr content would be very interesting.

3.5 Summary

A variety of techniques have been used to investigate the periodicity of growth banding of three gorgonians *Pseudoplexaura porosa*, *Plexaurella dichotoma* and *Plexaurella nutans*.

Although a successful protocol was developed to enable gorgonian colonies to be sampled, stained and replanted, the stains used: acid fuchsin, alizarin red S and tetracycline, were either unsuccessful at marking the skeletal material or were unable to be detected visually in the gorgonian skeletal components.

Isotopic marking using a ^{84}Sr spike was the most successful technique developed. The ^{84}Sr spike was incorporated and detected within calcite loculi using

SIMS ion microprobe techniques, and provided information on the periodicity of growth banding. For *Plexaurella dichotoma* and *Plexaurella nutans* the ^{84}Sr spiking results indicate that growth banding is annual as the majority of a band is formed during a six month period.

Chapter 4: Potential proxy records in the high-Mg calcite loculi of a Bermudian gorgonian *Plexaurella dichotoma*

4.1 Introduction

The banded skeletons of gorgonian corals (Cnidaria: Octocorallia) are potentially valuable archives of past climate. The utility of gorgonian corals as palaeoceanographic archives has been less well explored than that of the scleractinian corals. The limited number of investigations of the composition of calcified regions in the gorgonian skeleton, including sclerites embedded within the coenenchymal tissue, indicate that the elemental chemistry, especially the Mg/Ca content, may be a valuable proxy for ocean temperature [*Chave*, 1954; *Weinbauer and Velimirov*, 1995; *Weinbauer et al*., 2000; *Heikoop et al*., 2002; *Thresher et al*., 2004].

Compared with reef corals, the minute dimensions of the gorgonian skeleton prohibit the use of conventional bulk sampling techniques to produce highly resolved proxy time series. This chapter describes results of Secondary Ionisation Mass Spectrometry (SIMS) ion microprobe analyses of magnesium-to-calcium (Mg/Ca) and strontium-to-calcium (Sr/Ca) ratios in high-Mg calcite loculi accreted by a shallow water Bermudian gorgonian *Plexaurella dichotoma.*

4.2 Methods

4.2.1 Sample collection

A live colony of *Plexaurella dichotoma* was collected at 6 m depth from Bailey's Bay Flats (32°21.73'N, 064°44.84'W), an inner lagoon reef site on the north shore of the Bermuda platform, on 27th September 2001. This species was selected because its' axial skeleton is heavily mineralised (see Chapter 2, section 2.3.2). The base of the colony, 1.5 cm in diameter, was dried and the coenenchyme removed to reveal the axial skeleton. Sclerites isolated from the coenenchymal tissue were used to confirm the initial species identification (see Chapter 2, section 2.2.3).

4.2.2 Sample preparation for band counting

The axial skeleton was sectioned across its width into slabs 0.5 cm thick. Thin sections were prepared (as described in Chapter 2, section 2.3.3) to conduct growth band counts. A growth band is defined here as one high and low density couplet of organic gorgonin, including any embedded calcitic loculi. Counting of growth bands was conducted manually under microscope using objectives 1.5-20, both in transmitted and reflected light. Due to the difficulty in resolving individual bands in certain regions of the skeleton, a minimum of eight radial transects were counted across each section. Based on the variability in the number of bands distinguished in repeat counts of a single section, the estimated error is ±4 bands per section. Assuming the bands are annual accretions [Chapter 3, section 3.4.6; *Grigg*, 1974; *Druffel et al*., 1995; *Andrews et al*., 2002; *Risk et al*., 2002; *Marschal et al*., 2004; *Sherwood et al*., 2005], this translates to an age error estimate of ±4 years.

4.2.3 Sample preparation for ion probe analysis

One section was selected for SIMS ion microprobe analysis based on the clarity of banding and the continuity of calcite loculi across a radial transect. Samples for ion microprobe analysis were epoxy mounted in a 1" round aluminium ring. Sections were then ground using silicon carbide paper (350-1200 grade), highly polished with 1 μm alumina, followed by 0.2 μm colloidal silica and gold coated. The gorgonian samples were found to be "gassy" and so before ion microprobe analysis, samples were placed under vacuum (1×10^{-3} torr) overnight.

4.2.4 SIMS ion microprobe analyses

SIMS ion microprobe analyses were conducted using the Cameca IMS 3f (Figure 4.1) at the Northeast National Ion Microprobe Facility (NENIMF), Woods Hole Oceanographic Institution (WHOI), under the supervision of Dr. Anne Cohen, Dr. Graham Layne and Dr. Nobu Shimizu. The SIMS ion microprobe employs a high-energy primary beam of oxygen ions to dislodge or "sputter" atoms from the surface of a material. The dislodged atoms are ionised, separated by mass and counted in a spectrometer. The dislodged atoms represent the secondary ion beam.

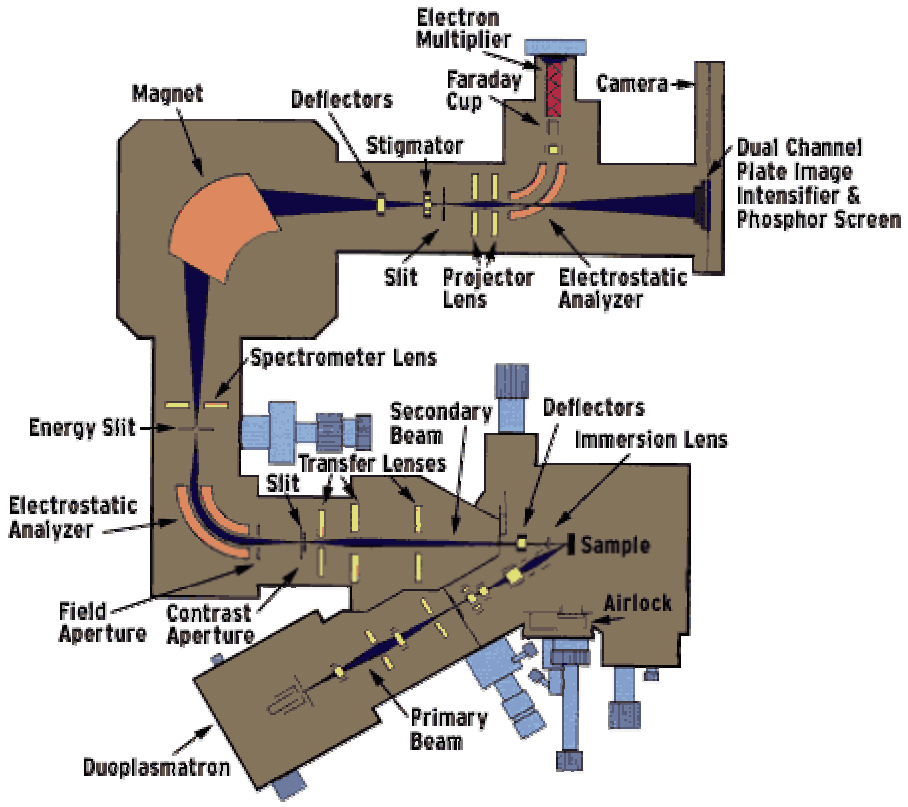

Figure 4.1 The Cameca IMS 3f ion probe at WHOI.

Source: http://www.whoi.edu/nenimf/instrument.html

For this project a 3 nA O^- primary ion beam was used to sputter select areas of successive calcite loculi in situ along a transect starting at the central core of the sectioned skeleton to the outermost band (Figure 4.2). Ion probe sample spots were 10-20 μm in diameter and approximately 5 μm deep. A single spot was occupied for 3 minutes while measuring secondary ion intensities for ^{24}Mg, ^{42}Ca and ^{88}Sr. Contributions from molecular ions including ^{44}Ca-dimer were suppressed using a 50-110 eV energy window that reduces molecular interferences to <0.1%. Cleanliness of the utilised mass spectrum has been demonstrated for Mg, Ca and Sr by measurement of isotope ratios [*Hart and Cohen*, 1996].

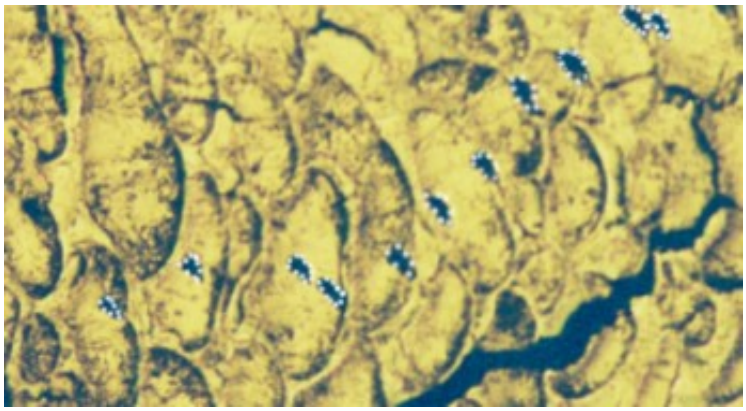

Figure 4.2 A portion of the ion probe transect measuring Mg/Ca and Sr/Ca. Ion probe spots (~ 10 µm diameter) are outlined in white.

Ion microprobe ratios were converted to molar ratios (see Table 4.1 and Equations 4.1 and 4.2) using a standard calcite (OKA C2) for which Mg/Ca and Sr/Ca ratios have been independently established [*Cohen et al*., 2001].

	OKA (ipu)	OKA (mmol/mol)	Conversion factor (ipu→mmol/mol)
Mg/Ca	0.18186	4.47	24.579
Sr/Ca	2.59	19.30	7.451

Table 4.1 OKA standard calcite values.

$$IMR_{corrected} = \left(\frac{OKA_{known}}{OKA_{measured}} \right) \times IMR_{measured}$$

(Equation 4.1)

$IMR_{measured}$ = *Sample ion microprobe ratio (raw data)*
$IMR_{corrected}$ = *Sample ion microprobe ratio corrected for machine variation*
OKA_{known} = *OKA standard value (Mg/Ca = 0.18186; Sr/Ca = 2.59)*
$OKA_{measured}$ = *OKA standard value measured for this ion probe session*

$$Sample\ Mg/Ca_{(mmol/mol)} = \left(\frac{IMR_{corrected}}{0.18186} \right) \times 24.579$$

$$Sample\ Sr/Ca_{(mmol/mol)} = \left(\frac{IMR_{corrected}}{2.59} \right) \times 7.451$$

(Equation 4.2)

$IMR_{corrected}$ = *Sample ion microprobe ratio corrected for machine variation*

Internal measurement precision for both Mg/Ca and Sr/Ca was 0.4% (2σ). The count rate data for each probe spot were checked and data points with low count rates (associated with probing a calcite/organic border) were discounted. When the transect was complete, a photo microscope was used to identify the exact location for each ion probe spot, to measure the distance between spots, and to determine the total transect distance. Band counts were performed along the transect line and the thickness of each band determined using the photomicroscope. Thirty-eight growth bands were counted across a radius of 4.75 mm, this indicates a colony age of 38 years, spanning the period 1963–2001. Growth band width measurements enabled the ion probe values to be assigned growth band numbers and hence years. Unfortunately, the low density of loculi in the outermost layers precluded analysis of the last 13 years of the record (Figure 4.3), so the Mg/Ca and Sr/Ca time series transect covers the period 1963-1988.

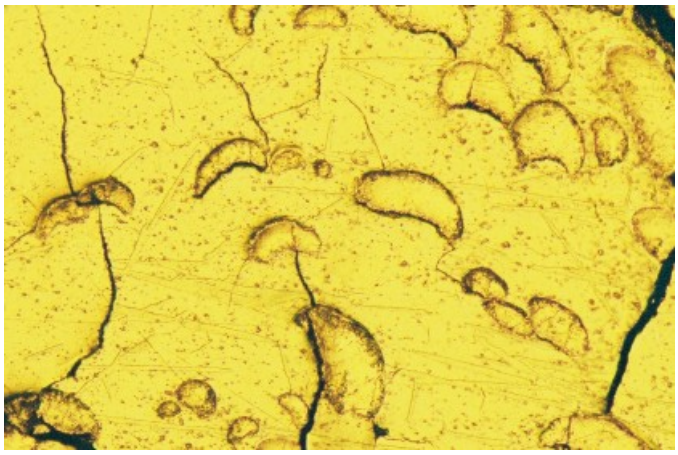

Figure 4.3 Photograph of the outermost regions of the ion probe section; loculi are less numerous here.

To further investigate loculi formation and to assess variability in the Mg/Ca and Sr/Ca content within each loculus, a series of measurements were made along the growth axes of several large loculi (100-140 μm width) (Figure 4.4).

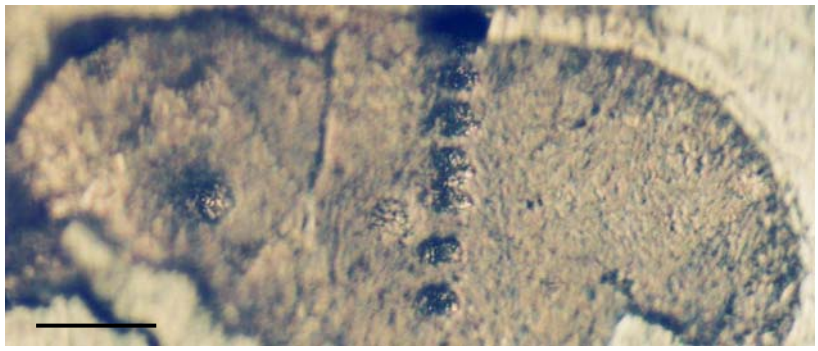

Figure 4.4 Microscope image showing high-resolution ion probe sample spots across the width of a calcite loculus. Scale bar 50 µm.

Calcite loculi grow upwards as well as outwards (Chapter 2, section 2.4.4) [*Lewis et al*., 1992] and upward growth rate was investigated by probing two loculi longitudinally. A further cross section of the basal skeleton was cut and sliced in half lengthways to reveal the rod shaped loculi. One 'longitudinal' section was prepared for ion probe work as described in section 4.2.3. Loculi grow to maximum lengths between 3 and 5 mm (Chapter 2, section 2.4.4) [*Lewis et al*., 1992]. The first longitudinal transect was completed on 11th September 2003 for a distance of 2.62 mm. For the second longitudinal transect, I wanted to ensure I probed the upward growth in its entirety and after careful microscopic examination I located a loculus ~5 mm long. This loculus was probed at 100 µm intervals, for a total distance of 4.3 mm on 15th June 2004 (Figure 4.5).

Figure 4.5 Longitudinal ion probe transect showing ion probe spots spaced ~100 µm apart. Scale bar = 100 µm.

4.2.5 Sea surface temperature data

Sea surface temperatures (SSTs) at the sample collection site were monitored in situ at 6 m depth, daily during 2000 and 2001 using calibrated Stoway data loggers (Onset Corp., ±0.1°C). To assess the representativeness of the Bailey's Bay site of open ocean conditions, the in situ logged SSTs were compared with SSTs (0–10 m depth) recorded at the open ocean Bermuda Atlantic Time-series Study (BATS) site (31º40'N, 64º10'W) for the corresponding time period (Figure 4.6A). Both absolute SSTs and the mean annual range of SSTs are similar at both sites although as the shallow lagoon responds to cool winter air temperatures, open ocean wintertime SSTs are approximately 1ºC higher.

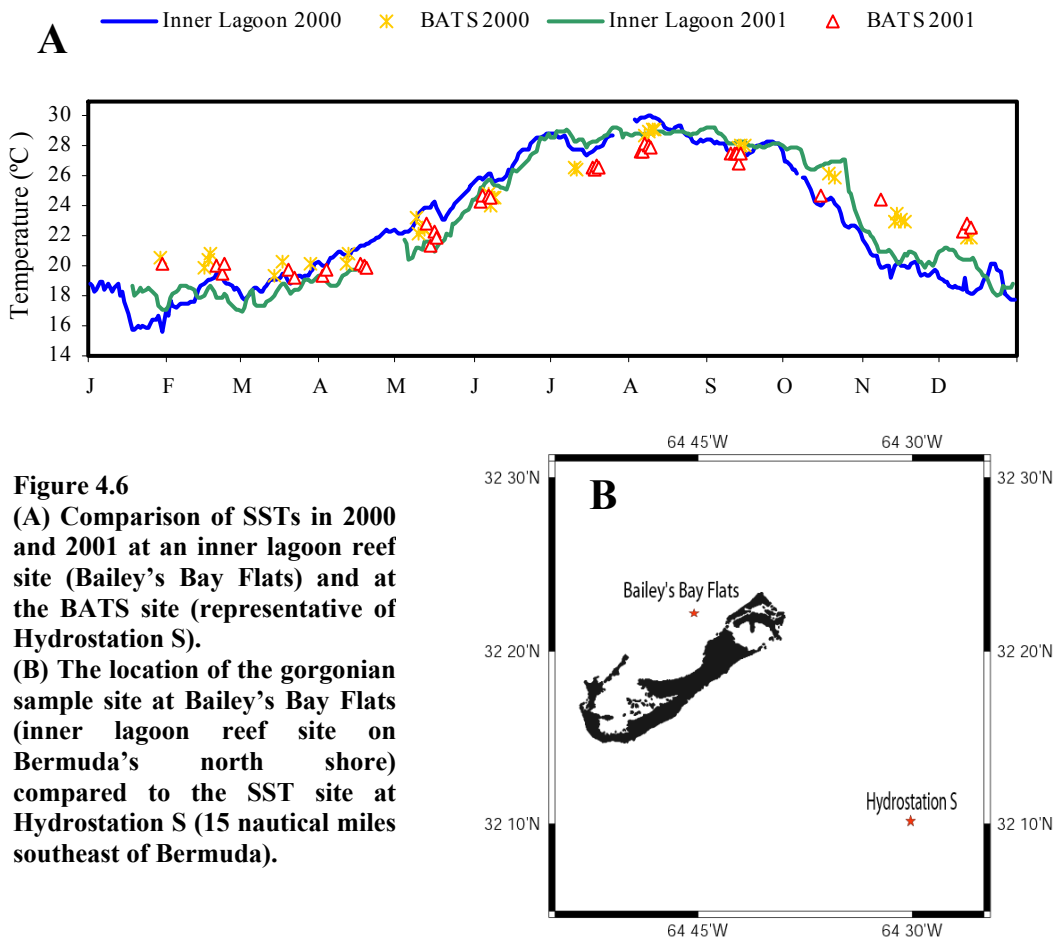

Figure 4.6
(A) Comparison of SSTs in 2000 and 2001 at an inner lagoon reef site (Bailey's Bay Flats) and at the BATS site (representative of Hydrostation S).
(B) The location of the gorgonian sample site at Bailey's Bay Flats (inner lagoon reef site on Bermuda's north shore) compared to the SST site at Hydrostation S (15 nautical miles southeast of Bermuda).

Due to the short duration of the in situ and BATS temperature records, the SST time series from Hydrostation S (32º10'N, 64º30'W), an open ocean site 15 nautical miles southeast of Bermuda (Figure 4.6B), was used to assess the potential of *Plexaurella dichotoma* Mg/Ca and Sr/Ca ratios as proxies for SST.

4.3 Results

4.3.1 Time series (ion probe horizontal transect)

4.3.1.1 Mg/Ca and Sr/Ca ranges

Mg/Ca ratios measured in the loculi of *Plexaurella dichotoma* range from 144.09 mmol.mol^{-1} to 341.15 mmol.mol^{-1} and Sr/Ca ratios range from 1.99 mmol.mol^{-1} to 3.53 mmol.mol^{-1}. These Mg/Ca ratios agree well with those reported by *Chave* [1954] for the sclerites of a Bermudian *Plexaurella* species (205 mmol.mol^{-1}) but are significantly higher than those reported by *Weinbauer et al*. [2000] for the high-Mg calcite skeleton of a Mediterranean red coral, *Corallium rubrum* (Mg/Ca ~115 mmol.mol^{-1}). However, the *Weinbauer et al*. [2000] *Corallium rubrum* values for Sr/Ca are remarkably similar to those for *P. dichotoma* at ~3 mmol.mol^{-1}.

4.3.1.2 Skeletal chemistry and average annual SSTs

Mg/Ca and Sr/Ca time series constructed along the radial transect were compared against SSTs recorded at Hydrostation S for the period 1963–1988. Mg/Ca and Sr/Ca ratios collected from loculi within each discrete growth band were averaged and normalised, and the correlation with SST determined with positive/negative time lags (e.g. Figure 4.7). Interannual variability in Mg/Ca correlates positively with interannual SST variability; the highest correlation (r^2 = 0.32) between annually averaged SSTs and Mg/Ca obtained with a 3 year lag. The best correlation between Sr/Ca and SST was inverse (r^2 = 0.35) obtained with an 8 year time lag. Although a time lag of 3 years for the Mg/Ca data could be explained due to band count error (band counts and hence associated years are only accurate to ±4 years, see section 4.2.2) the time lag for Sr/Ca of 8 years cannot and so these results are clearly inconclusive.

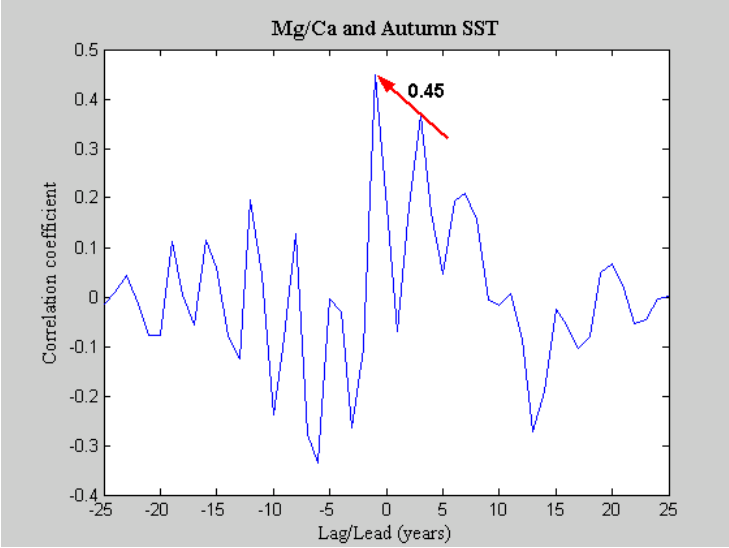

Figure 4.7 Example of MATLAB correlation coefficient plot for z scored data.

4.3.1.3 Skeletal chemistry and seasonal SSTs

Hypothesising that the bulk of a loculi is accreted over a shorter time frame than one year, correlations amongst seasonal SSTs and skeletal chemistry were explored. The highest correlations were obtained for the autumn season (October-December) (Figure 4.8A and B). Mg/Ca correlates positively with autumn SST: $r^2 = 0.45$ with zero lag ($P < 0.10$, df = 17) (Figures 4.7 and 4.8A). Sr/Ca correlates inversely with autumn SST for the first half of the time series: $r^2 = 0.43$ with zero lag ($P < 0.10$, df = 17), but fails to capture the SST variability after about 1976 (Figure 4.8B).

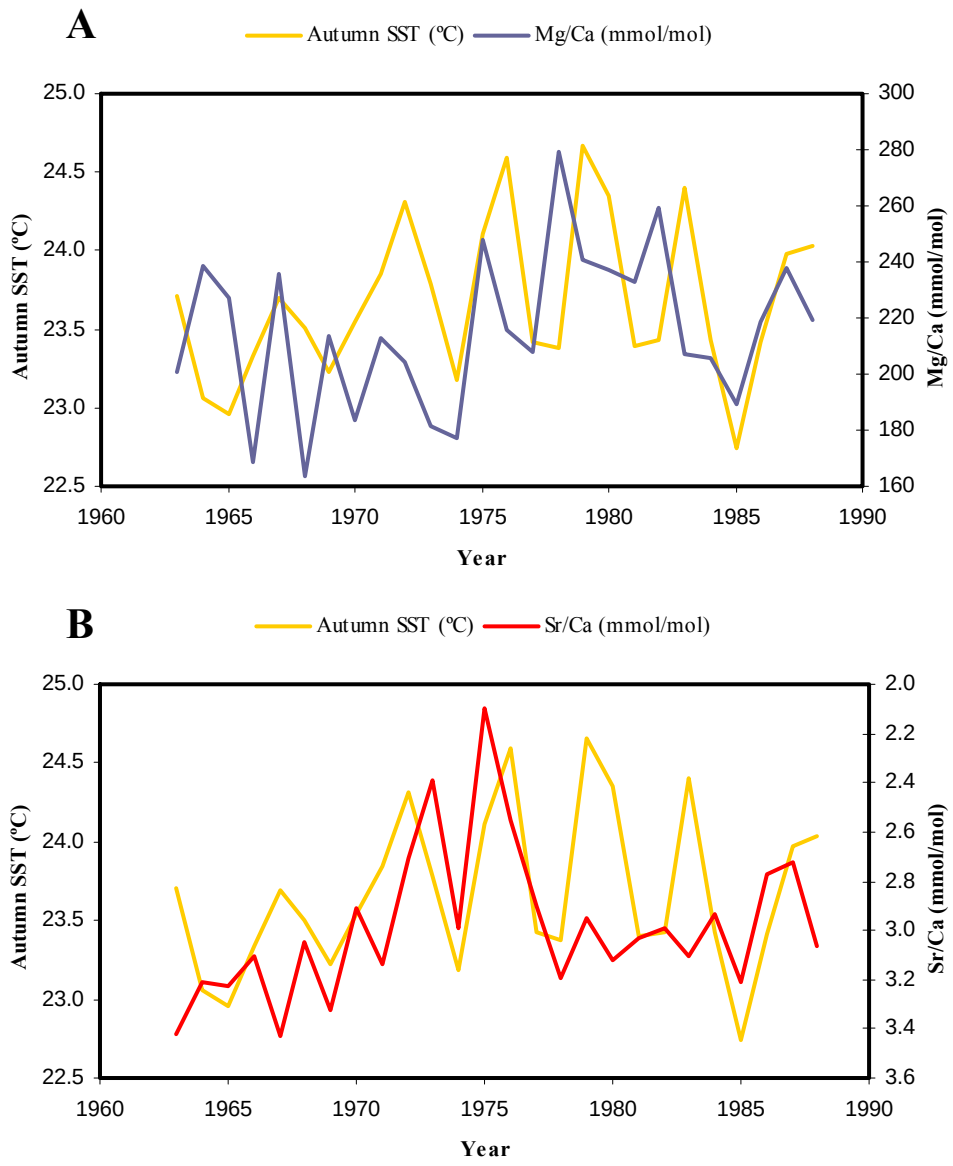

Figure 4.8
(A) Mg/Ca and (B) Sr/Ca time series spanning years 1963-1988 plotted against interannual SSTs averaged over the autumn period only.

4.3.1.4 Calculating a Mg/Ca temperature relationship

To explore the sensitivity of Mg/Ca in *Plexaurella dichotoma* calcite to changes in interannual SST (autumn), a Mg/Ca-SST relationship was calculated using the ion probe dataset (illustrated in Figure 4.8A and 4.9A). It is apparent that some of the Mg/Ca data points lag behind the equivalent SSTs by one year (Figure 4.8A and 4.9A), however this lag is within the proposed band count error of ±4 years. Data were then plotted against one another (Figure 4.9B) to reveal the Mg/Ca-SST relationship (Mg/Ca = 46.746*SST - 879.24). The slope of this relationship is significantly higher than that derived for other inorganic and biogenic calcites (see section 4.4.1).

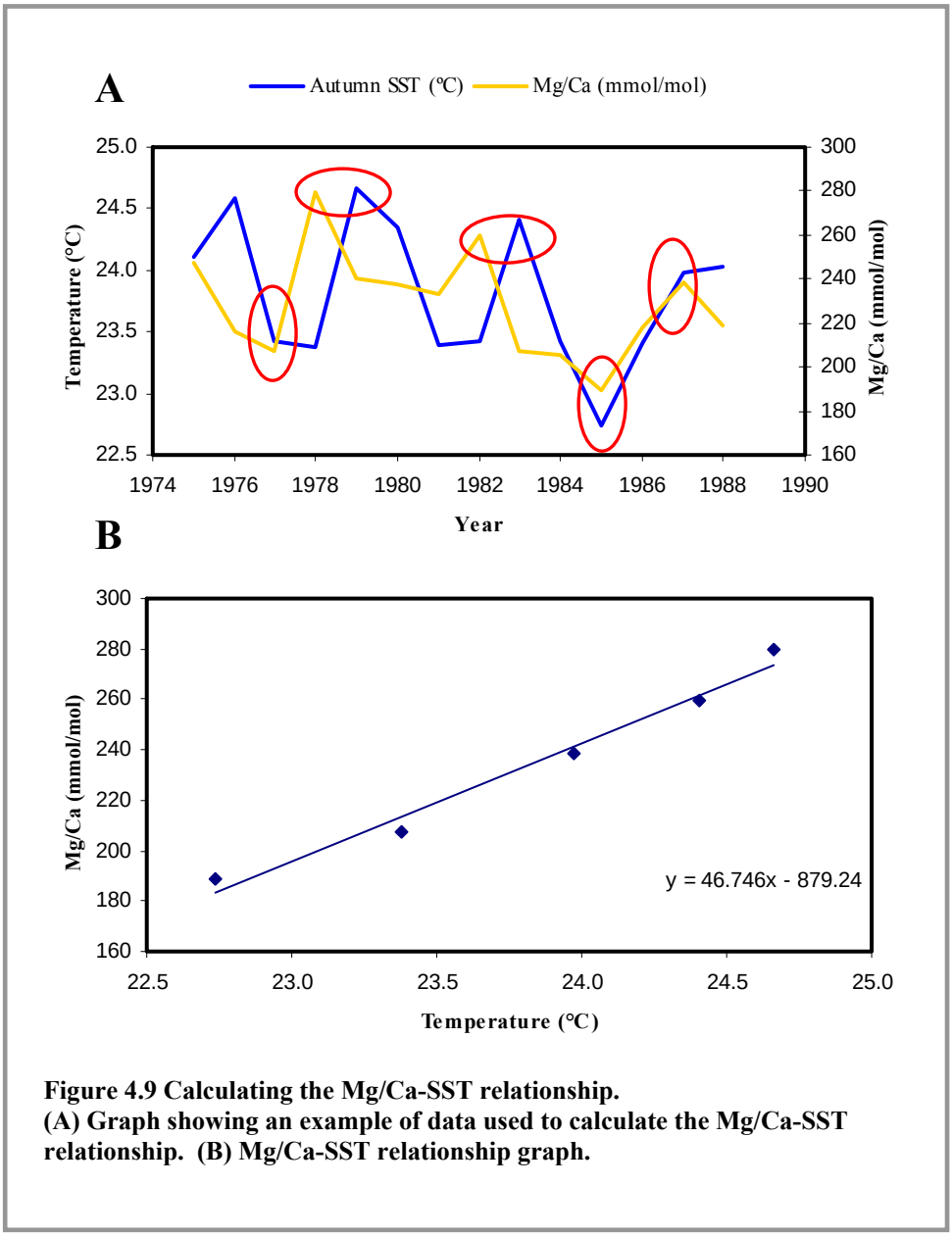

Figure 4.9 Calculating the Mg/Ca-SST relationship.
(A) Graph showing an example of data used to calculate the Mg/Ca-SST relationship. (B) Mg/Ca-SST relationship graph.

4.3.2 Variability within loculi

To assess within loculus skeletal chemistry variability, seven loculi (100-140 µm width) were analysed for Mg/Ca and Sr/Ca at high-resolution along the axis of maximum growth i.e. along a straight path from the calcification centre to the edge of the loculus (Figure 4.4). The Mg/Ca and Sr/Ca mean values and standard deviations were calculated for each within loculus transect and each growth band. Within loculus variation is compared to the yearly variation in Figure 4.10A and B.

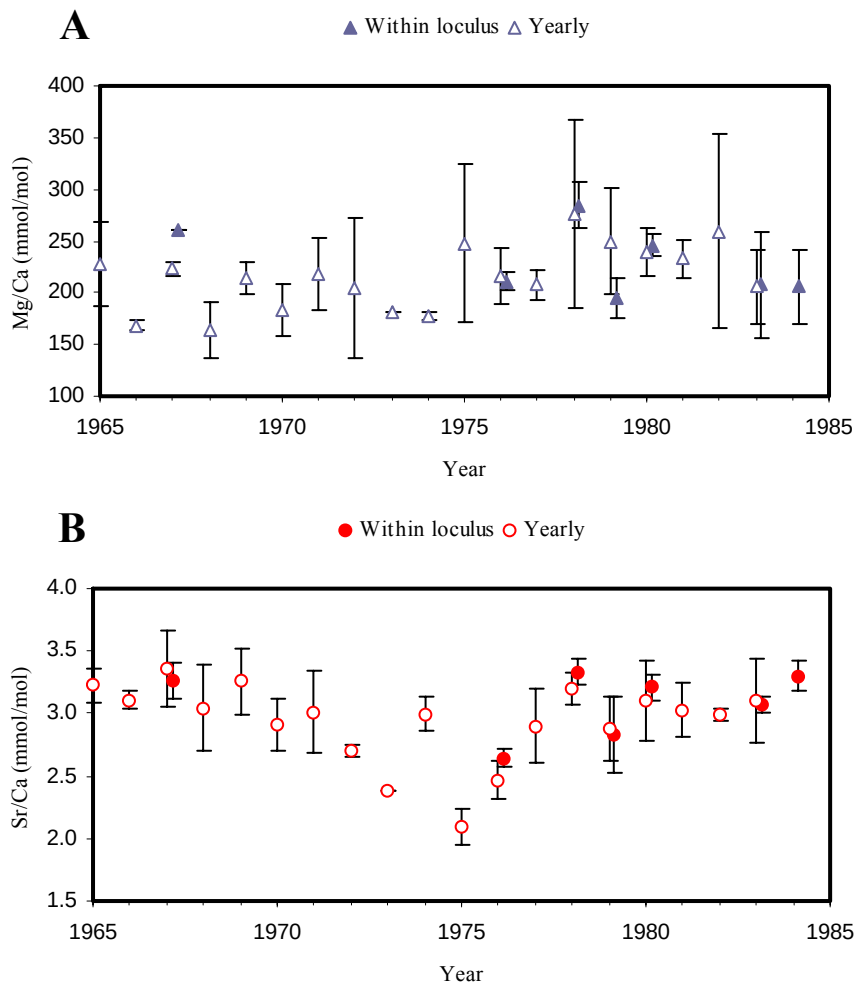

Figure 4.10 Within loculus variation compared to total yearly variation for (A) Mg/Ca and (B) Sr/Ca. Mean values are plotted for each band or loculus, error bars represent the variation of these values. The within loculus variation is generally small compared to total yearly variation.

For the within loculus data, with two exceptions, (1983 for Mg/Ca and 1979 for Sr/Ca), low variability observed along the major growth axis supports the hypothesis that the bulk of a loculus may be accreted over a short time frame (autumn). Larger variation is observed within the annual growth bands of 1975, 1978, and 1982 (Figure 4.10A). The data contributing to this large variability come from sample spots located at the lateral ends of the loculi, offset from the major growth axis. This observation suggests that subsequent lateral growth (widening) of the loculi may occur at different times of the year (other than autumn).

4.3.3 Longitudinal data

To further investigate loculus growth, two loculi were probed longitudinally at ~100 µm intervals. Longitudinal transect 1 covered a length of 2.6 mm, after this distance it was impossible to continue ion probing as the calcite loculus was buried under a layer of gorgonin. The Mg/Ca and Sr/Ca values for longitudinal transect 1 are shown in Figure 4.11. The two datasets are well matched, particularly for the second half of the transect. From ~1.5 mm the fluctuations in Mg/Ca and Sr/Ca values follow each other very closely. Mg/Ca and Sr/Ca are plotted against one another in Figure 4.12, which illustrates the degree of this correlation.

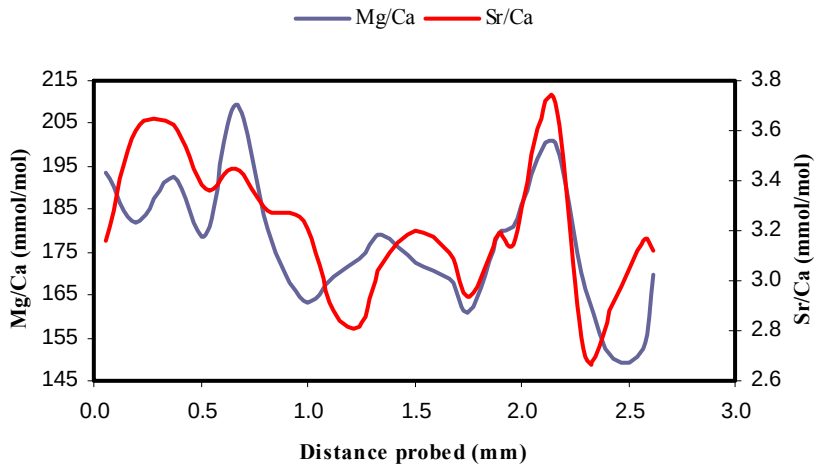

Figure 4.11 Longitudinal transect 1, Mg/Ca and Sr/Ca values measured along the upward growth of a calcite loculus.

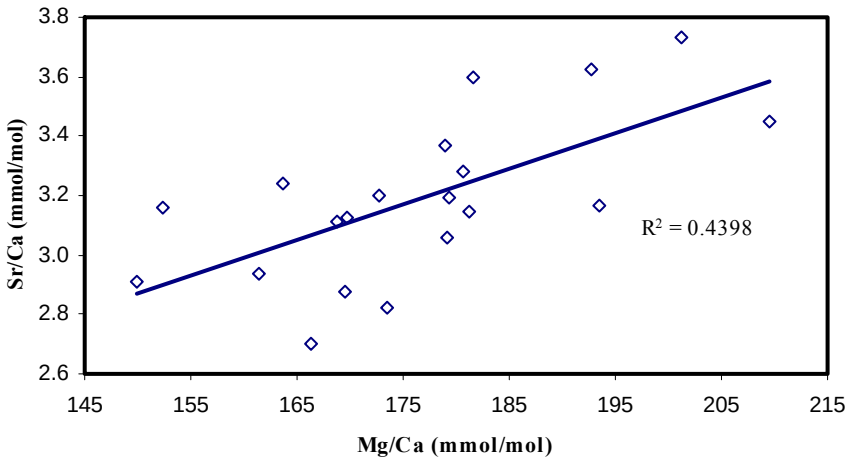

Figure 4.12 Longitudinal transect 1, cross correlation of Mg/Ca and Sr/Ca data.

For longitudinal transect 2 the entire length of a loculus was ion probed for Mg/Ca and Sr/Ca resulting in a transect 4.3 mm long (Figure 4.13).

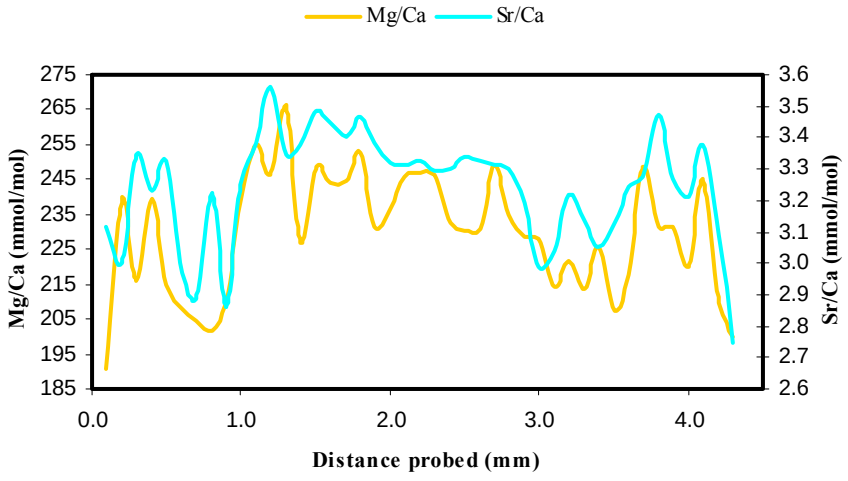

Figure 4.13 Longitudinal transect 2, Mg/Ca and Sr/Ca values measured along the entire length of a calcite loculus.

Again, as with longitudinal transect 1, Mg/Ca and Sr/Ca appear closely, positively correlated and the degree of this correlation is shown in Figure 4.14.

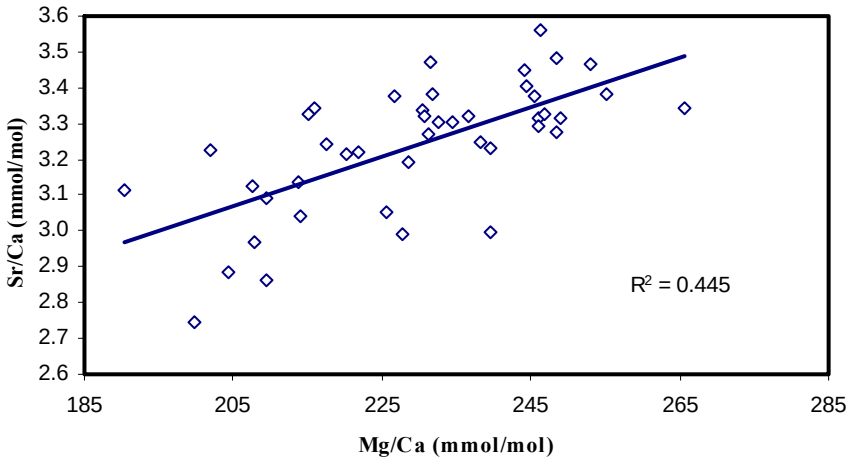

Figure 4.14 Longitudinal transect 2, cross correlation of Mg/Ca and Sr/Ca data.

This is the first time a correlation between Mg/Ca and Sr/Ca has been observed, no correlation was found for the horizontal transect data, nor the pooled within loculus data.

The range of the longitudinal Mg/Ca and Sr/Ca data is smaller than the horizontal transect data (Table 4.2). However some of the horizontal variability comes from ion probe spots laterally offset from the major growth axis (section 4.3.2). Longitudinal probe spots sampled along the centre of the loculus and so should avoid any 'lateral' effects.

	Horizontal transect	Longitudinal transect 1	Longitudinal transect 2
Mg/Ca (mmol/mol)	144.09 - 341.15 (197.06)	149.90 – 209.54 (59.64)	190.48 – 265.67 (75.19)
Sr/Ca (mmol/mol)	1.99 - 3.53 (1.54)	2.70 – 3.74 (1.04)	2.75 – 3.56 (0.81)

Table 4.2 Comparison of the range of data for longitudinal and horizontal transects.
The highest and lowest values are given in each case with the difference between them shown in brackets.

4.4 Discussion

4.4.1 Mg/Ca

The positive correlation between Mg/Ca and SST observed for *Plexaurella dichotoma* calcite is in agreement with that observed for a range of biogenic calcite skeletons, including gorgonians [*Chave*, 1954; *Weinbauer and Velimirov*, 1995; *Weinbauer et al*., 2000; *Thresher et al*., 2004], as well as data obtained from laboratory grown inorganic calcites [*Oomori et al*., 1987; *Mucci and Morse*, 1983; *Huang and Fairchild*, 2001]. Mg/Ca in biogenic calcites is used increasingly as a proxy for SST [*Chave*, 1954; *Dodd*, 1967; *Lea*, 2003]. Although the temperature sensitivity of Mg/Ca in high-Mg calcites has not been determined experimentally, this study suggests that Mg/Ca ratios in *Plexaurella dichotoma* high-Mg calcite may also respond to changes in SST and therefore, be a useful SST proxy. Despite the positive correlation obtained between Mg/Ca and SST, there are clearly phase offsets in some years. For example, peak SSTs obtained in 1979 and 1983 appear to be captured by peaks in Mg/Ca ratios exactly one year earlier (Figure 4.8A). This most likely reflects uncertainties in the age model based on band counting and the assumption that the outermost band was accreted during 2001. As sample collection took place at the end of the warm summer period (27th September, 2001) the bulk of the 2001 loculus growth may not yet have occurred. Nevertheless, the magnitude of the offsets is within our estimated age error of ±4 years.

In Figure 4.15 the Mg/Ca-SST relationship obtained in this study for *Plexaurella dichotoma* high-Mg calcite is compared with relationships reported for the red coral *Corallium rubrum* [*Weinbauer et al*., 2000], sclerites [*Chave*, 1954; *Weinbauer and Velimirov*, 1995], high-Mg foraminiferal calcite [*Toyofuku et al*., 2000] and inorganic calcite [*Oomori et al*., 1987]. The sensitivity of *Plexaurella dichotoma* Mg/Ca to changes in temperature is apparently much higher than has been observed for other biogenic and inorganic calcites and is a full order of magnitude higher than that reported by *Weinbauer et al*. [2000] for *Corallium rubrum*. The reasons for these differences are unclear but may be a function of the Mg/Ca content of the skeleton i.e. the higher the Mg content, the higher the sensitivity of Mg to temperature. The differences amongst Mg/Ca-SST relationships obtained for gorgonian calcites may, in addition, reflect the different calibration techniques used to derive them.

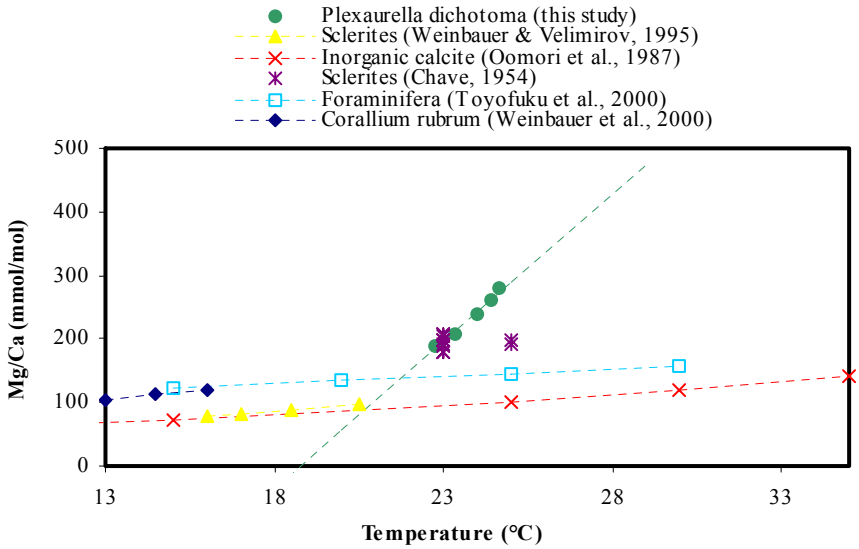

Figure 4.15 Comparison of Mg/Ca-SST relationships for inorganic and biogenic calcites.

For example, the relationship for *Plexaurella dichotoma* in this study was obtained by comparing interannual Mg/Ca variability within a single colony against interannual SST variability over the same time period, whereas other relationships have been established using different colonies collected at different sites or depths [for e.g., *Weinbauer et al.*, 2000].

4.4.2 Sr/Ca

Variability in *Plexaurella dichotoma* Sr/Ca ratios track the interannual SST variability for the first half of the record but fail to do so after 1976, remaining relatively invariant for the remaining 12 years (Figure 4.9B). This suggests that *Plexaurella dichotoma* Sr/Ca may be controlled by factors other than ocean temperature. Experimental determination of laboratory grown inorganic calcites indicate that the partitioning of Sr is dependent on calcite growth/precipitation rate [*Lorens*, 1981; *Mucci and Morse*, 1983; *Tesoriero and Pankow*, 1996; *Huang and Fairchild*, 2001]. These experiments have shown an increase in the partition coefficient of Sr into calcite (D_{Sr}) with greater rates of calcite precipitation [*Lorens* 1981; *Mucci and Morse*, 1983; *Tesoriero and Pankow*, 1996]. Growth rate effects on Sr incorporation into biogenic calcites have been observed in gorgonian sclerites [*Weinbauer and Velimirov*, 1995] and the axial skeleton of *Corallium rubrum*

[*Weinbauer et al*., 2000], in both these studies Sr was suggested to be inversely related to growth rate. *Heikoop et al*. [2002] reported an Sr/Ca-SST relationship for deep-sea gorgonians but suggested that growth rate may be a factor influencing Sr incorporation into the skeleton. Growth/calcification rate effects on Sr/Ca in calcite have also been noted for coccolithophores [*Stoll and Schrag*, 2000; *Rickaby et al*., 2002]. For these biogenic calcites the same relationship as with inorganic calcites is seen; the higher the growth rate the higher the Sr/Ca incorporated into the calcite structure.

To investigate the growth rate hypothesis for Sr/Ca in *Plexaurella dichotoma* calcite, I have looked into ways in which growth rate might be suppressed and thus indicated in the Sr/Ca data. Hurricanes and tropical storms cause significant perturbations to the water column, which in turn affect coral reef communities [e.g., *Dollar and Tribble*, 1993; *Bries et al*., 2004; *Gardner et al*., 2005]. Negative affects on coral colony growth rates have been observed through increases in sedimentation causing smothering of polyps, and turbidity related light reduction in the water column [e.g., *Fabricius*, 2005]. Bermuda hurricane season occurs during September and October. All tropical storms and hurricanes that affected the Bermudian islands between 1963 and 1989 are plotted with the autumn averaged Sr/Ca data in Figure 4.16.

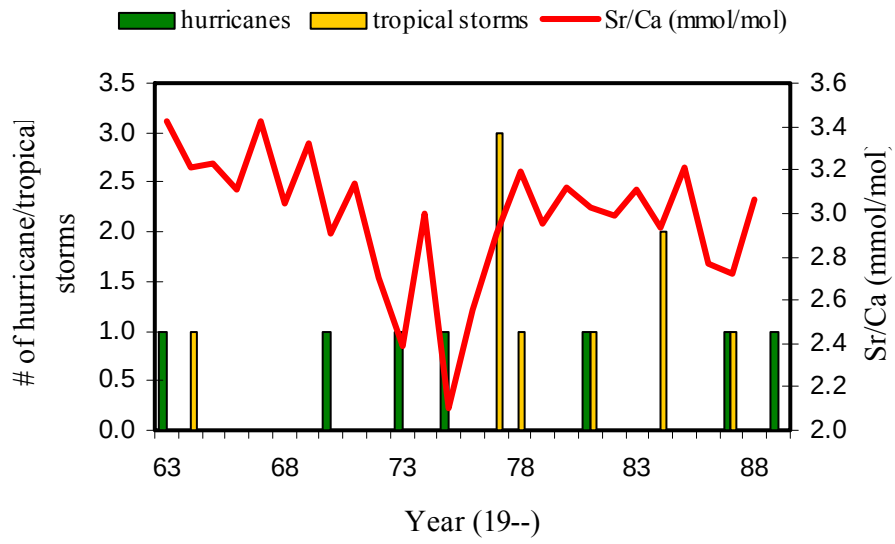

Figure 4.16 Hurricanes/tropical storm affects on Sr/Ca as potential indicator of growth rate. Hurricane/storm data from: http://stormcarib.com/climatology/TXKF_dec_isl.htm

In 1973 a level 1 hurricane passed through Bermuda, followed by a level 2 hurricane in 1975. From Figure 4.16 it is apparent that in both 1973 and 1975 Sr/Ca levels are low, perhaps indicating a decrease in growth rate caused by the hurricanes' disturbance of the water column. The tropical storms that occurred in 1977 have not suppressed the Sr/Ca ratios for this year, although there were three storm events within this year, tropical storms are not as severe weather events as hurricanes (see appendix 4.1) and this might be why colony growth rate appears unaffected. Although some correlation between hurricane activity and Sr/Ca is apparent which is encouraging for the growth rate hypothesis, there is still no clear explanation for why the variability within the Sr/Ca data drops off after ~1976. One possibility could be that by 1976, the colony at ~13 years old, was better established to cope with these perturbation events. Gorgonian mortality rates are strongly size dependent [*Lasker*, 1990], juveniles allocate resources to growth in order to enhance survival and thus delay reproduction for several years until a "species specific minimum size" is attained [e.g., *Brazeau and Lasker*, 1989; *Kapela and Lasker*, 1999]. Sr/Ca time series measurements within colonies of varying sizes from the same location would enable the degree of perturbation to be related to colony size and age, and thus this hypothesis to be tested.

There is also the question of how Sr/Ca responds to growth rate. Here I have taken the view that Sr/Ca will increase with increasing growth rate as has been found in inorganic calcite [*Lorens* 1981; *Mucci and Morse*, 1983; *Tesoriero and Pankow*, 1996] and coccolith calcite [*Stoll and Schrag*, 2000; *Rickaby et al*., 2002]. However, studies on *Corallium rubrum* suggest the opposite effect [*Weinbauer et al*., 2000]. Further work monitoring Sr/Ca in high-Mg calcite perhaps including experiments using gorgonians in aquaria where growth rate is suppressed would help to clarify this issue.

4.4.3 Seasonal locular growth

The increased correlation between Mg/Ca and SST for SSTs averaged over the time period October through December may indicate a preferred timing of calcite growth in this species, which is post-reproductive season for other *Plexauridae* on Bermuda [*De Putron*, 2002]. It is feasible to suggest that the maximum energy for growth occurs after the spawning period, July through September. In support of the seasonal growth hypothesis, *Cohen et al*. [2004] showed that colonies of the massive reef coral *Diploria labyrinthiformis* on Bermuda exhibited maximum linear skeletal extension rates from late September through February. Furthermore, the lack of

significant chemical variability within individual loculi may be further evidence that calcite growth occurs within a limited time window.

4.4.4 Longitudinal locular growth

Mg/Ca and Sr/Ca values measured along longitudinal locular growth co-varied. Relationships between Mg/Ca and Sr/Ca in calcite have been noted previously; the amount of Sr^{2+} partitioned into calcite increased with the Mg content of calcite both for inorganic Mg-calcite [*Mucci and Morse*, 1983] and biogenic Mg-calcite [*Ohde and Kitano*, 1984]. *Mucci and Morse* [1983] hypothesised that the larger sized Sr ion compensated for distortion caused by the incorporation of the smaller sized Mg ion into calcite via a co-precipitation mechanism (ionic radii: Sr^{2+} = 0.113 nm; Ca^{2+} = 0.099 nm; Mg^{2+} = 0.065 nm) [e.g., *Huheey et al*., 1993]. A significant positive correlation between Mg and Sr was also found in the calcite sclerites of the zooxanthellate gorgonian *Eunicella singularis* [*Weinbauer and Velimirov*, 1995] although no such relationship was found in the azooxanthellate species studied. If it is assumed that the longitudinal growth of a loculus occurs over the same time frame as the radial growth then the longitudinal transect provides an extremely detailed look into the time frame of loculus growth, and could be why a correlation between Mg/Ca and Sr/Ca is noted in this dataset only.

In both the longitudinal transects a rise and fall in Mg/Ca values is noticeable (Figures 4.11 and 4.13). This fluctuation perhaps reflects the SST pattern at the coral sample site. Although the bulk of a loculus is hypothesised to form in the autumn, probing of loculi longitudinally provides an extremely high-resolution picture of locular growth and could supply information on the non-bulk growth that may occur at other times throughout the year. In longitudinal section, skeletal banding is less clear, so it was not possible to ascertain the years from which the longitudinal transects came. If this were possible it would have been interesting to compare Mg/Ca fluctuations to SST variations recorded for that year.

In the future for a more accurate and detailed analysis, loculi could be isolated (dissolution of organics using bleach see Chapter 2, section 2.3.2) from a known year band and mounted for longitudinal ion probing. The Mg/Ca and Sr/Ca datasets could then be compared to other datasets for the year in question. For example SST fluctuations recorded at the sample site, documented dates/times of spawning and any storm/hurricane occurrences. It should also be possible to analyse the proportion of

growth attributed to the autumnal months as opposed to the rest of the year to further test the seasonal growth hypothesis.

4.5 Conclusions

Geochemical signals contained within the high-Mg calcite loculi of a shallow water gorgonian, *Plexaurella dichotoma*, from Bermuda were investigated using SIMS ion microprobe. Mg/Ca and Sr/Ca ratios were measured in skeletal calcite loculi from growth bands corresponding to 1963-1988 (±4 years) and at high-resolution in individual loculi both radially and longitudinally.

Mg/Ca ratios showed an overall, positive correlation with annual SSTs that is strongest in the autumn months (October-December). The sensitivity of Mg/Ca to interannual changes in average autumn temperatures is 0.47 mmol/mol per ºC.

Sr/Ca ratios fail to capture the interannual SST variability, indicating that temperature is not a primary control of Sr/Ca variability in the high-Mg calcite accreted by this species. Growth rate is considered to be the primary control on Sr/Ca in gorgonian calcite and this hypothesis was investigated using hurricane and tropical storm data as indicators of growth rate suppression.

High-resolution analyses along the radial growth axes of several large loculi showed that intra-loculi variability was small. This, together with the correlation of Mg/Ca with autumnal SST and the increased availability of energy in the post-reproductive season, suggest a preferred timing of calcite growth in this species during the autumn months.

Further longitudinal ion probing of loculi isolated from known year growth bands has the potential to confirm or reject many of these hypotheses.

These results indicate the potential for accessing information about past variability in the oceanic environment using gorgonian skeletal calcite in combination with in situ microbeam analytical techniques.

Chapter 5: Development of a method to measure tritium in gorgonian coral skeletons

5.1 Introduction

Tritium (^{3}H, the heaviest isotope of hydrogen) was produced by nuclear weapons testing in the 1950s and 1960s. It is an ideal transient tracer as it exists solely as part of a water molecule and is conservative, with no significant chemical or biological sources or sinks in the open ocean. Bomb tritium was produced largely in the northern hemisphere, in a spike-like fashion, and can be clearly seen propagating into the ocean [*Jenkins*, 1998]. The ability to replicate this observation would prove a critical test of any ocean circulation model performance. However, a significant limitation to the utility of tritium observations in ocean circulation models is our imperfect knowledge of the time history of surface water concentrations. Gorgonian corals have the potential to provide a detailed time history of surface water tritium concentrations at a variety of locations.

Bermuda has the most complete record of surface ocean tritium measurements, having data ranging from 1968 through to 1988 [e.g., *Jenkins*, 1998]. It was for this reason, and because gorgonian corals were so abundant there, that Bermuda was chosen as the sampling site for this project.

The aims of this chapter are to investigate whether the tritium concentrations measured within the gorgonin of the coral skeleton reflect the surface water tritium concentrations over the time period the skeleton was accreted. This aim is addressed in two ways. Firstly, by collecting water samples at each gorgonian coral sample site; the tritium signal in the water sample should reflect the tritium signal in the most recently formed skeletal material, and secondly, by comparing the gorgonian tritium time series results to the tritium surface ocean record measured between 1968 and 1988 at Bermuda.

Tritium has never previously been measured in gorgonian corals. This chapter describes the techniques that have been developed to reconstruct surface ocean tritium measurements using gorgonian coral skeletons.

5.2 Methods - Sampling

5.2.1 Sample collection

Coral samples were collected as described in Chapter 2, section 2.2. Samples were selected for tritium time series work that were long-lived, displayed clear banding patterns and contained no skeletal degradation (Table 5.1). Surface water samples were taken at each coral collection site and prepared for analysis following the procedure described in section 5.4.1.1.

Sample	Species	Location	Latitude and Longitude	Date	Depth (m)	Notes
2-1st	*Pseudoplexaura porosa*	Crescent Reef	N32°24.05 W064°47.95	7/12/2000	5	Tritium time series 3
2-2nd	*Pseudoplexaura porosa*	Bailey's Bay Flats	N32°21.73 W064°44.84	27/09/2001	6	Tritium time series 2
3-2nd	*Plexaurella dichotoma*	Bailey's Bay Flats	N32°21.73 W064°44.84	27/09/2001	6	Tritium time series 4
1-3rd	*Pseudoplexaura porosa*	Bailey's Bay Flats	N32°21.73 W064°44.84	11/10/2002	4	Tritium time series 1
4-3rd	*Pseudoplexaura porosa*	Bailey's Bay Flats	N32°21.73 W064°44.84	18/10/2002	7	Tritium time series 5

Table 5.1 Details of all gorgonian samples used for tritium work.

5.2.2 Band counting

The banding present in the organic gorgonin axial skeleton was used to give a chronology to the tritium measurements. The colony base and thicker branch sections were divided into slices ~0.5 cm thick using a band saw. Thin sections were prepared as described in Chapter 2, section 2.3.3 from a selection of coral slices from each skeletal area (i.e. base, lower branch or upper branch). Thin sections were then examined under microscope using transmitted and reflected light. A series of band counts were performed (at least eight per section) along a variety of growth radii. Errors for band counts equalled 4 bands per section as the number of bands differed by a maximum of four depending on growth radii selected. To investigate whether it was easier to perform band counts on larger, more visible sections a series of collages were made from photos taken of sections under magnification. These photo collages were used to plan and map out sampling strategies for each time series.

5.2.3 Gorgonin sampling techniques

Two techniques were used to sample material on a band per band basis for the tritium measurements. For both techniques the surface of each ~0.5 cm thick slice was highly polished so growth bands were clearly visible under magnification.

The first sampling technique involved shaving the outermost growth band from each polished slice using a scalpel whilst viewing the section under microscope. Shavings were transferred using tweezers to a pre weighed pot. Reweighing the pot once a band had been extracted determined the mass per band per slice. The corresponding band was extracted from the next slice and so on, the material from each slice was then combined to achieve a total mass per band for a particular year of growth. The sampled material was dried over night in a 40ºC nitrogen atmosphere oven and reweighed.

The second sampling technique used a dentist drill mounted with a microscope to drill material from each growth band. The inner edge of the band to be sampled was marked out using the smallest drill bit possible (~100 µm diameter) then the band was sampled by milling from the outer edge of the band inwards. The material drilled was collected on weighing paper and transferred to a pre weighed pot. The material was then treated as outlined above.

5.3 Methods – Exchange technique preparation

5.3.1 Background

The skeletal chemistry, specifically the amino acid composition, of the axial skeleton for a variety of gorgonian species is remarkably similar considering their morphological differences [*Goldberg*, 1976]. Axial skeleton gorgonin contains collagen-like amounts of glycine, proline and hydroxyproline [*Smanzt-Froelich*, 1974; *Goldberg*, 1974, 1976; *Leversee*, 1980].

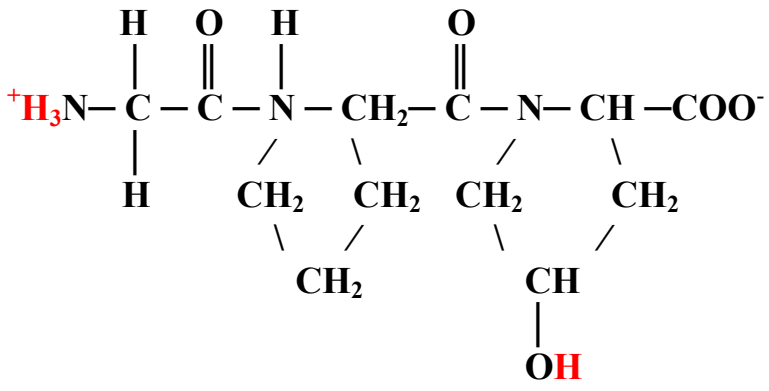

Figure 5.1 Simplified collagen primary structure (glycine-proline-hydroxyproline) showing exchangeable hydrogen sites.

Although carbon-bound hydrogen is conservative and non-exchangeable [e.g., *Schimmelmann*, 1991], it is possible that some of the hydrogen within the collagenous matrix may be susceptible to isotopic exchange with ambient water hydrogen after skeletal accretion. The protons most susceptible to such exchange are situated at the termini of the collagen chain (attached to the amino and carboxyl groups) and on the hydroxyl group of the hydroxyproline side chain (Figure 5.1). These protons may have exchanged with ambient water hydrogen since biosynthesis and thus need to be removed so the tritium levels measured reflect actual, historical tritium concentrations.

5.3.2 Verifying exchange is necessary

A series of bulk (4 x 10 g coral) samples were used to test the extent of contamination present due to the exchange of hydrogens outlined above. Bulk samples were sealed for tritium analysis from branch sections adjacent to the base of *Pseudoplexaura porosa* (sample 2-1st). Band counts on thin sections from the sampled branch material revealed an average of 43 bands. Assuming bands are annual, the bulk material sampled should contain the Bermudian surface water tritium signal from 1958-2000 decay corrected to the present (predicted from Figure 5.2 as ~1.06 TU).

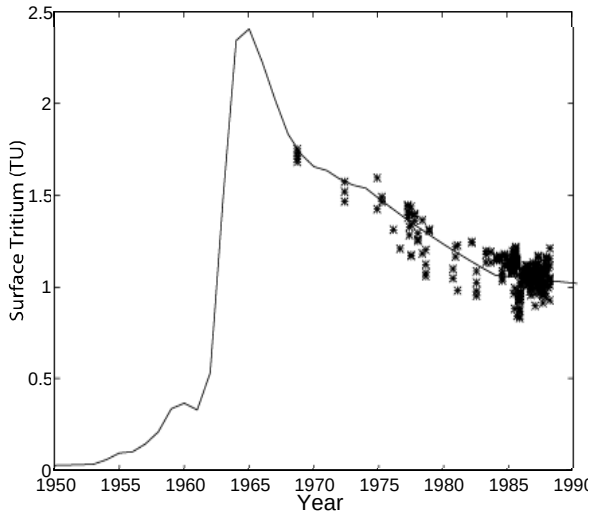

Figure 5.2 Box model estimate (line) of surface tritium concentrations in North Atlantic [*Dreisigacker and Roether,* 1978] compared to actual observations [e.g., *Jenkins,* 1998] decay corrected to 2000.

Two samples were treated to remove exchangeable hydrogen (as described in section 5.5.1) and two samples remained untreated. The data obtained from this experiment (Table 5.2) confirm that extraneous contamination is substantial and needs

to be removed. Samples that did not undergo treatment had tritium concentrations of up to 16 TU compared to the exchanged sample with a concentration within errors to 1 TU. Tritium values for the unexchanged samples are dramatically larger than seawater tritium values, the tritium contamination is also in excess of background water vapour levels (ambient water vapour at Bermuda ~2-3 TU and in England ~5-6 TU). The high levels of tritium contamination in the unexchanged samples may have come from luminous dials on diving equipment. These early results illustrated how important the exchange step would be in getting a clear, representative tritium time series from a gorgonian coral skeleton.

Sample	^{3}H in TU
Unexchanged sample 1	16.82 ±1.101
Unexchanged sample 2	7.42 ±0.511
Exchanged sample 3	Sample failed
Exchanged sample 4	<0.090

Table 5.2 Tritium concentrations for exchange test samples.
Where a result is preceded by '<' then the tritium signal present is lower than the detection limit, the number quoted (appendix 5.1).

5.3.3 Ideas behind exchange method

In an attempt to remove all hydrogen susceptible to exchange, each sample is reacted with tritium free sodium hydroxide (NaOH) to deprotonate the exchangeable groups. Then the gorgonin is for some samples, reacted with a tritium free phosphoric acid (H_3PO_4) solution, and for all samples, flushed with a large amount of tritium free water to re-protonate the exchangeable hydrogen sites, this time with hydrogen that does not contain any tritium.

To calculate the concentrations of reagents needed, the pK_a for each amino acid was investigated (Table 5.3).

Amino Acid	pK_a values		Source:
	α-carboxyl	α-amino	
Glycine	2.35	9.78	*Dawson et al*. [1969]
Proline	2.95	10.65	*Dawson et al*. [1969]
Hydroxyproline	1.82	9.66	*Smith et al*. [1942]

Table 5.3 pK_a values for collagen amino acids.

Table 5.3 shows that above pH 3 and below pH 9 these amino acids will be in the carboxylate and ammonium ion form (e.g., for glycine: $H_3N^+CH_2COO^-$). If pH < pK_a then the exchangeable groups will exist in the protonated form: COOH and N^+H_3. If pH > pK_a then the exchangeable groups will exist in the deprotonated form: COO^- and NH_2. Therefore, tritium free NaOH needed to be sufficiently strong to achieve a pH more basic than 10 to remove exchangeable Hs from the amino groups. The sample is then flushed with enough tritium free water to reach a neutral pH and to re-protonate the groups with Hs that are tritium free. This tritium free water flushing step should re-protonate any groups that sit in the protonated state at pH 7. To ensure the carboxylic acid groups are reprotonated with tritium free Hs, the pH would need to be decreased to below 2. However, when I experimented with the addition of a tritium free phosphoric acid step, for some samples there was obvious degradation of the collagenous matrix, I decided to include this step only for some samples (exchange technique test acid samples and time series 5).

This exchange technique is based on a hydrogen exchange method for hydroxyl groups in cellulose developed by *Feng et al*. [1993]. Adaptations to this technique were carried out in collaboration with Rachel Stanley and Sheila Stark [e.g., *Stark*, 2003; *Stark et al*., 2005].

5.4 Methods – Preparation of tritium free reagents for exchange

5.4.1 Tritium free water

5.4.1.1 Sampling procedure

In order to make tritium free reagents a supply of tritium free water was required. Tritium free water was collected from Calypso Soft Drinks Ltd. in Wrexham, North Wales and from St Mary's County Metropolitan Commission in Maryland, USA. In Wrexham, the tritium free water is sourced from spring water from the Lincolnshire limestone beds underneath the drinks factory. This water has been radiocarbon dated to 4938 years. The Maryland tritium free water is sampled from the 'Aquia' aquifer, which supplies drinking water to St Mary's County. This water has been radiocarbon dated to at least 30,000 years [*Aeschbach-Hertig et al*., 2002].

Glass bottles (1 litre) with polypropylene caps were used for tritium free water collection and storage. Prior to use the bottles are baked at 200°C overnight under an argon atmosphere to remove adsorbed water. The caps were evacuated to 1 x 10^{-3} torr

and filled with argon. The argon filled bottles were cooled to room temperature, capped, and sealed under tension with electrical tape.

Water was introduced to the bottles at a low flow rate leaving a 2 cm headspace. The bottles were kept vertical at all times during filling to maintain an argon layer over the water to help prevent contamination. To verify this water was tritium free, several samples from Wrexham and Maryland were degassed and analysed (section 5.6.2).

5.4.2 Tritium free reagents

Methods were researched and refined to produce tritium free sodium hydroxide (NaOH) and tritium free phosphoric acid (H_3PO_4) using tritium free water and reagents that contained no hydrogen.

5.4.2.1 Preparing a tritium free sodium hydroxide solution

The method to synthesise tritium free NaOH was adapted from *Cornog* [1921]. Following experimentation, it was decided that a solution of 14-17% NaOH was strong enough to obtain the pH required for the exchange reaction. Approximately 70 g of sodium were added to 900 ml tritium free water to achieve the desired concentration.

All glassware used in the procedure was pre baked at 40°C overnight in a nitrogen atmosphere to remove any traces of water. 900 ml of tritium free water were transferred to a 1500 ml separatory funnel under an argon atmosphere. Enough anhydrous ethyl ether (<0.08% water) was added to the separatory funnel to form a layer ~6 cm thick above the water. The two liquids were mixed by shaking whilst carefully releasing pressure and then left to settle out under an argon atmosphere. In an argon filled glove box metallic sodium was cut into small (~1 cm^3) pieces using a chisel and Stanley knife. Several pieces were placed in a crystallising dish filled with paraffin and transferred to the fume cupboard. Each piece of sodium was carefully blotted using low lint content paper towels and then added to the separatory funnel using tweezers. The sodium remains suspended in the ether layer and slowly reacts with any water present to form sodium hydroxide, which passes through to the water layer below. Using an ether layer prevents the highly exothermic results usually observed when metallic sodium reacts directly with water. *Cornog* [1921] remarked that as long as the ether layer was 3-4 times the diameter of the sodium pieces the reaction proceeded safely. More pieces of sodium were added (maximum of 3 pieces reacting at one time) and the ether layer topped up as required. The addition of an argon supply to the

separatory funnel increases the safety of the reaction and minimises potential contamination from water vapour. Figure 5.3 shows the experimental set up for the synthesis of tritium free NaOH.

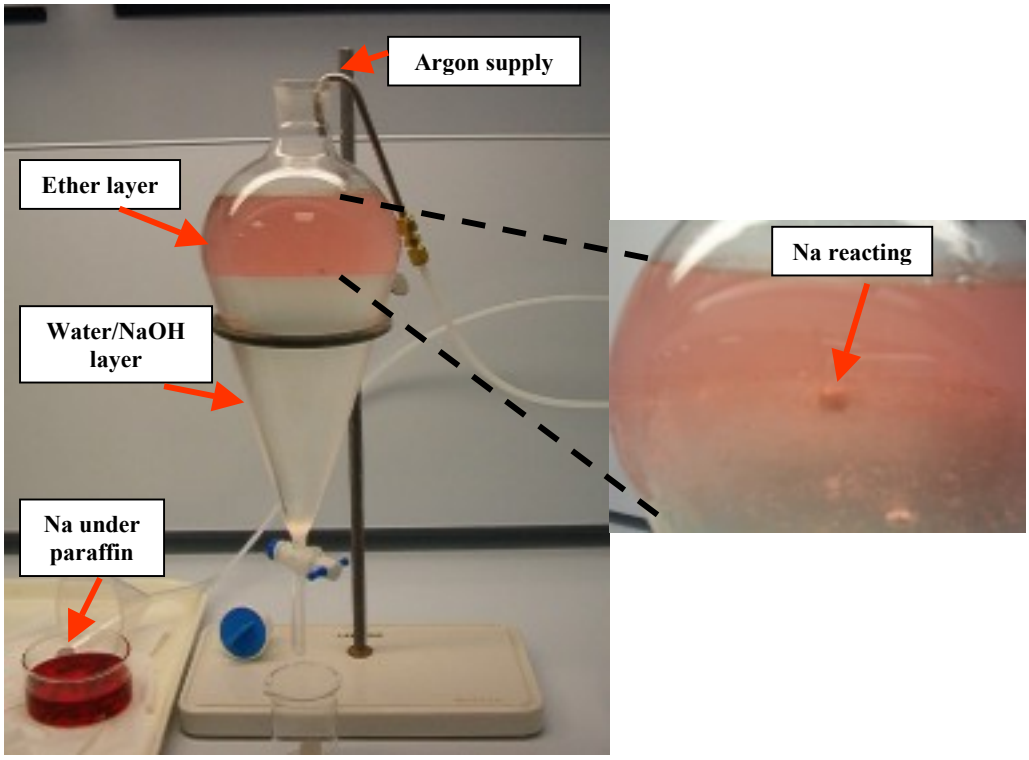

Figure 5.3 Experimental set up used for tritium free NaOH synthesis.

With time the ether layer turned pink as the paraffin coating the sodium was red in colour. When all the sodium had been added, the NaOH was drained into a pre weighed, argon filled 1 litre round bottomed flask. To remove any traces of ether, the flask was placed under an argon atmosphere in a spark-free heating mantle and the NaOH solution boiled for 25 minutes. The NaOH was then left to cool, still under argon. The strength of the NaOH solution was checked by titrating against 1M HCl using phenolphthalein as indicator. If the NaOH was too strong, it was diluted using tritium free water and if too weak, it was boiled further to concentrate the solution. Tritium free NaOH was transferred, in an argon atmosphere, to pre baked, argon filled bottles (prepared as described in section 5.4.1.1) for storage.

5.4.2.2 Tritium free sodium hydroxide test solution

Due to the time consuming and dangerous nature of the method for synthesising tritium free sodium hydroxide described above, I decided to test another method. I wanted to see how contaminated, with respect to tritium, a solution of NaOH would be if it were made simply using NaOH pellets and tritium free water in an argon atmosphere. To produce 1 litre of ~17% NaOH, 170 g of NaOH pellets were added to 1 litre of tritium free water in an argon filled glove box. The solution was swirled until the pellets had dissolved, transferred to an argon filled bottle (prepared as described in section 5.4.1.1) and allowed to cool under argon.

5.4.2.3 Preparing a tritium free phosphoric acid solution

Tritium free H_3PO_4 was made by reacting phosphorus pentoxide (P_4O_{10}) with tritium free water:

$$P_4O_{10} + 6H_2O \rightarrow 4H_3PO_4$$

(Equation 5.1)

To make 800 ml of H_3PO_4, ~135 g of P_4O_{10} were added to 800 ml of tritium free water. The reaction was carried out in a glove box that was continuously purged with a high flow rate of argon. The glove box was placed inside a fume cupboard so the acid fumes produced were safely vented. Tritium free water was transferred to a beaker and the P_4O_{10} powder added using a metal spoon (~5 ml). 40-45 spoonfuls were added in total and after every 4^{th} addition a break was taken to allow the acid fumes to vent from the glove box. Tritium free H_3PO_4 was transferred to an argon filled 1 litre bottle (prepared as in section 5.4.1.1), cooled under argon and capped and taped for storage. The strength of the acid was determined by titration against the tritium free sodium hydroxide solution using phenolphthalein as indicator.

5.5 Methods – The exchange

5.5.1. Exchanging coral samples

Coral material to be exchanged was dried overnight in a nitrogen oven at 40ºC. The sample was then transferred to an Erlenmeyer flask in an argon filled glove box and enough tritium free NaOH added to cover the sample. The sample was mixed using a stir bar and plate under argon for 3 hours (Figure 5.4) at which time the flask was capped, taped and left to exchange for a further 24 hours

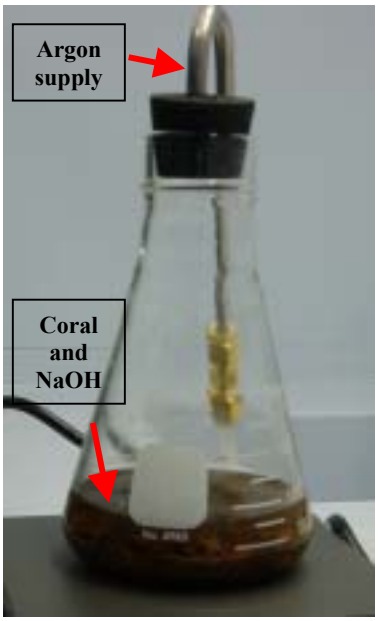

Figure 5.4 Gorgonin undergoing exchange with tritium free NaOH in an argon atmosphere.

.

If the acid step of the exchange was included (for exchange test acid samples and tritium time series 5), tritium free H_3PO_4 would be added, under an argon atmosphere, to the solution at this stage and the pH checked before leaving the solution to stir under argon for 30 minutes longer. The flask was then transferred to an argon filled glove box where the coral and exchange solution were decanted into a polypropylene centrifuge bottle. The flask was rinsed thoroughly with tritium free water to ensure minimal loss of coral material and the rinsings transferred to the centrifuge bottle. The coral and exchange solution were centrifuged at 2500 rpm for 5 minutes. The supernatant was decanted to waste, the centrifuge bottle refilled with tritium free water and shaken thoroughly before centrifuging at 2500 rpm again for 5 minutes. This washing procedure was repeated five times and the pH of the supernatant checked each time, the aim to remove all traces of acid and base. After the last rinse, if the pH was satisfactory (pH ~7), most of the water was decanted and the remaining coral and solution filtered. It was possible to process a maximum of four samples at one time.

5.5.2 Transferring coral sample to bulb

Coral sample bulbs (250 ml volume) were manufactured from Corning 1720 glass, which has extremely low helium permeability [*Clarke et al.*, 1976]. Before use, sample bulbs were baked overnight at 625°C in a helium-free nitrogen atmosphere to remove dissolved helium. Coral sample bulbs have a wide capillary to facilitate the insertion of a solid sample. Coral was transferred from the glass scinter of the filter apparatus to the neck of a pre weighed sample bulb using tweezers. The coral was then pushed down the capillary using a syringe needle. Tritium free water was introduced using a syringe to flush the capillary. The amount of water added to each sample was recorded. This procedure of sample transferral was very time consuming (60 minutes per gram of material) especially when processing four samples simultaneously, so the glove box was continually purged with a high flow rate of argon to prevent contamination from water vapour in the laboratory atmosphere. Following sample transfer the bulb was covered with parafilm and weighed before connection to the vacuum manifold for sample degassing.

5.6 Methods – Sample degassing and sealing

5.6.1 Degassing coral samples

Bulbs containing coral samples were connected to a dedicated vacuum manifold (Figure 5.5) using Viton o-ring couplings.

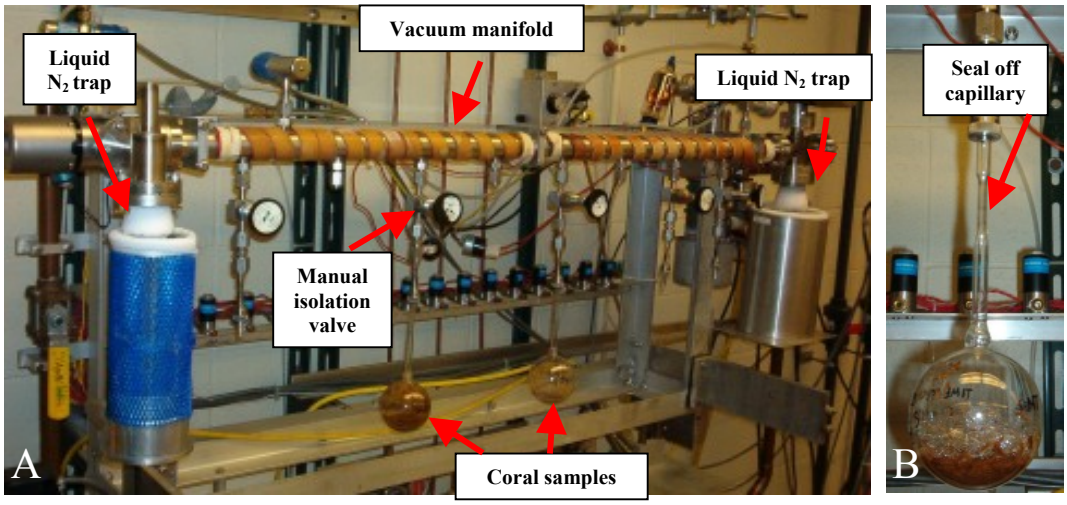

Figure 5.5 Degassing of coral samples.
(A) Vacuum manifold for degassing of coral samples. (B) Sample bulb containing coral and showing seal off capillary.

Samples were opened to a rough pump using the manual restriction valves above each sample bulb and the headspace pumped through a liquid nitrogen water trap. When pressure surges were sufficiently low (1×10^{-3} torr) the manifold was transferred to a diffusion pump. When degassing samples containing a significant amount of water ($\geq$ 10 ml), drying was hastened by submerging sample bulbs in a warm water bath. Care had to be taken not to completely freeze dry the samples as water vapour is needed to ensure good gas transfer when measuring samples on the mass spectrometer [*Postlethwaite*, 2002]. Samples were evacuated to a pressure of $< 1 \times 10^{-7}$ torr and flame sealed whilst still open to the diffusion pump to minimise helium contamination caused by heating glassware during sealing. The sealing time was recorded and the sample bulbs reweighed to calculate the wet sample weight. Sample bulbs were stored in vacuo, underground in a freezer, the cold temperature minimises helium permeation through the glass walls [*Clarke et al*., 1976]. Samples were left to decay for 12 months before mass spectrometric analysis of ^{3}He grown in from ^{3}H decay.

5.6.1.1 Sealing wide capillary sample bulbs

Sealing of the wider capillary bulbs required substantial skill. The glass needed to be heated thoroughly and evenly prior to focusing in on the required sealing area, if you focus in too quickly or on one area of the capillary for too long, the glass collapses in and, due to the width of the capillary, the opposite side is too far away for the glass to fuse so the vacuum and seal is lost. I had most problems with sealing following the start of a new batch of glassware; I failed to seal the first three sample bulbs from this batch (total sealing failure rate = 6%). When this happened, the sample in question would be flooded with argon, removed from the manifold, covered with parafilm and taken back to the argon filled glove box to be re-exchanged with tritium free water, re-stuffed into a new bulb, degassed and sealed.

5.6.2 Degassing liquid samples

To determine the tritium content of liquid samples, the samples are first degassed. The degassing procedure works by removing any gases present in the sample. The sample is then sealed under vacuum and after a period of storage, the in-growth of ^{3}He produced by tritium decay is measured. Liquid samples were degassed for tritium analysis on a vacuum manifold (Figure 5.6). Prior to degassing, to remove any ambient water vapour and to check for leaks, the degassing line was diffusion

pumped to at least 5 x 10^{-7} torr. Around 500 g of sample was transferred from the glass sample collection bottles under an argon blanket into pre weighed, 1 litre alumino-silicate glass bulbs. Sample bulbs were manufactured from glass (Corning 1720) and were treated prior to use as described in section 5.5.2. After sample transfer, flow-restricting valves above each sample were closed and the headspace above each sample pumped for 5 minutes through a liquid nitrogen water trap. The degassing sections were isolated and all samples shaken for 30 minutes to enhance gas transfer across the water/headspace interface. The pump/shake cycle was repeated at least seven times, first pumping on a rough pump and when pressure surges were sufficiently low, transferring to a diffusion pump. Samples were flame sealed at a pressure of less than $1x10^{-7}$ torr whilst still open to the diffusion pump to minimise the helium contamination caused by heating glassware during sealing. Sealing times were recorded and the sample bulbs reweighed to calculate sample weights. Samples were stored in vacuo, underground and left for at least six months before mass spectrometric analysis.

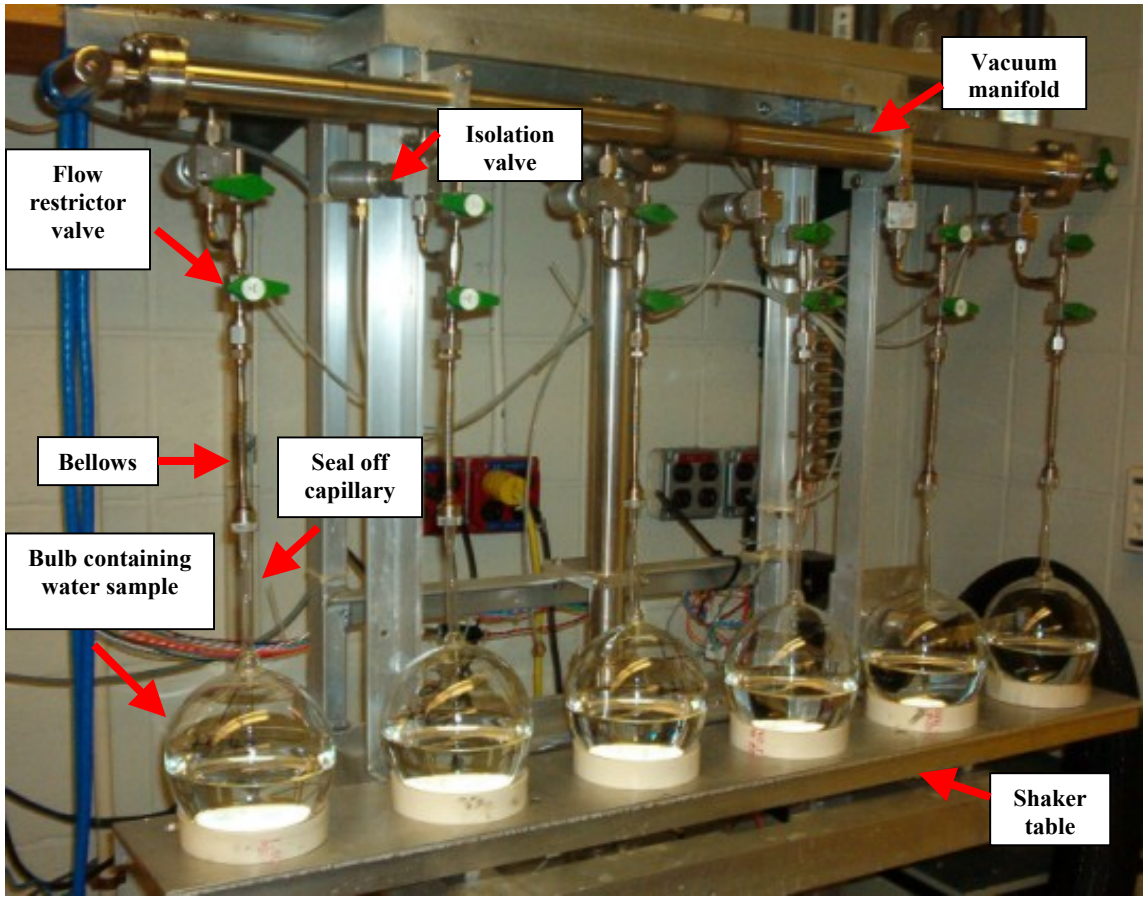

Figure 5.6 The degassing line at WHOI used for liquid samples.

5.7 Methods – Tritium sample analysis

5.7.1 Sample transfer

Following the helium in-growth period and prior to analysis, tritium sample bulbs are loaded onto a rotary shaker table and gently shaken for ~8 hours in order to ensure equilibrium of the helium between the water and headspace.

To allow automated processing of samples, they are transferred to stainless steel containers with pneumatic valves ('bunnies', Figure 5.7). Sample bulbs are attached using Viton o-ring couplings to a vacuum system transfer line, eight samples can be transferred at one time. Empty 'bunnies' are connected with VCR copper gaskets and the system is evacuated to less than 1 x 10^{-6} torr. The 'bunnies' are cooled with liquid nitrogen, the sample bulb nubs broken and the sample head-space gases transferred across. The 'bunnies' are then closed and moved to the mass spectrometer manifold for automated processing of the samples.

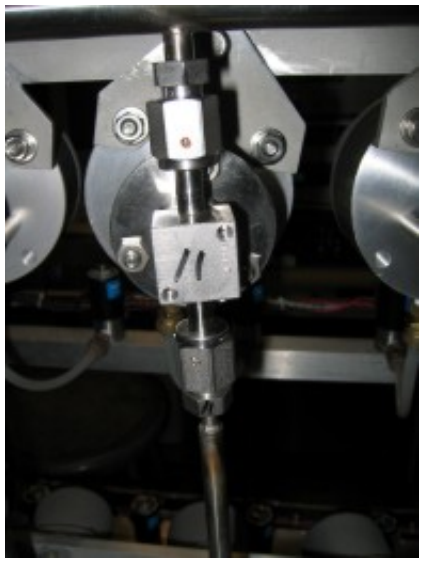

Figure 5.7 Samples are transferred to 'bunnies' to enable automated processing on the mass spectrometer.

5.7.2 Sample processing and analysis

During sample processing gases are progressively purified using four cryogenic traps at decreasing temperatures. The ultra high vacuum in the low temperature cryotrap, the magnetic sector mass spectrometer and the quadrupole mass spectrometer is maintained using ion pumps. The whole system is controlled using a Pentium based PC.

The sample processing line is isolated and the 'bunny' valve opened introducing the sample to the cold-water trap (cooled with liquid nitrogen to 180-250°K), which eliminates water vapour from the sample. At this point the pressure in the processing line is monitored and if above a critical level, sample processing would be aborted. Next, the sample is drawn through a high temperature cryotrop (activated charcoal operated at 60°K), this trap removes all gases but neon and helium. Following a second pressure check, helium and neon are drawn onto the surfaces of a low temperature cryotrap (activated charcoal operated at 10-15°K). The low temperature trap is then isolated and warmed to 40°K at which temperature the helium will be released and the neon retained. An aliquot of the sample is introduced into the mass spectrometer (QMS, Balzers Model QMG-112) for helium isotope analysis.

5.7.3 Air standards and blanks

Samples are calibrated against air standards that are treated in the same way as the samples except that air standards are not processed through the water trap. Air standards are prepared by collecting marine air whilst recording temperature, pressure and relative humidity. Measurements of air standards are interspersed with samples and standard curves are determined on a weekly basis.

Line blanks are run every three hours during sample analysis to determine the magnitude of the blank signal in the machine so it can be corrected for. Manifold blanks are run before the analysis of a sample group to check for leaks in the sample manifold. Processing of the samples is aborted if the manifold blank is above a specified level.

5.8 Methods - Calculating tritium

5.8.1 Calculating coral sample mass

Due to the number of transfer steps involved in the exchange procedure and associated sample losses, coral sample masses could not be accurately ascertained until after mass spectrometric analysis. Following analysis, samples were weighed and dried thoroughly in an oven at 50ºC. The dry gorgonin was removed from the sample bulb, which was then cleaned, dried and re weighed to determine the mass of coral for each sample.

5.8.2 Calculating mass of liquid associated with each sample post seal off

Most of the tritium free water used to wash the coral material down the capillary and into the bulb was pumped away during the degassing procedure but the samples were sealed wet to ensure good gas transfer at the analysis stage. The mass of liquid retained in each sample is calculated using Equation 5.2. Each sample is weighed post seal off with the glass nub to give the total mass (M_T). The sample mass (M_c) is calculated as described in section 5.8.1. The empty glass bulb is weighed prior to stuffing to give M_b enabling the calculation of M_l.

$$M_T = M_c + M_b + M_l$$

(Equation 5.2)

M_T = *total mass*
M_c = *mass of coral sample*
M_b = *mass of glass bulb*
M_l = *mass of liquid*

5.8.3 Corrections applied to data

5.8.3.1 Degassing correction

During degassing a certain mass of water is pumped away for each sample (Table 5.4). Preferential evaporation of lighter isotopes causes fractionation of hydrogen in the water molecules and hence, a slight tritium enrichment in the remaining water [*Clarke et al*., 1976]. This must be corrected for in the final calculations. The fractionation factor (α) for this evaporation is 1.15 ±0.02 at 20°C [*Clarke et al*., 1976] for water. As the specific fractionation factor for the reagents is unknown it was assumed to be the same as for water. The correction is calculated from Equation 5.3 and displayed for each sample type in Table 5.4.

$$\frac{W + \frac{W_E}{\alpha}}{W + W_E}$$

(Equation 5.3)

W = *mass of water retained in sample*
W_E = *mass of water removed from sample*
α = *fractionation factor*

Sample	W	W_E	Correction
Tritium free water	364.43	3.76	0.999
Seawater	382.48	3.06	0.999
Reagents	443.17	1.77	0.999
Gorgonin	1.84	15.36	0.880

Table 5.4 Degassing corrections for samples.

5.8.3.2 Liquid correction

As noted in section 5.8.2, a certain mass of tritium free water is associated with the sealed coral sample. The mass of this liquid can be calculated using Equation 5.2 and then is corrected for, as it will contribute to the tritium signal of the sample.

5.8.4 Calculating tritium from measured helium

The amount of tritium present in a given sample is calculated from measured ^{3}He using the radioactive decay equation (Equation 5.4)

$$N = N_o e^{-\lambda t}$$

(Equation 5.4)

N = *non decayed tritium*
N_o = *initial tritium in sample before decay*
t = *amount of time tritium has been left to decay*
λ = *decay constant*

Therefore $N_o - N =$ the decayed tritium in the sample and hence the tritiugenic ^{3}He measured by the mass spectrometer in cm^3 (Equation 5.5).

$$N_o = \frac{^3He}{1 - e^{-\lambda t}}$$

(Equation 5.5)

$$\lambda = \frac{\ln 2}{t_{1/2}}$$

(Equation 5.6)

$t½$ = *half life of tritium*

The half-life of tritium is equal to 4500 days [*Lucas and Unterweger*, 2000].

The volume of tritiugenic helium present in each sample is converted into cm^3 of tritium using Equation 5.7.

$$N_o = \frac{^3He}{1 - e^{-\ln 2.t/4500}}$$

(Equation 5.7)

Low level tritium measurements are normally expressed in tritium units (TU). 1 TU is equivalent to 1 ^3H atom per 1 x 10^{18} ^1H atoms. In order to convert cm^3 to TU the volume of tritium in cm^3 is divided by 22.4 x 10^3 (the volume 1 mole of gas occupies at STP) to give tritium in moles. This is then divided by the amount of hydrogen in moles present in the sample. As the exact structure of gorgonin is unknown, collagen is used in its place (section 5.3.1). Moles of hydrogen are calculated using Equation 5.8 where for reagents or water their respective relative molecular mass (RMM) would be used.

$$^1H\,(mol) = \left(\frac{sample\ mass}{RMM\ collagen}\right) x \quad unexchangeable\ hydrogens$$

(Equation 5.8)

Finally the amount of tritium in the sample in TU is given by Equation 5.9.

$$Tritium\,(TU) \quad = \quad \frac{^3H(mol)}{^1H(mol)}\, x\, 10^{18}$$

(Equation 5.9)

5.9 Results and Discussion - Liquid samples

5.9.1 Tritium free water

The results calculated for tritium free water from Wrexham and Maryland are shown in Table 5.5.

Sample	Tritium (TU)	Notes
Wrexham samples:		
Wrexham 1	0.007±0.0009	
Wrexham 2A	0.004±0.0005	
Wrexham 2B	0.008±0.0007	
Wrexham 3A	<0.001±0.0000	
Wrexham 3B	0.003±0.0000	
Wrexham 4A	0.008±0.0113	
Wrexham 4B	0.013±0.0005	
Wrexham 5	0.005±0.0103	
Wrexham 6	<0.006±0.0125	
Wrexham 7	0.008±0.0057	
Wrexham 8	0.009±0.0091	
Wrexham 9	0.005±0.0081	
Tritium free test 1	<0.009±0.0124	Half of bottle used and stored
Tritium free test 2	<0.006±0.0178	Half of bottle used and stored
Tritium free test 3	0.007±0.0002	Half of bottle used and stored
Wrexham average	*0.007*	
Maryland samples:		
Aquia 1	0.009±0.004	
Aquia 2	0.011±0.006	
Aquia 3	0.014±0.006	
Aquia 4	0.008±0.004	
Aquia 5	0.005±0.004	
Aquia 6	0.010±0.008	
Aquia 7	0.008±0.006	
Aquia test	<0.002±0.004	Bottle opened under argon and then stored
Aquia average	*0.008*	
Patapsco 2	0.009±0.006	New Maryland source
Patapsco 3	0.013±0.006	New Maryland source

Table 5.5 Tritium free water results measured by helium in-growth.

Where a result is preceded by '<' then the tritium signal present in that sample is lower than the detection limit, the number quoted (appendix 5.1). The tritium free water results show that the Wrexham and Maryland water is tritium free to as good a detection limit as is currently possible. 'Tritium free test 1,2,3' and 'Aquia test' were samples degassed after the sample bottle had been opened under argon, some of the water used and then recapped and sealed followed by a period of storage. This is an important test as it replicates how the water was used during the exchange procedure. Results for these samples indicate that this process does not contaminate the samples with respect to tritium.

5.9.2 Tritium free reagents

After synthesis and some use, reagents were degassed, sealed and stored in vacuo (section 5.6.2). It was important to know how much tritium the ideally 'tritium free' reagents contained. Results for NaOH, test NaOH and H_3PO_4 are shown in Table 5.6.

Sample	Tritium (TU)	Notes
NaOH samples:		
Zoe NaOH	0.135 ± 0.021	
NaOH SOC 1	0.091 ± 0.003	
NaOH SOC 2	0.130 ± 0.005	
NaOH WHOI 1	0.039 ± 0.006	Used argon atmosphere
NaOH WHOI 2	0.061 ± 0.015	Used argon atmosphere
NaOH 20/02/04	0.069 ± 0.009	Used argon atmosphere
NaOH 13/04/04	0.043 ± 0.006	Used argon atmosphere
NaOH test samples:		
NaOH test 1	0.791 ± 0.016	Made using NaOH pellets
NaOH test 2	0.780 ± 0.011	Made using NaOH pellets
H_3PO_4 samples:		
H_3PO_4 SOC 1	0.307 ± 0.057	
H_3PO_4 SOC 2	0.204 ± 0.032	
H_3PO_4 26/03/04	0.238 ± 0.009	
H_3PO_4 10/03/04	0.300 ± 0.008	

Table 5.6 Results for tritium free reagents NaOH, test NaOH and H_3PO_4 measured by helium in-growth.

For the tritium free NaOH samples, those reagents made after the addition of an argon source to the separatory funnel (see Figure 5.3) have lower levels of tritium than those made before the technique was modified. The addition of the argon atmosphere also improves the safety of the technique; purging the flammable ether fumes from the separatory funnel and preventing water vapour from reacting with the metallic sodium pieces as they are added to the reaction vessel.

As the synthesis of tritium free NaOH is a dangerous and time consuming procedure, I investigated the simpler, alternative method of dissolving NaOH pellets in tritium free water under an argon atmosphere. Unfortunately, the results show that this 'NaOH test' has more than 10 times as much tritium as the traditionally made 'tritium free NaOH' and thus this is not a viable substitute technique.

Phosphoric acid has higher levels of tritium than NaOH, however the acid was only used for some of the coral exchanges (see section 5.3.3). It is apparent that both reagents have elevated tritium concentrations in comparison with the tritium free water (~0.008 TU). Contamination for NaOH is probably from the paraffin that coats the

sodium pieces. However, during NaOH synthesis, only the ether layer turned pink (Figure 5.3) and not the water/NaOH layer. For H_3PO_4, contaminants present within the matrix of the P_4O_{10} could explain the high tritium levels and this is unfortunately unavoidable. Other tritium contamination sources for both reagents might be from water vapour in the laboratory atmosphere. Although reagents were always opened and dispensed within the argon filled glove box, continual transfer of lab equipment into and out of the glove box means some air could potentially enter this argon atmosphere. Purging the glove box for longer and at higher flow rates following any transfer should reduce this source of contamination.

5.9.3 Seawater samples

At each gorgonian coral sample site a seawater sample was taken. Table 5.7 shows the tritium results for seawater sampled at the surface during this project and also for two precipitation samples collected during a period of heavy rainfall. Surface water values of the inshore reefs vary from 0.609 ±0.006 TU to 0.921 ±0.008 TU and compare well with other surface seawater values measured in the area (e.g. Figure 5.2).

Sample	Sample site Latitude and Longitude	Date collected	Tritium (TU)
Castle Harbour 1	32º20.40N, 064º41.90W	04/DEC/2000	0.900 ±0.033
Castle Harbour 2	"	04/DEC/2000	0.869 ±0.037
Whalebone Bay 1	32º21.90N, 064º42.85W	04/DEC/2000	0.805 ±0.051
Whalebone Bay 2	"	04/DEC/2000	0.632 ±0.036
Bermuda Precipitation 1	N/A	10/DEC/2000	1.474 ±0.069
Bermuda Precipitation 2	N/A	10/DEC/2000	1.218 ±0.090
Bailey's Bay Flats 1	32°21.73N, 064°44.84W	27/SEP/2001	0.617 ±0.018
Tyne's Bay 1	"	30/SEP/2001	0.767 ±0.022
South Shore Kate 1	32°19.64N, 064°41.14W	14/OCT/2002	0.721 ±0.011
South Shore Kate 2	"	14/OCT/2002	0.609 ±0.006
Bailey's Bay Flats 1A	32°21.73N, 064°44.84W	15/OCT/2002	0.612 ±0.013
Bailey's Bay Flats 1B	"	15/OCT/2002	0.716 ±0.012
Bailey's Bay Flats 2A	"	15/OCT/2002	0.673 ±0.013
Bailey's Bay Flats 2B	"	15/OCT/2002	0.673 ±0.010
Crescent Reef 1A	32°24.05N, 064°47.95W	16/OCT/2002	0.730 ±0.014
Crescent Reef 1B	"	26/OCT/2002	0.717 ±0.013
Bailey's Bay Flats 3A	32°21.73N, 064°44.84W	22/OCT/2002	0.724 ±0.011
Bailey's Bay Flats 3B	"	22/OCT/2002	0.672 ±0.012
Bailey's Bay Flats 4A	"	22/OCT/2002	0.818 ±0.013
Crescent reef 2A	32°24.05N, 064°47.95W	19/OCT/2003	0.849 ±0.009
Crescent reef 2B	"	19/OCT/2003	0.885 ±0.007
Crescent reef 3A	"	21/OCT/2003	0.906 ±0.008
Crescent reef 3B	"	21/OCT/2003	0.921 ±0.008

Table 5.7 Results for seawater samples measured by helium in-growth.

5.10 Results and Discussion - Gorgonian coral samples

5.10.1 Samples prepared and sealed for analysis

A list of all coral samples prepared and sealed for tritium analysis are displayed in Tables 5.8 and 5.9. Unfortunately, data are not available for all samples. Some samples were lost due to cracking and shattering of the glassware housing the coral samples, whilst some samples had detection limits (appendix 5.1) too high to be analysed in time for inclusion in this thesis (D.L. too high, Table 5.8 and 5.9) and remain in storage.

Sealed at Location?	Sample	Year	Seal off pressure (torr)	Sealed on	Data?
Test technique samples					
WHOI	Test- base 1	recent branch	3.00E-08	19-Mar-04	Yes
WHOI	Test- base 2	recent branch	3.80E-08	19-Mar-04	Yes
WHOI	Test- acid 1	recent branch	3.50E-08	19-Mar-04	Yes
WHOI	Test- acid 2	recent branch	3.80E-08	19-Mar-04	Yes
WHOI	Test- branch tips	2003	5.00E-08	17-Mar-04	D.L. too high

Table 5.8 Exchange technique test gorgonian samples prepared for tritium analysis.

5.10.2 Sample housing glassware problems

During the helium in-growth period samples were stored in a freezer to minimise helium permeation through the sample bulb glass walls [*Clarke et al*., 1976]. When samples were removed from the freezer prior to analysis, cracks in the glass developed running from the seal off capillary, down the glass tubing and into the bulb (Figure 5.8A). In some cases the glass tubing shattered (Figure 5.8B). Of the 37 samples having detection limits low enough for helium-3 analysis, 13 samples were lost due to cracking of the glass sample bulbs (see Table 5.8 and 5.9), equal to a loss-rate for tritium samples of 35%.

Location	Sample	Year	Seal off (torr)	Sealed on	Data?
P. porosa	**Sample 1 3rd trip**				
SOC	TS1-1A	1990-2002	1.10E-07	30-May-03	Yes
SOC	TS1-1B	1990-2002	1.80E-07	14-May-03	Yes
SOC	TS1-2A	1980-1990	3.60E-07	16-May-03	Yes
SOC	TS1-2B	1980-1990	3.50E-07	16-May-03	No-seal not broken
SOC	TS1-3A	1975-1980	1.20E-07	22-May-03	Yes
SOC	TS1-3B	1975-1980	1.30E-07	22-May-03	Yes
SOC	TS1-4A	1970-1975	4.50E-08	28-May-03	Yes
SOC	TS1-4B	1970-1975	5.10E-08	28-May-03	Yes
SOC	TS1-5A	1968-1970	1.10E-07	29-May-03	Yes
SOC	TS1-6A	1966-1968	9.10E-08	29-May-03	No-bulb cracked
SOC	TS1-6B	1966-1968	9.70E-08	29-May-03	Yes
SOC	TS1-7A	1965-1966	1.30E-07	30-May-03	No-bulb cracked
SOC	TS1-8A	1964-1965	3.20E-08	05-Jun-03	Yes
SOC	TS1-9A	1962-1964	2.40E-08	11-Jun-03	Yes
SOC	TS1-10A	1955-1962	1.00E-08	17-Jun-03	Yes
SOC	TS1-10B	1955-1962	1.50E-08	18-Jun-03	No-bulb cracked
SOC	TS1-11A	1950-1955	1.30E-08	18-Jun-03	Yes
SOC	TS1-12A	1942-1950	2.20E-08	10-Jun-03	Yes
SOC	TS1-13A	1935-1942	4.70E-08	06-Jun-03	No-bulb cracked
SOC	TS1-14A	1927-1935	3.40E-08	05-Jun-03	Yes
P. porosa	**Sample 2 2nd trip**				
SOC	TS2-1	2001-1997	4.70E-08	17-Jun-03	Yes
SOC	TS2-2	1996-1992	4.30E-08	17-Jun-03	No-bulb cracked
SOC	TS2-3	1991-1987	4.40E-08	17-Jun-03	Yes
SOC	TS2-4	1986-1983	6.00E-08	13-Jun-03	Yes
SOC	TS2-5	1982-1979	5.40E-08	13-Jun-03	Yes
WHOI	TS2-6	1978-1975	3.20E-08	12-Mar-04	D.L. too high
WHOI	TS2-7	1974-1968	3.10E-08	12-Mar-04	D.L. too high
WHOI	TS2-8	1968-pre bomb	3.30E-08	06-Apr-04	D.L. too high
P. porosa	**Sample 2 1st trip**				
WHOI	TS3-1	post bomb	5.00E-08	17-Mar-04	No-bulb cracked
WHOI	TS3-2	bomb spike	8.20E-08	02-Apr-04	No-bulb cracked
WHOI	TS3-3	bomb spike	5.80E-08	02-Apr-04	D.L. too high
WHOI	TS3-4	pre bomb	6.00E-08	02-Apr-04	No-bulb cracked
P. dichotoma	**Sample 3 2nd trip**				
WHOI	TS4-1	1959-1965	3.50E-08	06-Apr-04	D.L. too high
WHOI	TS4-2	1965-1970	3.00E-08	07-Apr-04	D.L. too high
WHOI	TS4-3	1970-1975	2.60E-08	07-Apr-04	D.L. too high
WHOI	TS4-4	1975-1985	3.10E-08	08-Apr-04	No-bulb cracked
WHOI	TS4-5A	1985-2001	3.80E-08	08-Apr-04	No-bulb cracked
P. porosa	**Sample 4 3rd trip**				
WHOI	TS5-1	1950-1960	3.90E-08	16-Apr-04	D.L. too high
WHOI	TS5-2	1960-1968	3.40E-08	16-Apr-04	D.L. too high
WHOI	TS5-3	1968-1980	3.00E-07	16-Apr-04	No-bulb cracked
WHOI	TS5-4A	1980-2002	4.50E-08	22-Apr-04	Yes
WHOI	TS5-4B	1980-2002	3.70E-08	22-Apr-04	No-bulb cracked

Table 5.9 Time series gorgonian samples prepared for tritium analysis.

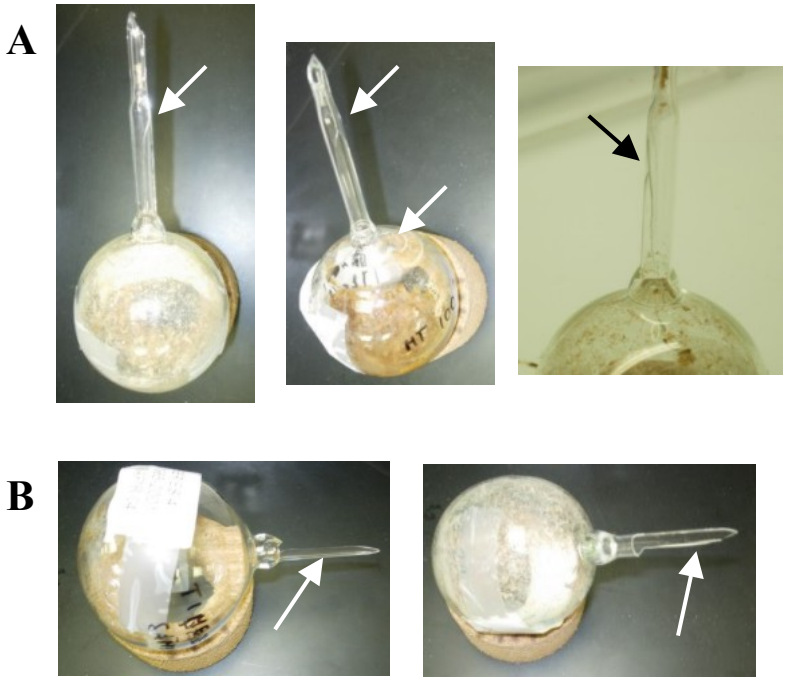

Figure 5.8 (A) Examples of three coral samples unable to be analysed for helium-3 due to cracks in the glass sample bulbs. Arrows point to cracks running from the seal off capillary, down the glass tubing and into the bulb itself. (**B) Examples of coral samples where the glass tubing shattered after cracks developed in the sample bulb tubing.**

The development of cracks in the sample bulbs could be due to stress build up in the glass. Micro-scale cracks can develop at the capillary if the seal off area hasn't been adequately annealed. However, early on in this project, problems with micro-scale cracks were encountered during the preparation of the samples sealed to verify if the exchange was necessary (section 5.3.2), and hence, I was very careful to thoroughly anneal all samples sealed after this time. As noted in section 5.6.1.1, the wide capillary glass bulbs are hard to seal. In some cases the seal off point can be at an angle, which sets up an unequal distribution of stress in the glass. When the glassware was removed from the freezer, the temperature change coupled with this stress point could cause the glass to crack, and in some cases, shatter. However, no problems were encountered when samples sealed in Southampton were transferred from a freezer to room temperature conditions to be prepared for shipping to Woods Hole for analysis. This may be due to the storage freezer being maintained at a lower temperature in Woods Hole, furthermore, most samples lost to glassware cracking were stored in the boxes at the bottom of the freezer and hence at the coldest temperatures.

In future, it is recommended that other sample containers be used to house coral samples (section 5.11.1). If glassware were used, it would be prudent during the in-growth period to store samples in a refrigerator rather than a freezer, or to move samples from the freezer to a refrigerator prior to analysis to lessen potential temperature shock effects.

5.10.3 Exchange technique test samples

Four bulk (~5 g) samples were prepared and sealed to test the exchange technique. All the samples were branch sections of coral representing the time period ~1990-2001. Two of the samples were exchanged using NaOH only, whilst for the remaining two samples, the H_3PO_4 step of the exchange was included. The results are shown in Table 5.10. These samples were prepared to see whether including the acid step in the exchange would affect the measured tritium signal.

Sample	Tritium (TU)	Uncertainty (TU)
Exchange Test Base 1	3.508	±0.642
Exchange Test Base 2	3.661	±0.479
Exchange Test Acid 1	5.162	±0.696
Exchange Test Acid 2	5.304	±0.451

Table 5.10 Tritium results for exchange technique test samples measured by helium in-growth.

The reproducibility is excellent for the base 1 and 2 samples and the acid 1 and 2 samples. However, the exchange test acid samples have higher tritium levels (by ~1.60 TU) than the exchange test base samples. This implies the acid step is introducing contamination with respect to tritium. This contamination could come from the acid itself, which has higher tritium content than the base (section 5.9.2), or from the extra steps introduced to the exchange procedure. Another possibility is that the acid is breaking down the structure of the gorgonin and opening up more hydrogen sites to exchange. Fortunately, samples where the acid step was included in the exchange process are limited to the two exchange test acid samples mentioned above and the tritium time series 5 (TS 5) samples. When the TS 5 samples are analysed (detection limits were too high for these samples to be analysed and included in this thesis; Table 5.8) it will be interesting to compare their tritium results with the other time series' to investigate whether the increase in tritium associated with the acid step is as reproducible as it is for the test exchange samples.

Although it is hard to say more from these data, the important point is that leaving out the acid step should not affect the efficiency of the exchange. In fact, it appears from these results that the exchange works better (tritium values are lower) without the acid step.

5.10.4 Tritium time series samples

During this project many valuable samples were lost due to cracking of glassware. Furthermore, some samples had detection limits too high to be analysed in time to be included in this thesis. The reduced dataset for tritium time series samples is shown in Table 5.11.

Sample	Year	Sealed on	Tritium (TU)	Uncertainty (TU)
Time Series 1				
TS1-1A	1990-2002	30-May-03	-6.803	±1.322
TS1-1B	1990-2002	14-May-03	5.484	±1.736
TS1-2A	1980-1990	16-May-03	5.096	±0.899
TS1-3A	1975-1980	22-May-03	3.412	±1.109
TS1-3B	1975-1980	22-May-03	2.565	±0.772
TS1-4A	1970-1975	28-May-03	3.721	±1.444
TS1-4B	1970-1975	28-May-03	1.067	±0.389
TS1-5A	1968-1970	29-May-03	7.970	±0.756
TS1-6A	1966-1968	29-May-03	-294.515	±12.470
TS1-6B	1966-1968	29-May-03	4.674	±0.600
TS1-8A	1964-1965	05-Jun-03	-9.750	±1.418
TS1-9A	1962-1964	11-Jun-03	-7.359	±2.710
TS1-10A	1955-1962	17-Jun-03	2.280	±0.849
TS1-11A	1950-1955	18-Jun-03	<0.285	±1.977
TS1-12A	1942-1950	10-Jun-03	-11.215	±3.055
TS1-14A	1927-1935	05-Jun-03	-10.985	±2.643
Time Series 2				
TS2-1	2001-1997	17-Jun-03	7.101	±1.831
TS2-3	1991-1987	17-Jun-03	<0.445	±2.015
TS2-4	1986-1983	13-Jun-03	-34.466	±2.246
TS2-5	1982-1979	13-Jun-03	2.296	±1.069
Time Series 5				
TS5-4A	1980-2002	22-Apr-04	<0.158	±0.637

Table 5.11 Tritium results for gorgonian time series samples measured by helium in-growth. Where a result is preceded by '<' then the tritium signal present is lower than the detection limit, the number quoted (appendix 5.1).

5.10.4.1 Samples lost due to glassware problems

In Table 5.11 three samples are highlighted blue, during their preparation and processing, problems with glassware were encountered. Sample TS2-4 was sealed poorly, a bubble developed during seal off and only a very thin film of glass maintained the vacuum. Small cracks likely developed in this seal allowing helium to diffuse through and contaminate the sample. Leaks were also detected in TS1-6A apparent from the associated tritium signal and large error. Concerning TS1-5A, when this sample was connected to the vacuum line for degassing, the top of the glass capillary cracked and so the top of the glass tubing was scored, broken off and annealed in an effort not to lose the sample. This procedure meant the sample was open to atmospheric conditions in the laboratory for ~15 minutes and was not flooded with argon during this time. The elevated tritium value associated with this sample is probably due to contamination with water vapour from the atmosphere. These problems again highlight the difficulties of working with glassware and other methods of housing coral samples are discussed in section 5.11.1.

5.10.4.2 Negative numbers

Following mass spectrometric analysis, it was noted that several samples (Table 5.11, in red) had sub atmospheric helium ratios ($^3He/^4He$ < 1Ra, where Ra = atmospheric helium isotope ratio) resulting in negative excess helium values (^3He due to tritium decay) and hence negative tritium. This is an unphysical result and affected samples sealed after 30th May 2003. Figure 5.9 shows the raw data for the time series samples. In Figure 5.9A the size of the samples increase with time. The size of a sample should be related to the amount of tritium in that sample and should have no relationship with time, as my samples were sealed in no particular order. Samples sealed post 30th May 2003 have negative excess ^3He values (Figure 5.9B) and $^3He/^4He$ ratios below 1 (Figure 5.9C), which is sub atmospheric and suggests these samples have been contaminated with radiogenic ^4He ($^3He/^4He$ ~0.1 Ra).

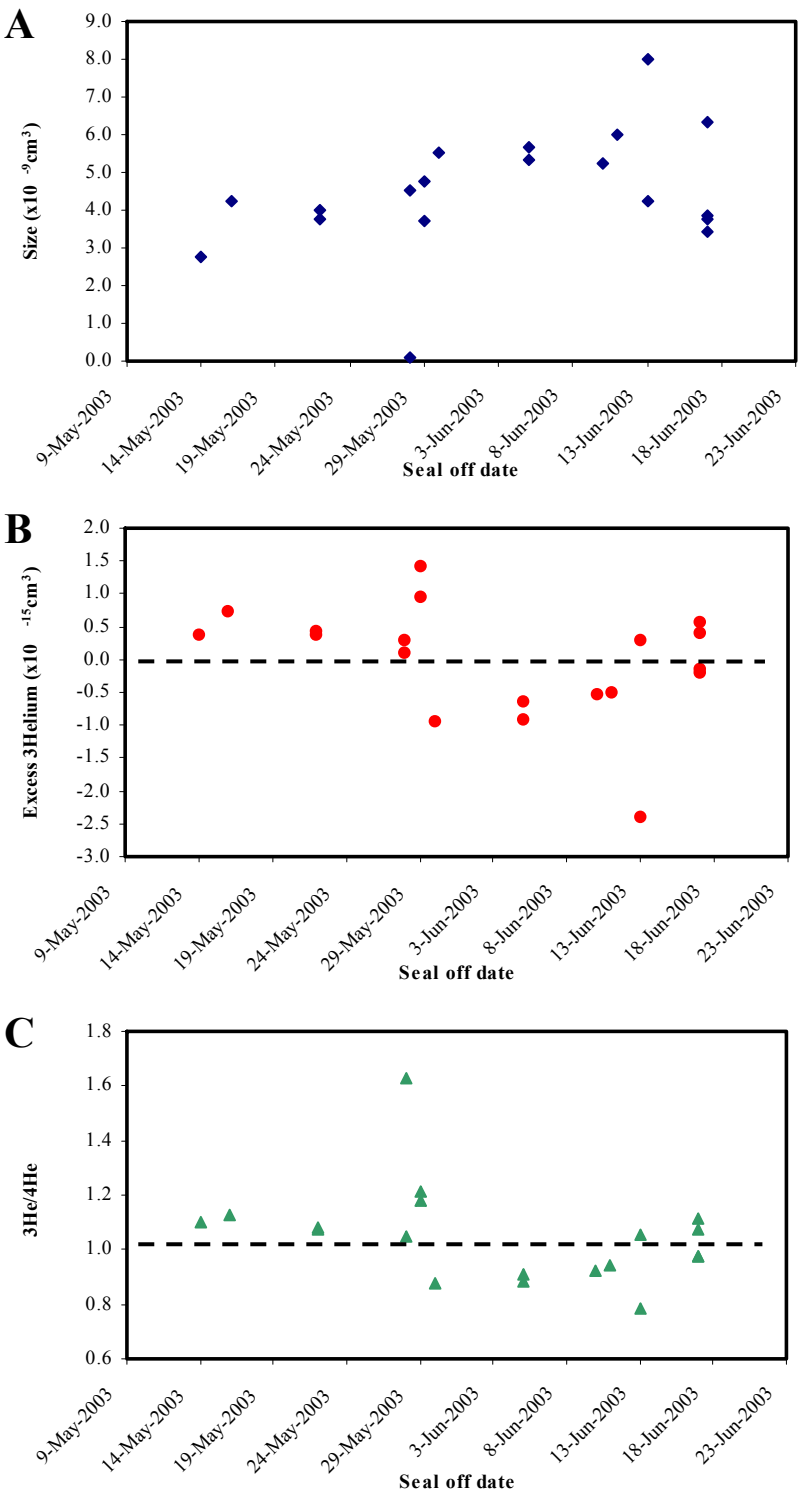

Figure 5.9 Plots to show anomalies with data after 30th May 2003 seal off date. (A) The size of samples is increasing with time (B) Negative excess helium values post 30th May 2003 (C) Sub atmospheric (<1) $^{3}He/^{4}He$ ratios post 30th May 2003.

On the 30th May 2003, I changed the argon tank in the sample preparation lab. Argon gas (high purity grade) is used to maintain a helium free atmosphere for all laboratory procedures (e.g. sections 5.5.1 and 5.5.2) and the coral is in constant contact with this gas. One explanation is that the helium contamination came from the argon tank. However correcting for this is not possible as the amount, uniformity with time, or isotopic ratio of contamination is unknown. In fact, samples sealed on or after 13th June 2003 appear unaffected (Table 5.11). Samples TS1-11A and TS2-3 are both sub detection limit and the other samples (TS1-10A, TS2-1 and TS2-5) are all positive.

As the reason for and source of contamination for samples with negative tritium is unknown, the only option is to discount them from the dataset. This is very unfortunate considering the months of work dedicated to producing these data. In future it is recommended that gases from cylinders used for inert atmospheres be analysed to check their content.

5.10.4.3 Measurement errors

Uncertainty in the tritium values for some coral samples is high (Table 5.10 and 5.11). Measurement errors are inversely proportional to the storage time and mass of sample. Therefore, increasing the storage time and enlarging the sample size can reduce these errors. Larger samples were used for the test exchange samples and these generally have smaller errors when compared to the smaller sized time series samples.

Reducing the helium blank associated with sample preparation and analysis will also reduce the error because the error is proportional to the square root of the number of ^{3}He atoms collected. This has two implications; firstly, the larger tritium signals will have a larger absolute error but a smaller relative error and secondly, when a sample has been significantly contaminated with atmospheric helium, the error will be inflated due to 'poisson statistical dilution' from the background atmospheric ^{3}He (e.g. sample TS1-6A). One source of atmospheric helium contamination is from incomplete degassing of the sample. The ^{4}He content of a sample should be high if atmospheric helium was not removed via degassing and this does not appear to be a problem with the coral samples.

Another source of contamination from atmospheric helium is from the glass bulbs used to house the samples. If small cracks develop in the glass then helium can diffuse through the glass into the sample (e.g., TS1-6A and TS2-4). These cracks are most likely to form when the glass cools too quickly after sealing. Further attention when sealing samples can reduce this source of contamination. Using a different

material to house coral samples that does not require flame sealing would eliminate this source of error (section 5.11.1).

5.10.5 Gorgonian coral versus surface seawater

Tritium values successfully extracted from gorgonian coral are shown in Table 5.12.

Sample	Year	Gorgonian coral tritium (TU)	Uncertainty (TU)
Time Series 1			
TS1-1B	1990-2002	5.484	±1.736
TS1-2A	1980-1990	5.096	±0.899
TS1-3A	1975-1980	3.412	±1.109
TS1-3B	1975-1980	2.565	±0.772
TS1-4A	1970-1975	3.721	±1.444
TS1-4B	1970-1975	1.067	±0.389
TS1-6B	1966-1968	4.674	±0.600
TS1-10A	1955-1962	2.280	±0.849
TS1-11A	1950-1955	<0.258	±1.977
Time Series 2			
TS2-1	2001-1997	7.101	±1.831
TS2-3	1991-1987	<0.445	±2.015
TS2-5	1982-1979	2.296	±1.069
Time Series 5			
TS5-4A	1980-2002	<0.158	±0.637
Test exchange			
Base 1	1990-2001	3.508	±0.642
Base 2	1990-2001	3.661	±0.479
Acid 1	1990-2001	5.162	±0.696
Acid 2	1990-2001	5.304	±0.451

Table 5.12 Tritium values successfully extracted from gorgonian coral.

The aims of this chapter were to investigate whether tritium concentrations measured within the gorgonin of coral skeletons reflected surface seawater concentrations. Tritium surface water values prior to 1965 have never been measured and a natural tritium concentration of 0.20 ±0.06 TU is estimated [*Dreisigacker and Roether*, 1978].

Gorgonian coral samples TS1-10A and TS1-11A span the time periods 1955-1962 and 1950-1955 respectively. TS1-11A is sub detection limit (<0.258 ±1.069 TU), which might well be expected for pre bomb levels, whereas TS1-10A with a value of 2.280 ±0.849 TU, is several times the expected natural tritium concentration of 0.20 ±0.06 TU. Oceanic deposition of nuclear weapons testing fallout started in about 1952

and reached peak levels of ~18 TU between 1963 and 1964 [*Dreisigacker and Roether*, 1978; *Doney and Jenkins*, 1988]. Following this pattern the nearest 'peak' gorgonian sample would be TS1-6B spanning 1966-1968 with a measured tritium concentration of 4.674 ±0.600 TU. A peak tritium value of 18 TU decay corrected (see appendix 5.2) to 2004 equals 1.90 TU but the gorgonian value is twice that. Following the bomb spike, surface water tritium values have decreased quickly due to radioactive decay, dilution with older waters from depth and the influx of southern hemisphere low tritium surface waters [e.g., *Jenkins*, 1998]. The gorgonian tritium concentrations also decrease until 1980, however, post 1980 all gorgonian tritium values are elevated with the exception of TS5-4A and TS2-3, which although sub detection limit, are both within errors of the measured surface seawater tritium. Gorgonian tritium data are displayed with measured surface water values and box model estimates (pre 1964) for the North Atlantic in Figure 5.10. Although there are some satisfactory matches, in the majority of cases, gorgonian reconstructed surface water tritium is greater than both the box model estimates and the measured seawater values.

A series of hypotheses are put forward in an attempt to explain and understand the elevated tritium values extracted from coral gorgonin.

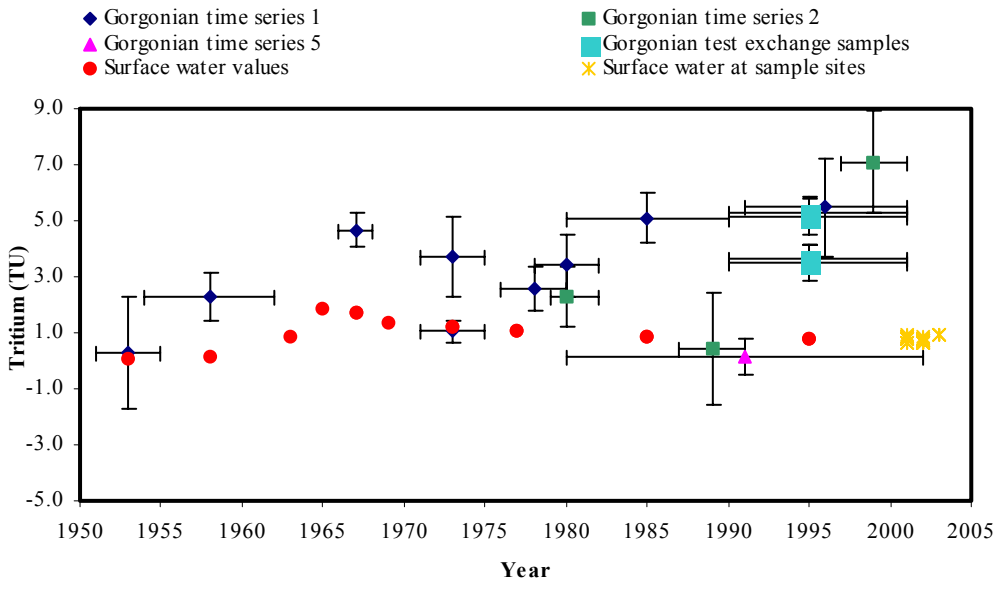

Figure 5.10 Tritium data measured in gorgonian coral skeletons from Bermuda compared to surface water tritium values in the North Atlantic.
Tritium surface water values 1953-1964 (red) are adapted from *Dreisigacker and Roether* [1978] box model calculations, measured samples 1965-1995 (red) from *Jenkins* [1998]. For coral data y-axis error bars represent uncertainty in measurements, x-axis error bars represent number of years each coral sample spans. All values decay corrected to 2004.

5.10.5.1 Elevated tritium or a real signal

Are the gorgonian reconstructed tritium values too high? This thesis is, to my knowledge, the first attempt to reconstruct past surface water tritium concentrations. The North Atlantic is the best-characterised location with respect to surface water tritium measurements but pre 1964 no tritium measurements had been made [e.g., *Dreisigacker and Roether*, 1978]. Unfortunately, although nine pre bomb coral samples were prepared for tritium analysis (Table 5.8), I only have data for two of these samples. The oldest sample has no detectable tritium concentration but TS1-10A spanning 1950-1955 has an extremely high value of 2.280 ±0.849 TU. Could surface water tritium values have been this high? Is this actually a real signal? If tritium decay were reversed to take 2.280 ±0.849 TU back to its 1955 value, then the surface water tritium signal would have been equal to about 32.03 TU. This is impossible for pre bomb tritium, during the bomb spike the maximum value reached was around 18 TU [*Dreisigacker and Roether*, 1978; *Doney and Jenkins*, 1988]. Even if the age model for sampling were incorrect and the 1950-1955 sample was actually spanning the bomb spike (1964-1965) the values are still too high. The gorgonian samples are definitely reflecting an increased tritium surface water signal. This is again apparent from the seawater samples collected at the coral sample site in comparison to the most recent tritium values obtained from the coral gorgonin (Figure 5.10).

5.10.5.2 Molecular structure for gorgonin

Axial skeleton gorgonin contains collagen-like amounts of glycine, proline and hydroxyproline [*Smanzt-Froelich*, 1974; *Goldberg*, 1974, 1976; *Leversee*, 1980] and as the exact structure of gorgonin is unknown, collagen is used in its place. During calculations to determine gorgonian tritium concentrations, the simplified structure of collagen containing the repeating sequence of amino acids glycine, proline and hydroxyproline is used. What would be the effect on our gorgonian tritium numbers if this molecular structure for gorgonin were incorrect or over simplified? Could this account for the high tritium values measured in the gorgonian skeleton?

Table 5.13 shows the resultant tritium concentrations when the molecular structure of 'gorgonin' is changed. Altering the sequence of amino acids for gorgonin does not significantly change the calculated tritium concentration, which remains within the measurement uncertainty of each sample. Even if the assumption of treating gorgonin as a simplified collagen structure were incorrect, the resulting influence on

gorgonian tritium would be insufficient to account for the differences between gorgonian tritium and surface seawater measurements.

Sample	Tritium $(Gly\text{-}Pro\text{-}Hyp)_n$ (TU)	Tritium $(Gly\text{-}Gly\text{-}Pro)_n$ (TU)	Tritium $(Gly\text{-}Pro\text{-}Pro)_n$ (TU)	Tritium $(Gly\text{-}Pro\text{-}Hyp\text{-}Gly)_n$ (TU)
Time Series 1				
TS1-1B	5.484 ±1.736	5.767	4.908	4.939
TS1-2A	5.096 ±0.899	5.359	4.560	4.589
TS1-3A	3.412 ±1.109	3.588	3.053	3.073
TS1-3B	2.565 ±0.772	2.698	2.296	2.310
TS1-4A	3.721 ±1.444	3.913	3.330	3.351
TS1-4B	1.067 ±0.389	1.124	0.955	0.961
TS1-6B	4.674 ±0.600	4.926	4.184	4.211
TS1-10A	2.280 ±0.849	2.410	2.041	2.054
TS1-11A	<0.285 ±1.977	<0.335	<0.285	<0.285
Time Series 2				
TS2-1	7.101 ±1.831	7.468	6.355	6.395
TS2-3	<0.445 ±2.015	<0.523	<0.445	<0.445
TS2-5	2.296 ±1.069	2.415	2.055	2.068
Time Series 5				
TS5-4A	<0.158 ±0.637	<0.186	<0.158	<0.158
Test exchange				
Base 1	3.508 ±0.642	3.697	3.131	3.151
Base 2	3.661 ±0.479	3.860	3.263	3.284
Acid 1	5.162 ±0.696	5.437	4.611	4.641
Acid 2	5.304 ±0.451	5.588	4.735	4.765

Table 5.13 Tritium results calculated for varying collagen molecular structures.
(Gly = Glycine, Pro = Proline and Hyp = hydroxyproline).

Although changing the amino acid sequence has no measurable consequence for tritium, there are some structural issues that require discussion. The amino acids that make up the collagenous structure probably come from two sources. Firstly, from external sources e.g. food for the gorgonian colony, this should not influence the tritium signal, as phytoplankton tritium should be in equilibrium with surface water tritium. The second potential source of amino acids is preparation by the organism via its own biosynthetic route. This may have an implication on the results as during formation, water and other small molecules could become incorporated into macrocyclic structures, the tritium associated with this water is unknown and these molecules may be unaffected by the exchange procedure.

If this study were to be repeated it might be worthwhile attempting to extract pure collagen from the coral samples prior to the exchange and tritium analysis so that the results could be computed with more accuracy.

5.10.5.3 Exchangeable sites

The exchange technique has been shown to be necessary (section 5.3.2) but does it go far enough to correct the tritium values measured in the gorgonian samples?

The extent of exchange for coral gorgonin has been estimated but is not known. To ascertain a clearer picture of hydrogen exchange in the coral samples, a series of exchange experiments using solutions of differing tritium concentrations could be completed. Alternatively, the use of deep-sea corals that should have very low, if any, tritium in their skeletons has potential. Suspending these corals in high tritium concentration water with both the water and the skeletal gorgonin sampled and analysed for tritium over the course of the experiment might provide important insight into the rate of exchange.

For tree ring cellulose, *Feng et al.* [1993] illustrated that the degree of exchange could be calculated by completing a series of deuterium exchanges, of a potential 30% exchangeable hydrogen, 25.5% was removed. The exchange technique used for coral gorgonin is adapted from the *Feng et al.* [1993] method. Therefore it is highly probable that the gorgonian samples contain hydrogen open to exchange and possibly contaminated with tritium that has not been removed by the exchange technique. *Feng et al.* [1993] also noted that the exchangeability of hydrogen varies from sample to sample, this could be why some of our samples appear to reflect seawater tritium whilst others remain elevated.

A further issue for the exchange concerns the exchangeable hydrogen successfully replaced with either –OH from NaOH or –H from tritium free water. The assumption is made that the replacement hydrogen is tritium free, however, the water and reagents used in the exchange procedure contain some tritium (section 5.9.1 and 5.9.2) and so need to be corrected for. Although this is an important correction to make, the tritium free reagents and tritium free water contained very little tritium and with only 19% hydrogen estimated to be exchangeable this correction should be small. At the largest, the correction would be equal to the measured tritium level in the tritium free NaOH and the tritium free water. Table 5.14 shows the tritium data with this exchangeable hydrogen correction factor added to the measurement uncertainty.

Although the increased breadth of error brings some values closer (within errors) to the seawater tritium signal the magnitude of correction is not sufficient for the majority of samples.

Sample	Year	Gorgonian coral tritium (TU)	Uncertainty (TU)
Time Series 1			
TS1-1B	1990-2002	5.484	±1.855
TS1-2A	1980-1990	5.096	±1.018
TS1-3A	1975-1980	3.412	±1.228
TS1-3B	1975-1980	2.565	±0.891
TS1-4A	1970-1975	3.721	±1.563
TS1-4B	1970-1975	1.067	±0.508
TS1-6B	1966-1968	4.674	±0.719
TS1-10A	1955-1962	2.280	±0.968
TS1-11A	1950-1955	<0.285	±2.096
Time Series 2			
TS2-1	2001-1997	7.101	±1.950
TS2-3	1991-1987	<0.158	±2.134
TS2-5	1982-1979	2.296	±1.188
Time Series 5			
TS5-4A	1980-2002	<0.445	±0.899
Test exchange			
Base 1	1990-2001	3.508	±0.695
Base 2	1990-2001	3.661	±0.532
Acid 1	1990-2001	5.162	±0.958
Acid 2	1990-2001	5.304	±0.713

Table 5.14 Gorgonian tritium values with the exchangeable hydrogen correction factor added to measurement uncertainty.

5.10.5.4 Contamination of samples

None of the above hypotheses has provided an adequate reason as to why the gorgonian coral tritium measurements are higher than the surface seawater tritium values.

The additional tritium signal most probably has been added after the samples were collected. Contamination could have come from tap water, water vapour, luminous dials on diving equipment, a luminous dial watch in the laboratory, there are many possible sources. What we can say from the data is that extraneous contamination is substantial and therefore needs to be removed. The exchange is working to a certain extent as some samples are within errors of the seawater signal. The main problem areas appear to be post 1990. All the post 1990 samples include the outermost bands of skeletal material, which during storage would have been in constant contact with the

atmosphere and so water vapour containing tritium. In the future it might be worth discarding the outer most layers and starting the sampling at a fresh new layer, which has been protected from the atmosphere during storage.

The exchange might be working very well and the contamination could occur post exchange when the samples are transferred to and from the argon glove box and to the sample degassing line. In the future it would make sense to have the degassing line in the same laboratory as the sample preparation areas to minimise the risk of contamination during sample transferral.

5.10.5.5 Averaged gorgonian tritium values

Tritium data from all gorgonian coral samples were averaged over the time period the samples spanned and are displayed compared to surface water data in Figure 5.11. Averaging the pre bomb samples gives an excellent fit to the box model tritium data. For the remaining years from 1963 onwards, although the gorgonian tritium values are elevated when compared to surface seawater tritium, the shape of the curve is good. For a first attempt at measuring a bomb tritium time series in gorgonian coral with the use of a difficult and challenging technique, the data are encouraging.

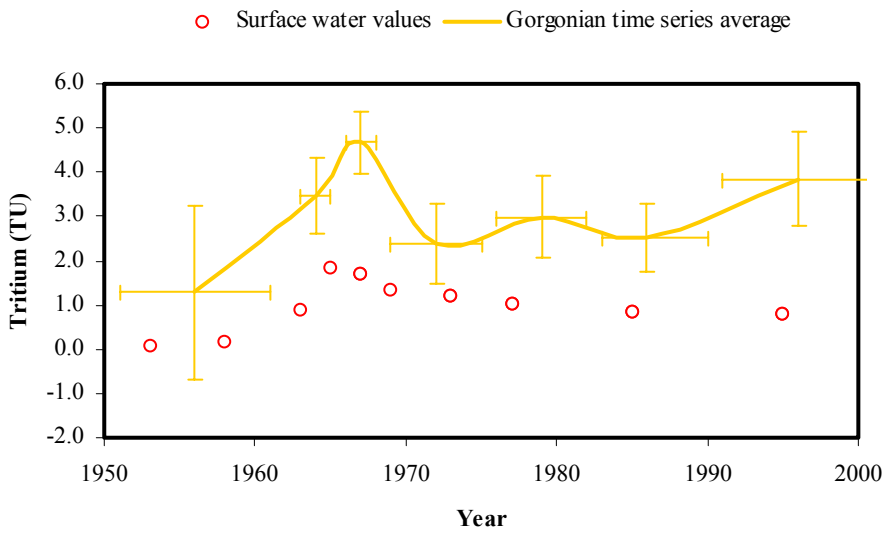

Figure 5.11 Gorgonian time series averaged tritium data compared to surface water tritium values. Tritium surface water values 1953-1964 (red) are adapted from *Dreisigacker and Roether* [1978] box model calculations, measured samples 1965-1995 (red) from *Jenkins* [1998]. All values decay corrected to 2004.

5.11 Conclusions and future improvements to the technique

It is very difficult given all the problems encountered with the development of this method and the extensive loss of samples through glassware cracking and possible helium contamination of argon gas cylinders to build a case for what is happening with the data. If more numbers were available perhaps the story would be clearer.

This thesis has succeeded in developing a technique for extracting tritium from the banded skeletons of gorgonian coral. As tritium has never previously been measured in gorgonian corals this marks an important step forward. There are however many ways in which the technique could be improved.

5.11.1 Sample housing improvements

If this technique is to be viable in the future certain changes are needed. Following the many problems encountered using glassware the technique used to house coral samples needs updating. Recent advances have meant that glass is no longer used for solid samples and in its place metal chambers have been designed (Figure 5.12).

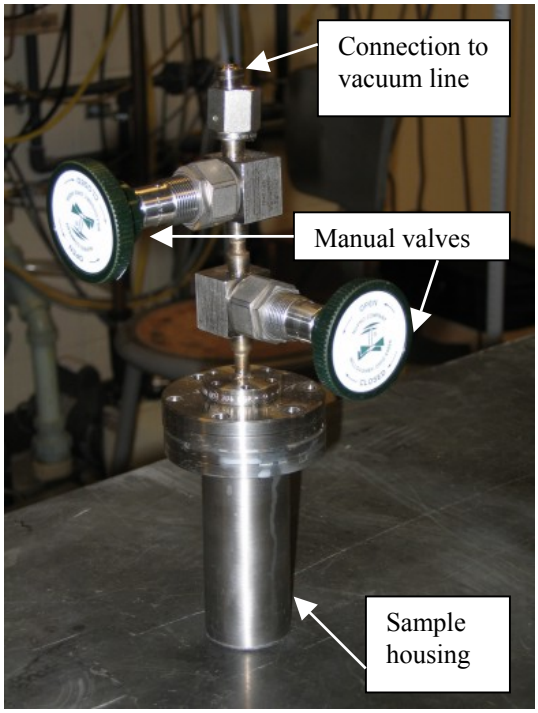

Figure 5.12 Metal solid sample housing, a replacement for glassware.

There are several benefits of these new metal containers over the glass sample bulbs. Firstly, the time consuming process of stuffing the coral sample through the capillary no longer exists, as with the metal chambers the sample can be spooned or transferred using tweezers directly into the wide necked sample housing. This will minimise potential sources of contamination as previously the sample sat in the glove box for at least one hour during stuffing. Secondly, the samples can be degassed to dryness as no water vapour pump is required for analysis, meaning, there would be less water correction needed (section 5.8.3.2) and sample weights would be more accurate (sections 5.8.1 and 5.8.2). Thirdly, there are no problems associated with flame sealing, cutting down the loss of samples at this stage, when the sample has been adequately degassed, the metal chambers are sealed simply by closing a valve. This seal off technique gives rise to further benefits; the degassing efficiency of each sample can be monitored mass spectrometrically prior to storage as the chamber sample can be re sealed again after the check and also, at the sample analysis stage, each sample could be re-measured without exposure to the atmosphere. Fourthly, with the metal chambers atmospheric contamination during storage is at least an order of magnitude smaller than with glass, meaning better detection limits are achieved due to less poisson statistical dilution (section 5.10.4.3). The final benefit is that there is no sample loss due to glass cracking, during this project 35% of samples were lost due to glassware cracking so this is an important breakthrough. The use of metal chambers to house samples definitely seems to be the way forward if this technique is to prove viable in the future, the only downfall to the metal containers being that each sample chamber is expensive. However chambers can be re used following sample analysis.

5.11.2 Improving accuracy of measurements

If this study were to be repeated it would be worthwhile attempting to extract pure collagen from the coral samples prior to the exchange step to enable tritium results to be computed with increased accuracy.

Completing the experiments outlined in section 5.10.5.3 would help to ascertain a clearer picture of the rate and extent of hydrogen exchange in the coral samples.

5.11.3 The exchange

The results for the exchange test technique samples proved, as hypothesised, that the acid step of the exchange is not required. In fact this step appears to introduce contamination to the tritium signal and so should be avoided.

I would, in future, introduce additional rinsing steps using tritium free water and ensure the pH of coral gorgonin be tested (not just the rinsings) to verify the base has been thoroughly neutralised and thus would not contribute to the measured tritium signal.

If viable, I would encourage the introduction of a totally tritium free lab where running tap water is only used in emergency, this would help to minimise atmospheric water vapour contamination.

It is recommended that glove boxes be continually purged using a high flow rate of argon to help reduce contamination possibly encountered during the transfer of items to and from the glove box. Argon cylinder content should be analysed before use to check content and purity.

5.11.4 Summary

The aims of this chapter were to investigate whether the tritium concentrations measured within the gorgonin bands of the coral skeleton reflected surface water tritium concentrations over the time period the skeleton was accreted.

A technique has been developed which succeeded in extracting the bomb tritium signal stored in gorgonian coral skeletons. With further work to improve on contamination issues and to reduce measurement uncertainty it is entirely possible that this tritium measurement technique could be used to reconstruct ocean circulation of the recent past in regions of the world where this information would be otherwise unavailable.

Chapter 6: Radiocarbon time series from a gorgonian coral skeleton

6.1 Introduction

Radiocarbon (^{14}C) was produced artificially in the late 1950s and early 1960s due to the testing of atmospheric nuclear weapons. Bomb ^{14}C is a useful tracer of oceanic mixing processes. The scleractinian coral skeleton records the ambient carbon isotopic composition of the surrounding seawater as it grows. The first measurements of radiocarbon in modern corals were made by *Knutson and Buddemeier* [1973] who detected bomb ^{14}C in the outer layers of a massive coral from Fanning Island. Radiocarbon measurements in Bermudian corals have been documented previously. *Nozaki et al*. [1978] measured ^{14}C in a 200 year old brain coral *Diploria labyrinthiformis* sampled from 5 m depth at North Rock, Bermuda. *Druffel* [1989] determined radiocarbon in cores taken from living coral colonies (*Diploria strigosa* and *Diploria labyrinthiformis*) at 11 m depth at two sites on Bermuda, Sam Hall's Bay (32°21'N, 64°46 W) and North Rock (32°29'N, 64°46'W).

The aim of this chapter is to attempt to recreate the bomb radiocarbon curve previously measured in scleractinian corals at Bermuda by *Nozaki et al*. [1978] and *Druffel* [1989], using a gorgonian coral colony. Comparison of the radiocarbon curve in the gorgonian to that documented from the scleractinia would enable confirmation of the skeletal banding chronology in the gorgonian skeleton.

Radiocarbon has been measured previously in deep-sea gorgonians. *Griffin and Druffel* [1989] used ^{14}C measurements to investigate carbon sources to the organic and calcareous portions of the coral skeleton. They found that although calcite was formed from dissolved inorganic carbon (DIC) from the depth of coral growth, the carbon source for the coral organic matter (polyps and gorgonin) was derived from particulate organic matter (POM) rained down from the surface and consumed by the corals at depth. Therefore, the isotopic composition of the carbonate fraction should record deep-sea conditions, whereas the isotopic composition of the gorgonin and polyps could be a proxy for surface productivity [*Griffin and Druffel*, 1989]. These findings have recently been confirmed by *Roark et al*. [2005] who used radiocarbon measurements to age deep-sea bamboo corals from the Gulf of Alaska. *Sherwood et al*. [2005] used radiocarbon measurements in the deep-sea gorgonian *Primnoa resedaeformis* to prove that skeletal growth banding was annual in periodicity.

This chapter will document the first radiocarbon measurements in organic gorgonin from a surface dwelling gorgonian *Pseudoplexaura porosa*.

6.2 Methods

6.2.1 Sample collection and preparation chemistry

The gorgonian coral sample used for radiocarbon measurements was collected as described in Chapter 2, section 2.2.2 and the sample details are shown in Table 6.1.

Sample	Species	Trip	Location	Latitude and Longitude	Date	Depth (m)
3	*Pseudoplexaura porosa*	3rd	Bailey's Bay Flats	N32°21.73 W064°44.84	16/10/2002	6

Table 6.1 Gorgonian sample used for radiocarbon time series.

The banding present in the gorgonian axial skeleton was used to provide chronology for radiocarbon sampling (Figure 6.1). Samples were prepared for band counting and examination as described in Chapter 5, section 5.2.2.

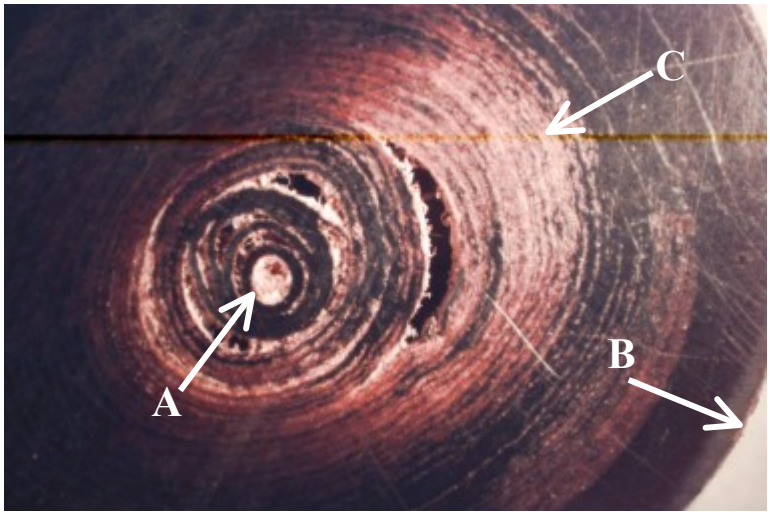

Figure 6.1 Gorgonian coral section used for radiocarbon sub sampling. Arrows indicate (A) Central core, (B) Outer edge and (C) mineralised area of skeleton.

Radiocarbon chemical preparation and analysis techniques required small chunks of material rather than powder, so the scalpel micro sampling method described in Chapter 5, section 5.2.3 was used. After drying at 40ºC overnight, each sample was weighed and the sample mass recorded. Radiocarbon analysis required a minimum of 5 mg carbon per sample. The structural formula for collagen (~50% carbon) was used in

the place of gorgonin (Chapter 5, section 5.3.1) to calculate the approximate mass required per sample. In the high carbonate areas of the skeleton (Figure 6.1) more material was sampled to ensure sufficient mass remained following the demineralisation step. Radiocarbon time series sample details are displayed in Table 6.2. Sampling was designed to span the same time period as that sampled by *Druffel* [1989] to enable a direct comparison of data.

Sample Number	Year	Sample mass (g)	NOSAMS code
1	1945-1948	0.07	OS- 43839
2	1949-1952	0.06	OS- 43840
3	1953-1958	0.07	OS- 43841
4	1959-1962	0.06	OS- 43842
5	1963-1967	0.09	OS- 43843
6	1968-1970	0.15	OS- 43844
7	1971-1972	0.11	OS- 43845
8	1973-1975	0.31	OS- 43846
9	1976-1978	0.37	OS- 43847
10	1979-1981	0.35	OS- 43848
11	1982-1983	0.38	OS- 43849
12	1984-1985	0.24	OS- 43850

Table 6.2 Samples prepared for radiocarbon analysis.

Weighed samples were transferred to acid cleaned, pre baked test tubes and washed several times in Milli-Q water. Samples were then demineralised in 1M HCl overnight, thoroughly rinsed in Milli-Q water until a neutral pH was obtained and then dried to constant weight at 40ºC.

6.2.2 Radiocarbon analysis

Following the pre treatment techniques described above, gorgonian samples were submitted for preparation and radiocarbon analysis to the National Ocean Sciences Accelerator Mass Spectrometer (NOSAMS) located at the Woods Hole Oceanographic Institution.

At the NOSAMS sample preparation lab, the gorgonian samples were combusted at high temperature to produce carbon dioxide (CO_2). The CO_2 generated through combustion was reduced via an Fe/H_2 catalyst to form graphite. The graphite derived from each sample was compressed into an aluminium 'target' which was then analysed on the Accelerator Mass Spectrometer (AMS) along with standards and process blanks.

The 'target' acts as a cathode in the ion source; the surface of the graphite is sputtered with cesium ions to generate a negative carbon ion beam. The ions produced are extracted and accelerated in the AMS system. After acceleration and removal of electrons, the emerging positive ions are magnetically separated by mass. The lighter ion beams (^{12}C and ^{13}C) are measured in Faraday Cups and the ^{14}C ions are analysed in a gas ionisation detector. Radiocarbon results are reported as $\Delta^{14}C$ (‰) [*Stuiver and Polach*, 1977] and include a background and $\delta^{13}C$ correction.

6.3 Results and Discussion

6.3.1 Radiocarbon in Pseudoplexaura porosa

Results for the radiocarbon time series measured in the organic gorgonin of the *Pseudoplexaura porosa* axial skeleton are listed in Table 6.3 and shown in Figure 6.2.

Sample Number	NOSAMS code	Year	$\Delta^{14}C$ (‰)
1	OS- 43839	1945-1948	-67.9
2	OS- 43840	1949-1952	-71.6
3	OS- 43841	1953-1958	-63.4
4	OS- 43842	1959-1962	-59.3
5	OS- 43843	1963-1967	-64.6
6	OS- 43844	1968-1970	-64.4
7	OS- 43845	1971-1972	-62.8
8	OS- 43846	1973-1975	-51.9
9	OS- 43847	1976-1978	-35.1
10	OS- 43848	1979-1981	-51.8
11	OS- 43849	1982-1983	30.7
12	OS- 43850	1984-1985	-23.7

Table 6.3 Radiocarbon results for *Pseudoplexaura porosa* skeletal gorgonin

The gorgonian radiocarbon results are relatively invariant reflecting pre bomb concentrations [e.g., *Broecker and Peng*, 1982] until ~1975 when the values increase slightly (from -51.9 ‰ in 1973-1975 to -35.1 ‰ in 1976-1978), before decreasing again in 1979-1981 and then increasing dramatically to 30.7 ‰ in 1982-1983. Could this increase represent the input of bomb ^{14}C? If so, then the results are puzzling and the ages assigned to samples must be incorrect as the onset of the increase due to bomb radiocarbon should occur around 1958 [*Nozaki et al*., 1978; *Druffel*, 1989].

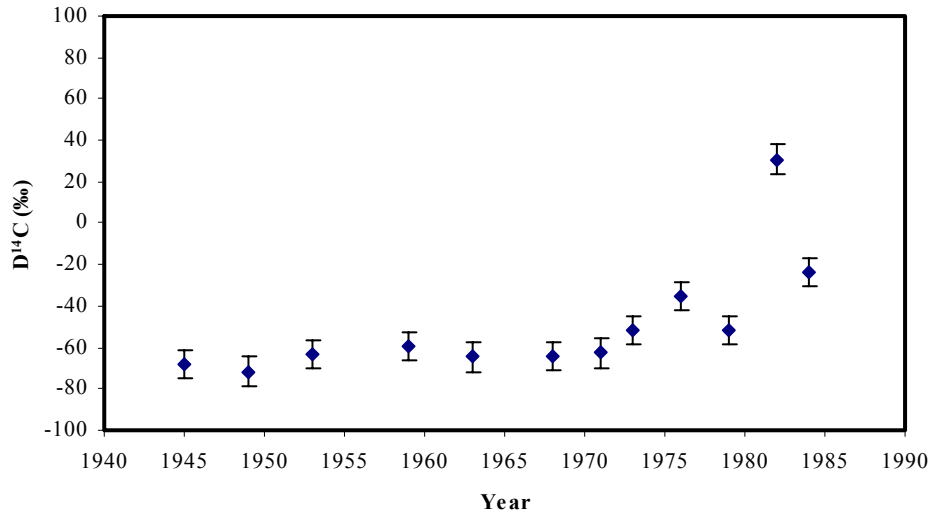

Figure 6.2 Radiocarbon results for organic gorgonin in *Pseudoplexaura porosa* from Bermuda

6.3.2 Gorgonian radiocarbon compared to scleractinian radiocarbon

The gorgonian ^{14}C time series data are compared to ^{14}C results from Bermudian scleractinian corals measured by *Nozaki et al*. [1978] and *Druffel* [1989] in Figure 6.3.

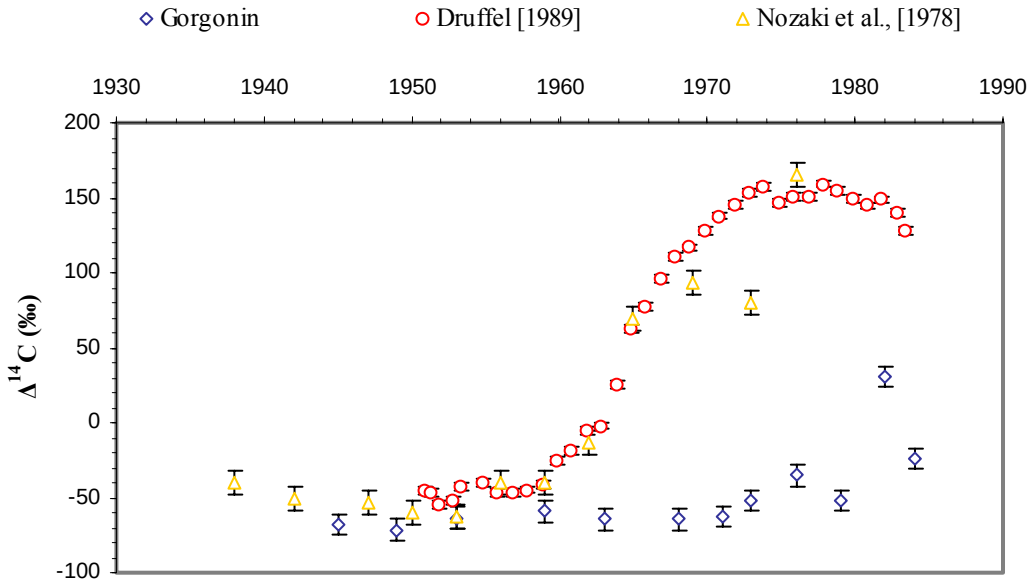

Figure 6.3 Radiocarbon in corals from Bermuda. Gorgonian radiocarbon results from organic gorgonin compared to scleractinian results from coral aragonite. Data from *Nozaki et al*. [1978] and *Druffel* [1989].

When compared to the ^{14}C measurements from scleractinian aragonite, the gorgonian coral ^{14}C measurements vary little and the increase, possibly associated with bomb radiocarbon, is very late (~1982) (Figure 6.3). The *Nozaki et al*. [1978] and *Druffel* [1989] data agree well with only two discrepancies (~1969-1973), which *Nozaki et al*. [1978] attribute to the influence of an influx of deep water to the coral growth site with lower radiocarbon than normal Sargasso Sea values. The possibility that the gorgonian coral was influenced by the influx of low radiocarbon water, from 1945 until 1981, seems unlikely given that the gorgonian sample site is located within the inner lagoon. In fact, one of the sample sites used by *Druffel* [1989], Sam Hall's Bay, is very close in location to the gorgonian sample site at Bailey's Bay Flats (Figure 6.4) and no indication of low ^{14}C water is apparent in those results (Figure 6.5).

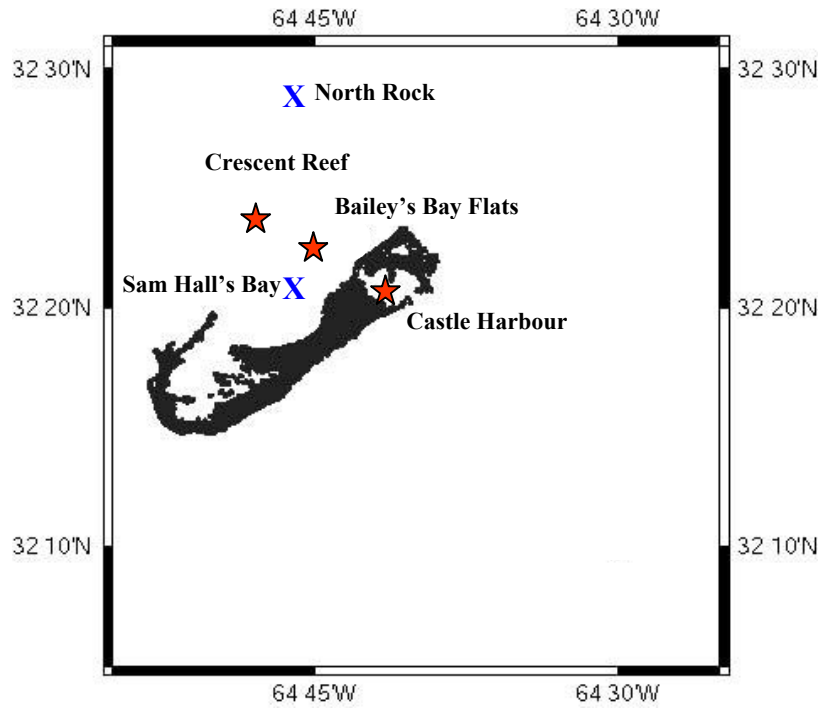

Figure 6.4 Map to show locations of coral sample sites on Bermuda.
North Rock – *Nozaki et al*. [1978] and *Druffel* [1989], Bailey's Bay Flats – this study, and Sam Hall's Bay – *Druffel* [1989].

Figure 6.5 shows the similarity between ^{14}C results from the two different coral sample sites used by *Druffel* [1989]. It would appear that the low radiocarbon measured in the gorgonian sample is not related to coral growth location.

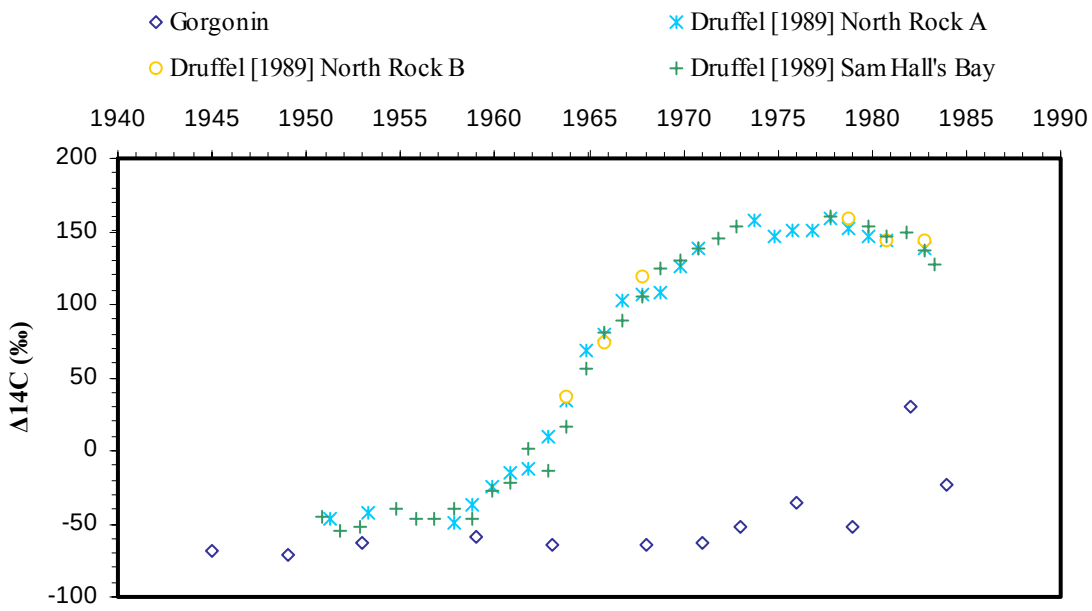

Figure 6.5 Radiocarbon results from *Druffel* [1989] for individual coral sites compared to the gorgonian coral radiocarbon data.

One possibility is that the years assigned to the gorgonian samples are wrong. However, the error in band counting would have to be out by ~20 years to bring the gorgonian radiocarbon time series in line with the scleractinian results. The band count error has been calculated previously (Chapter 5, section 5.2.2) as ±4 bands, the same band counting techniques were used for radiocarbon and so it is unlikely the band count error would have increased. Another possible way that the years assigned to the samples could be in error is through the sampling technique used. As chunks of material were required for the radiocarbon sample preparation and measurement techniques, the scalpel sampling method rather than the micro drill sampling method was used. The scalpel method is less exact than the micro drill and tends to over sample material meaning that instead of sampling two bands the scalpel might, in error, cross over into a third or fourth band. However, in this instance the sampling commenced from the central core and so if additional bands were sampled in error the effect would be to push the radiocarbon results to a more modern signal and that is not what is happening.

Unfortunately, for this study resources were available for only 12 radiocarbon analyses, but one way to verify whether the years assigned to gorgonian samples were incorrect would be to analyse the remainder of the sampled material (from 1986 to 2001) to see if the bomb radiocarbon curve is apparent there. If so, then the years assigned to samples are incorrect, if not, then for some reason gorgonian coral skeletal organic matter is not taking up ^{14}C.

6.3.3 Radiocarbon sources to organic gorgonin

In deep-sea gorgonians the carbon source for organic matter (polyps and gorgonin) is derived from particulate organic matter (POM) rained down from the surface and consumed by the corals at depth [*Griffin and Druffel*, 1989; *Roark et al*., 2005]. Therefore, the isotopic composition of gorgonin and polyps in deep-water gorgonians would reflect surface productivity. Hence, radiocarbon measured in a surface water dwelling gorgonian should reflect what the colony is feeding on. Gorgonians have been observed feeding on zooplankton [e.g., *Coma et al*., 1994], suspended particulate matter [e.g., *Lasker*, 1981], dissolved organic matter [e.g., *Murdock*, 1978], and microplankton [e.g., *Ribes et al*., 1998a]. Furthermore, *Pseudoplexaura porosa* colonies use photoautotrophic as well as heterotrophic food sources, they host zooxanthellae (dinoflagellate microalgae) within the body wall of their polyps enabling them to utilise photosynthetic products. How would these varying sources of carbon affect the measured radiocarbon signal in the skeletal gorgonin? It is the $\Delta^{14}C$ of DIC that determines the $\Delta^{14}C$ signature of phytoplankton and hence particulate organic carbon in the euphotic zone [*Druffel*, 1987; *Williams and Druffel*, 1987]. Thus, radiocarbon measured in organic skeletal material should reflect radiocarbon measured in carbonate skeletons formed from DIC. The assimilation of dissolved organic carbon (DOC) in substantial quantities by gorgonians could influence and reduce the radiocarbon signal recorded in the coral skeleton, as DOC has low radiocarbon content [e.g., *Bauer et al*., 2001] compared to DIC. However, *Sorokin* [1991] showed that dissolved organic matter, as a food source for gorgonians, was quantitatively unimportant. The main carbon source for symbiotic gorgonians like *Pseudoplexaura porosa* is through photoautotrophic means. Therefore it seems unlikely that the low radiocarbon signal measured in *Pseudoplexaura porosa* is due to an old carbon source for the gorgonian.

6.4 Conclusions and future work

A radiocarbon time series has been measured for the first time in a shallow dwelling gorgonian *Pseudoplexaura porosa*. The aim of this chapter was to use radiocarbon measurements of skeletal banding to confirm banding chronology; this has not been possible. Comparisons of the gorgonian ^{14}C time series with ^{14}C measured in scleractinian corals also from Bermuda showed the gorgonian values to be very low. In fact only three values showed post bomb levels of radiocarbon (> -50 ‰ [*Druffel*, 1989]) indicating the years assigned to samples could be incorrect meaning the bomb curve had not been sampled in its entirety.

Investigation of the sources of radiocarbon to the organic gorgonin skeleton failed to provide an explanation for low ^{14}C carbon.

Further radiocarbon measurements would allow clarification of why the ^{14}C measured in skeletal gorgonin is so low. If the remainder of the sampled material (from 1986 to 2001) were analysed for ^{14}C, the results containing either bomb radiocarbon or a lack of it, would indicate whether the age model for these samples were indeed incorrect.

It may be that skeletal gorgonin is not taking up and recording radiocarbon within its skeleton. It would be very interesting to extract both a gorgonin sample and a calcite sample from one or several growth bands to see if their radiocarbon concentrations were comparable.

In the future if the chronology of a specific gorgonian needed testing then radiocarbon measurements throughout the skeletal gorgonin should be carried out in combination with the determination of a radiocarbon time series in a neighbouring scleractinian coral.

Chapter 7: Synthesis and future work

7.1 Introduction

Scleractinian corals have been used extensively to obtain proxy information about palaeoclimates, however gorgonian corals have been little studied. The skeletons of gorgonian corals are potentially valuable archives of past oceanic conditions. With banded skeletons formed of organic gorgonin and calcite, the possibility exists to measure previously unobtainable proxy records.

This thesis has investigated the potential of gorgonian corals to record the conditions of the seawater in which they grew. Using Bermudian shallow water gorgonians (*Pseudoplexaura porosa*, *Plexaurella dichotoma* and *Plexaurella nutans*) the structure and growth of these corals was investigated. In order to extract reliable proxy information it is important to understand how the coral skeletons are formed. The banding present in the gorgonian skeleton was to be used as a guide to sampling for the proxy work, therefore the periodicity of this banding was investigated. A variety of techniques were utilised and developed to extract proxy information from the coral skeletons. Mg/Ca and Sr/Ca ratios were measured in the calcite loculi of *Plexaurella dichotoma*, and tritium and radiocarbon time series were determined in the gorgonin of *Pseudoplexaura porosa*.

7.2 Structural investigation

For the first time an investigation of the skeletal structure of *Pseudoplexaura porosa* and *Plexaurella dichotoma* was undertaken. For both species skeletal growth bands are formed of one high- and one low-density gorgonin couplet. For *Pseudoplexaura porosa* colonies, axial skeleton gorgonin is highly cross-linked and the small amount of calcite present is secreted in thin sheet like layers. The skeleton of *Plexaurella dichotoma* is highly calcified (containing up to 30% calcite by weight) and the gorgonin fibrous. Both species live in the surge zone and are subjected to current and wave generated water movements, encountering particularly high forces during storm conditions. As the skeleton's task is to act as a support system, the axis must be rigid enough to hold the fragile polyps off the substratum, and must be able to withstand the total water velocities at the colony site. The two species studied here strengthen their skeletons in different ways. *Pseudoplexaura porosa* employs extensive cross-

linking of skeletal gorgonin and the secretion of cement-like calcium carbonate deposits between the organic layers. *Plexaurella dichotoma* uses solely calcite deposition with calcite 'loculi' being distributed in specific areas of the skeleton to provide structural support.

Skeletal structure helped to determine the proxy measurement possibilities for each species. *Plexaurella dichotoma* appeared ideal to use for the Mg/Ca and Sr/Ca measurements. The calcite loculi were clearly visible within the coral skeleton and as loculi measured a minimum of 10 μm in diameter, using SIMS ion microprobe, it was possible to probe even the smallest of loculi. *Pseudoplexaura porosa* with its skeleton formed almost entirely of gorgonin seemed perfect to enable the extraction of a maximum mass of gorgonin per band for tritium measurements and the clarity of banding facilitated sampling for radiocarbon analysis.

7.3 Periodicity of growth banding

Prior to this study no work had been carried out to investigate the periodicity of growth banding in *Plexaurella* spp. and *Pseudoplexaura porosa*. During this thesis in situ staining and isotopic marking experiments were carried out on Bermuda to study the growth banding periodicity for these species. Although an original protocol was developed allowing gorgonian colonies to be sampled, stained and replanted, the stains used: acid fuchsin, alizarin red S and tetracycline, were either unsuccessful at marking the skeletal material or were unable to be detected visually in the gorgonian skeletal components. However, experiments undertaken employing a novel technique of isotopic spiking using ^{84}Sr were successful.

7.3.1 Plexaurella dichotoma

Isotopic marking using ^{84}Sr in skeletal calcite for *Plexaurella dichotoma* and *Plexaurella nutans* illustrated that the majority of a band is formed in a six month period (October-May). This result is a strong indication that banding for this species is annual in periodicity.

Investigation of the loculi structure together with measurements of *Plexaurella dichotoma* skeletal calcite chemistry provided further information on the growth and timing for loculi formation. The spherulitic morphology of crystals in the calcite loculi is indicative of rapid growth rates. This is further supported by high-resolution analyses

of Mg/Ca and Sr/Ca along the radial growth axes of several large loculi which demonstrated that intra-loculi variability in these elements was small and thus suggested the bulk of a loculus is accreted over a short time frame. Time series (1963-1988) SIMS ion microprobe measurements of Mg/Ca within calcite loculi showed an overall, positive correlation with autumnal (October-December) SSTs. These results indicate a preferred timing of calcite growth for *Plexaurella dichotoma*. The spawning period for *Plexauridae* on Bermuda occurs from July through to September [*De Putron*, 2002], thus the maximum energy available for growth would be after this time period.

The isotopic marking experiments together with the SIMS ion microprobe analyses indicate the majority of calcite growth occurs in the post-reproductive season, in the autumn and winter months. Following this, calcite locular growth is constrained along the major growth axis by the formation of an organic gorgonin layer. It is upon this organic layer that the calcification centres for future locular growth will eventually form the following autumn.

Drawing all the evidence together it is possible to outline a suggested model for the formation of annual growth banding in *Plexaurella dichotoma* (Figure 7.1). Each skeletal annual band is composed of calcite loculi and organic gorgonin, the amounts of which will depend upon the particular area of the coral's skeleton being considered. In a heavily calcified region of the skeleton, it is in the autumn months following the reproductive season, when the bulk of the calcite growth occurs. After this time, locular calcite growth along the major growth axis is restricted by organic gorgonin. Gorgonin growth then takes over and continues for the remainder of the year (Figure 7.1A and B). In the portions of the skeleton where loculi are less abundant, annual banding is still present. Here the distinction between high-density and low-density gorgonin is clearly evident (Figure 7.1C) with the low-density (lighter) band appearing in place of the calcite loculi and thus forming in the autumn months.

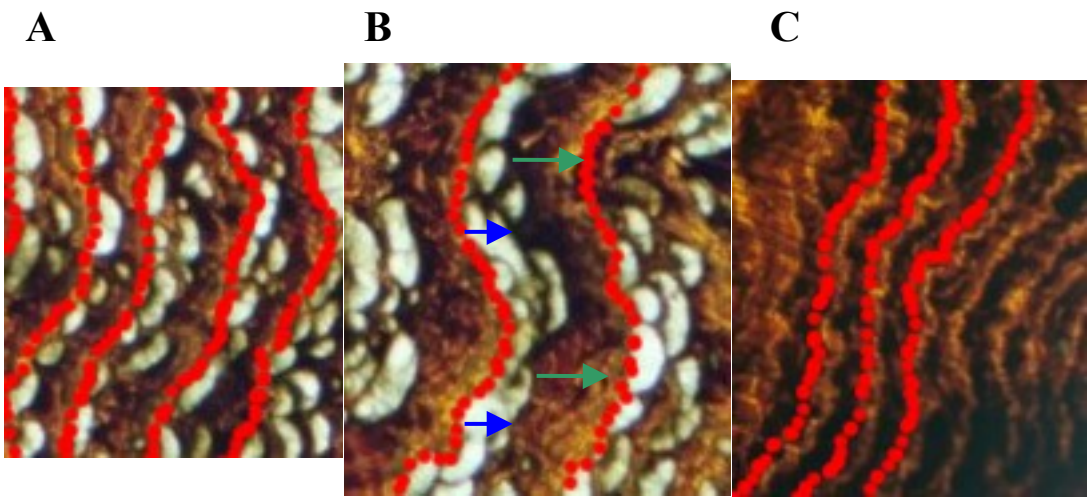

Figure 7.1 Annual growth banding in *Plexaurella dichotoma*.
(A) Each annual band (outline in red) is composed of calcite loculi (white) and organic gorgonin (brown).
(B) Growth model for annual banding. The bulk of a calcite loculus forms in the autumn months (October –December) after which time calcite growth along the major growth axis is restricted by organic gorgonin. The blue arrow indicates growth occurring in the autumn. The green arrow highlights gorgonin growth, which takes place throughout the remainder of the year.
(C) In the portions of the skeleton where loculi are less abundant annual banding is still present. Here the distinction between high-density and low-density gorgonin is clearly evident with the low-density (lighter) band appearing in place of the calcite loculi and thus forming in the autumn months.

7.3.2 Pseudoplexaura porosa

The small amounts of calcite present within the *Pseudoplexaura porosa* axial skeleton meant that the isotopic spiking technique was not viable. Thus the only information on banding periodicity for this species was from the tritium and radiocarbon time series measurements. However, neither technique provided results that were sufficiently accurate or to a good enough resolution to enable the periodicity of banding to be determined. Having performed numerous band counts both of various sections throughout individual colonies (Figure 7.2) and of sections from colonies over a wide size range, my opinion is that it is highly likely that the skeletal banding found within *Pseudoplexaura porosa* is annual in periodicity. It is noticeable when performing band counts from different colonies, which are similar in height and basal width, that the number of growth bands present is also comparable.

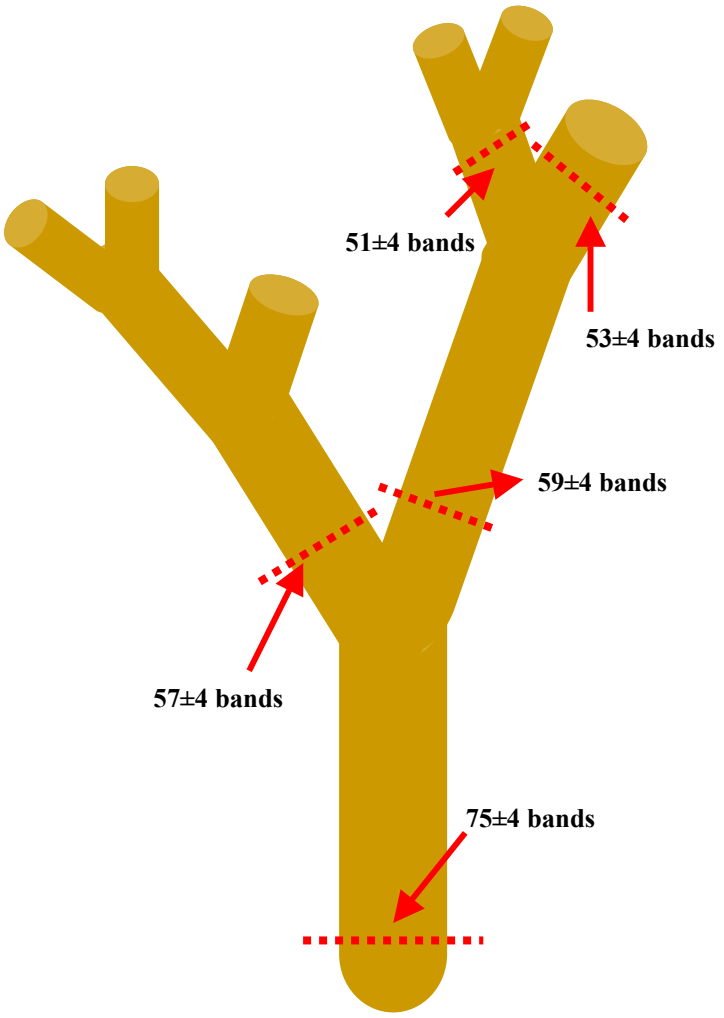

Figure 7.2 Skeletal banding counts throughout a *Pseudoplexaura porosa* colony. The red dashed lines show where thin sections were made throughout the colony's lower branches and base. Repeat band counts were performed on each section (a minimum of eight counts per section), error in band counting is equal to ±4 bands.

Every *Pseudoplexaura porosa* skeleton examined had the same banding pattern comprising alternative layers of high-density (dark) and low-density (light) gorgonin, the two together representing a single growth band. Reasons for the difference in density also point toward annual periodicity in banding. The gorgonian axial skeleton is synthesised and tanned within the axial epithelium [*Szmant-Froelich*, 1974]. The fastest growing parts of the colony soon become separated from the axial epithelium by new depositions, whereas the slower growing parts remain in contact with the epithelium for longer and have more time to become tanned (cross-linked). *Szmant-Froelich* [1974] suggested that many new layers are added to the skeleton in rapid succession during the

times of the year more favourable to growth resulting in a lighter band. For the rest of the year, the deposition rate of new gorgonin layers is slower, resulting in more tanned, darker layers. Thus the proposed *Pseudoplexaura porosa* model for skeletal growth banding would be akin to the *Plexaurella* spp. model in the areas of the skeleton with an absence of calcite loculi.

7.3.3 Future work to investigate the periodicity of growth banding

This thesis documents the first usage of ^{84}Sr as an isotopic spike to investigate growth processes in calcite. It is a powerful tool and has the potential to further constrain the growth hypotheses outlined here and to investigate growth rates for other corals.

Use of the ^{84}Sr spike to study the time frame of longitudinal growth of loculi would be valuable. Longitudinal transects provide an extremely detailed look into the loculus growth process. Mg/Ca measured longitudinally at high-resolution along the entire growth history of a calcite loculus appear to reflect the yearly SST pattern at Bermuda, suggesting loculi continue to grow lengthways unrestricted throughout the whole year. Isotopic spiking work using ^{84}Sr would provide further information on the timing of longitudinal growth of loculi.

Growth rate was considered to be the primary control on the Sr/Ca time series measured in gorgonian calcite. This hypothesis requires validation but if proven would constitute a powerful means of investigating annual periodicity. Sr/Ca, through the suppression of growth rate, would record past "known-year" events e.g. hurricanes and coral bleaching episodes, and thus measurements of Sr/Ca would enable these years to be identified and labelled.

7.4 Gorgonians as archives of past oceanic conditions

A variety of techniques were utilised and developed to extract proxy information from gorgonian coral skeletons.

7.4.1 Sea surface temperature

Interannual variability in Mg/Ca measured within calcite loculi from *Plexaurella dichotoma* correlated positively with interannual sea surface temperatures recorded at Bermuda over the same time period (1963-1988). The strongest correlation was between Mg/Ca and SSTs averaged over the autumn months (October-December). The

sensitivity of Mg/Ca to interannual changes in average autumn temperatures was calculated at 0.47 mmol/mol per ºC.

Having demonstrated that Mg/Ca ratios measured within gorgonian skeletal calcite correlate with changes in SST, the reliability and accuracy of the technique needs to be validated further. However, the future prospects for this technique are wide ranging, the great geographic and depth range of gorgonians compared to hermatypic species make them potentially invaluable sources of proxy information about deep and bottom water temperature variability in the mid- to high-latitudes.

7.4.2 Tracer measurements

7.4.2.1 Radiocarbon

A radiocarbon time series was measured for the first time in a shallow dwelling gorgonian *Pseudoplexaura porosa*. Unfortunately, the sampling strategy used failed to capture the bomb spike in its entirety. Additional analyses would have to be carried out to allow clarification of why the ^{14}C measured in skeletal gorgonin was so low. Further measurements of radiocarbon also represent an important opportunity to clarify that the two gorgonian skeletal components, gorgonin and calcite, are recording comparable seawater signals.

7.4.2.2 Tritium

Tritium has never previously been measured in gorgonian corals. This thesis described the development of a new technique, which succeeded in extracting the bomb tritium signal stored within the gorgonian coral skeleton. Further work is needed to improve on contamination issues and to reduce measurement uncertainty but the use of newly designed and constructed metal sample chambers should go a long way to addressing these concerns. In the future the tritium measurement technique described here could be used to reconstruct ocean circulation of the recent past in regions of the world where this information would be otherwise unavailable.

There are two major areas that would benefit from this technique. Firstly, the main problem in the establishment of tritium history is that although there is a relatively good record of tritium in precipitation, there is no corresponding record of tritium in the surface oceans. The reconstruction of this record would permit an improved knowledge of the hydrologic coupling of tritium to the ocean. Thus offering a more thorough understanding of tritium's "boundary conditions" and enhancing its use to constrain

oceanic circulation models. Additionally, this technique provides the possibility to reconstruct the surface water response to the tritium transient in areas other than the better-known locales. Sparsely sampled areas could be targeted allowing for a better understanding of the whole ocean system.

A second application for this technique would be to study ENSO (El Niño Southern Oscillation) events to try and characterise the changes in subsurface exchange between the northern and southern hemispheres. The large inter hemispheric contrast in tritium provides an important signal of the origins of water masses and their variations on seasonal, inter annual and longer time scales. With the reconstructed time history of surface tritium concentrations, changes associated with El Niño could be examined.

Finally, questions could be addressed regarding the food sources to gorgonians living at considerable depth in the world's oceans. *Griffin and Druffel* [1989] conducted a study using radiocarbon to track the sources of carbon (detrital vs DIC) to organic and calcareous skeletons of deep-sea corals. A potentially powerful tool would be to combine tritium and radiocarbon measurements to examine the pathways of organic material through the food chain, since the modern tritiated organic carbon would contrast with the low ambient tritium levels in the surrounding, old water.

7.5 Summary

This thesis has successfully combined a wide range of techniques, some newly developed, to illustrate the potential of gorgonian corals as recorders of seawater conditions in the recent past. Due to their wide geographic and depth distribution, as well as their important organic and inorganic skeletal components, gorgonian corals, although largely over looked thus far, should prove important archives of past oceanic conditions in the future.

Appendix 4.1

Hurricane and Tropical Storm Classifications

Source: http://stormcarib.com/guide.htm#defin

Tropical Systems:

- **Tropical disturbance, tropical wave**:

Unorganised mass of thunderstorms, very little, if any, organised wind circulation.

- **Tropical depression**:

Evidence of closed wind circulation around a centre with sustained winds from 20-34 knots (23-39 mph).

- **Tropical storm**:

Maximum sustained winds are from 35-64 knots (40-74 mph).
The storm is named once it reaches tropical storm strength.

- **Hurricane**:

Maximum sustained winds exceed 64 knots (74 mph).

Saffir Simpson Hurricane Intensity Scale:

***Category One* - A Minimal Hurricane**
Winds: 74-95 mph, 64-83 kts, 119-153 km/h
Minimum surface pressure: higher than 980 mbar
Storm surge: 3-5 ft, 1.0-1.7 m

***Category Two* - A Moderate Hurricane**
Winds: 96-110 mph, 84-96 kts, 154-177 km/h
Minimum surface pressure: 979-965 mbar
Storm surge: 6-8 ft, 1.8-2.6 m

***Category Three* - An Extensive Hurricane**
Winds: 111-130 mph, 97-113 kts, 178-209 km/h
Minimum surface pressure: 964-945 mbar
Storm surge: 9-12 ft, 2.7-3.8 m

***Category Four* - An Extreme Hurricane**
Winds 131-155 mph, 114-135 kts, 210-249 km/h
Minimum surface pressure: 944-920 mbar
Storm surge: 13-18 ft, 3.9-5.6 m

***Category Five* - A Catastrophic Hurricane**
Winds: greater than 155 mph, 135 kts, 249 km/h
Minimum surface pressure: lower than 920 mbar
Storm surge: higher than 18 ft, 5.6 m

Appendix 5.1

Detection limit calculations

The precision of all tritium measurements depends on the ^{3}He detection limit of the noble gas mass spectrometer. The atom detection limit for a gas is calculated as the standard deviation of a series of line blanks. This detection limit is determined by background ion scattering of hydrogen species (H2, HD, H3) and ^{4}He by the mass spectrometer [*Lott and Jenkins*, 1984]. This memory effect and hence the detection limit are lowered by running a series of line blanks before any low level tritium samples are analysed. The ^{3}He measured in the line blanks will decrease as embedded ions are released, effectively cleaning the machine and thus reducing the detection limit. Instrument retuning to increase sensitivity prior to sample analysis will also decrease the detection limit.

Once the detection limit of the noble gas mass spectrometer is known the detection limit for individual samples can be calculated as follows:

Consider 1 g collagen at 1 TU:

$$^1H\,(mol) = \left(\frac{sample\ mass}{RMM\ collagen}\right)x \quad unexchangeable\ hydrogens$$

$$^1H\,(mol) = \left(\frac{1}{286}\right)x \quad 17$$

$$^1H\,(mol) = \left(\frac{17}{286}\right)$$

$$^3H\,(mol) = \left(\frac{17}{286}\right)x\ 10^{-18}$$

$$^3H\,(atoms) = {}^3H\,(mol)\ x\ 6.02\ x\ 10^{23}$$
$$= 35776$$

35776 ^{3}H atoms in 1 g collagen at 1 TU

If the mass spectrometer detection limit for ^{3}He = x atoms

$$Detect: \frac{35776}{x}\ atoms\ per\ TUg$$

Detection limit for 1 g collagen at 1 TU $\frac{x}{35776}\ TUg$

Therefore, the detection limit for a sample of mass M (g) which has been sealed for helium ingrowth for a period of time t (days) is equal to:

$$\frac{x}{35776}.\frac{1}{M}.\frac{1}{\lambda t}$$

$$as\ \lambda = \frac{\ln 2}{t_{1/2}} = \frac{\ln 2}{4500}$$

t = *amount of time tritium has been left to decay*
λ = *decay constant*
$t½$ = *half life of tritium*

The half-life of tritium is equal to 4500 days [*Lucas and Unterweger*, 2000].

Therefore, the detection limit for a sample of mass M (g) which has been sealed for helium ingrowth for a period of time t (days) is equal to:

$$\frac{x}{35776}.\frac{4550}{\ln 2.M.t}\ \text{TU}$$

Appendix 5.2

Decay correction calculations

When working with tritium data, the effect of radioactive decay needs to be taken into account. Therefore tritium values are decay corrected to a common date.

The decay correction is calculated using the radioactive decay equation as follows:

$$N = N_0 e^{-\lambda t}$$

Where:

N = *The tritium value after decay correction*

N_0 = *The tritium value before decay correction*

$$\lambda = \frac{\ln 2}{t_{1/2}} = \frac{\ln 2}{4500}$$

t = *The time (days) between the date on which N_0 was determined and the date to which the value needs correcting*

REFERENCE LIST

Aeschbach-Hertig, W., Stute, M., Clark, J.F., Reuter, R.F. and Schlosser, P., 2002, A paleotemperature record derived from dissolved noble gases in groundwater of the Aquia Aquifer (Maryland, USA), *Geochimica et Cosmochimica Acta*, 66(5), 797-817.

Andrews, A.H., Cordes, E.E., Mahoney, M.M., Munk, K., Coale, K.H., Cailliet, G.M. and Heifetz, J., 2002, Age, growth and radiometric age validation of a deep-sea, habitat-forming gorgonian (*Primnoa resedaeformis*) from the Gulf of Alaska, *Hydrobiologia*, 471, 101-110.

Barnes, D.J., 1970, Coral skeletons: an explanation of their growth and structure. *Science*, 170, 1305-1308.

Barnes, D.J. and Lough, J.M., 1993, On the nature and causes of density banding in massive coral skeletons, *Journal of Experimental Marine Biology and Ecology*, 167(1), 91-108.

Bayer, F.M., 1956, Coelenterata: Octocorallia. In: Moore R.C. (ed), Treatise on Invertebrate Paleontology, Part F. Geological Society of America and University of Kansas Press, ppF167.

Begemann, F. and Libby, W.F., 1957, Continental water balance, ground water inventory and storage times, surface ocean mixing rates and world wide water circulation patterns from cosmic ray and bomb tritium, *Geochimica et Cosmochimica Acta*, 12, 277-296.

Beiring, E.A. and Lasker, H.R., 2000, Egg Production by colonies of a gorgonian coral, *Marine Ecology Progress Series*, 196, 169-177.

Bevelander, G., 1963, Effect of Tetracycline on Crystal Growth, *Nature*, 198(4885), 1103.

Bauer, J.E, Druffel, E.R.M., Wolgast. D.M. and Griffin, S., 2001, Sources and cycling of dissolved and particulate organic radiocarbon in the northwest Atlantic continental margin, Global Biogeochemical Cycles, 15(3), 615-636

Brazaeu, D.A. and Lasker, H.R., 1989, The reproductive cycle and spawning in a Caribbean gorgonian, *Biological Bulletin* mar biol Lab, Woods Hole 176, 1-7.

Bries, J.M., Debrot, A.O. and Meyer, D.L., 2004, Damage to the leeward reefs of Curacao and Bonaire, Netherlands Antilles from a rare storm event: Hurricane Lenny, November 1999, *Coral Reefs*, 23(2), 297-307.

Broecker, W.S. and Peng, T.H., 1982, Tracers in the sea, Eldigo Press, Palisades, New York,

Broecker, W.S. and Östlund, H.G., 1979, Property distributions along the σ_θ=26.8 isopycnal in the Atlantic Ocean, *Journal of Geophysical Research*, 84(C1), 1145-1154.

Broecker, W.S., Peng, T.H. and Östlund, H.G., 1986, The distribution of bomb tritium in the ocean, *Journal of Geophysical Research*, 91(C12), 14331-14334.

Bryan, W. H., and Hill D., 1941, Spherulitic crystallization as a mechanism of skeletal growth in the hexacorals, *Proceedings of the Royal Society of Queensland*, 52, 78-91.

Chave, K.E., 1954, Aspects of the biogeochemistry of magnesium 1. Calcareous marine organisms, *Journal of Geology*, 62, 266-283.

Clarke, W. B., Jenkins, W.J. and Top, Z., 1976, Determination of tritium by mass spectrometric measurement of ^{3}He, *International Journal of Applied Radiation and Isotopes*, 27, 515-522

Coffroth, M.A. and Lasker, H.R., 1998, Larval paternity and male reproductive success of a broadcast-spawning gorgonian, *Plexaura kuna*, *Marine Biology*, 131, 329-337.

Cohen, A.L, Layne, G.D., Hart, S.R. and Lobel, P.S., 2001, Kinetic control of skeletal Sr/Ca in a symbiotic coral implications for the paleotemperature proxy, *Paleoceanography*, 16(1), 20-26.

Cohen, A.L., Smith, S.R., McCartney, M.S. and van Etten, J., 2004, How brain corals record climate: an integration of skeletal structure, growth and chemistry of *Diploria labyrinthiformis* from Bermuda, *Marine Ecology Progress Series*, 271, 147-158.

Coma, R., Gili, J.M., Zabala, M. and Riera, T., 1994, Feeding and prey capture cycles in the aposymbiotic gorgonian *Paramuricea clavata*, *Marine Ecology Progress Series*, 155, 257–270.

Coma, R., Ribes, M., Zabala, M. and Gili, J.M., 1995a, Reproduction and cycle of gonadal development in the Mediterranean gorgonian *Paramuricea clavata*, *Marine Ecology Progress Series*, 117, 173-183.

Coma R. and Lasker, H.R., 1997, Small scale heterogeneity of fertilization success in a broadcast spawning octocoral, *Journal of Experimental Marine Biology and Ecology*, 214, 107-120.

Coma, R., Ribes, M., Zabala, M. and Gili, J.M., 1998, Growth in a modular colonial invertebrate, *Estuarine, Coastal and Shelf Science*, 47, 459-470.

Cook, F.C., 1904. The chemical composition of some gorgonian corals, *American Journal of physiology*, 12, 95-99.

Cornog, J., 1921, A Simple Method for the Production of Sodium Hydroxide free from Carbon Dioxide, *Journal of the American Chemical Society*, 43, 2573-2574.

Dawson, R.M.C, Elliot, D.C., Elliot, W.H. and Jones, K.M., 1969, Data for Biochemical Research (2nd ed.), p1-63, Oxford University Press.

De Putron, S.J., 2002, The reproductive ecology of two corals and one gorgonian from sub-tropical Bermuda, Ph.D. thesis, University of Wales, Swansea.

Dodd, J.R., 1967, Magnesium and strontium in calcareous skeletons: a review, *Journal of Paleontology*, 6(42), 1313-1329.

Dodge, R.E., Wyers, S.C., Frith, H.R., Knap, A.H., Smith, S.R., Cook C.B. and Sleeter, T.D., 1984, Coral calcification rates by the buoyant weight technique: effects of alizarin staining, *Journal of Experimental Marine Biology and Ecology*, 76, 217-232.

Dollar, S.J. and Tribble, G.W., 1993, Recurrent storm disturbance and recovery – A long-term study of coral communities in Hawaii, *Coral Reefs*, 12(3-4), 223-233.

Doney, S.C. and Jenkins, W.J., 1988, The effect of boundary conditions on tracer estimates of thermocline ventilation rates, *Journal of Marine Research*, 46, 947-965.

Dreisigacker, E. and Roether, W., 1978, Tritium and 90Sr in the North Atlantic surface water, *Earth and Planetary Science Letters*, 38, 301-312.

Druffel, E.R.M., 1987, Bomb radiocarbon in the Pacific: Annual and seasonal timescale variations, *J Marine Research*, 45, 667-698.

Druffel, E.R.M., 1989, Decade time scale variability of ventilation in the north Atlantic: high precision measurements of bomb radiocarbon in banded corals, *Journal of Geophysical Research*, 94(C3), 3271-3285.

Druffel, E.R.M., Griffin, S., Witter, A., Nelson, E., Southon, J., Kashgarian, M. and Vogel, J., 1995, *Geradia:* Bristlecone pine of the deep-sea? *Geochimica et Cosmochimica Acta,* 59(23), 5031-5036.

Dunbar, R.B. and Cole, J.E., 1999, Annual records of tropical systems (ARTS), PAGES workshop Report, Series 99-1, pp71.

Eriksson. E., 1965, An account of the major pulses of tritium and their effects in the atmosphere, *Tellus*, 17, 118-130.

Esford, L.E. and Lewis, J.C., 1990. Stiffness of Caribbean gorgonians (Coelenterata, Octocorallia) and Ca/Mg content of their axes, *Marine Ecology Progress Series*, 67, 189-200.

Fabricius, K.A., 2005, Effects of terrestrial runoff on the ecology of corals and coral reefs: review and synthesis, *Marine Pollution Bulletin*, 50, 125-146.

Fabricius, K. and Alderslade, P., 2001, Soft corals and sea fans: a comprehensive guide to the tropical shallow water genera of the central-west Pacific, the Indian Ocean and the Red Sea, Australian Institute of Marine Science, Queensland, Australia, pp16.

Feng X., Krishnamurthy, R.V. and Epstein S., 1993, Determination of D/H ratios of nonexchangeable hydrogen in cellulose: A method based on the cellulose-water exchange reaction, *Geochimica et Cosmochimica Acta,* 57, 4249-4256.

Fine, R.A. and Östlund, H.G., 1977, Source function for tritium transport models in the Pacific, *Geophysical Research Letters*, 4 (10), p461-464.

Gardner, T.A., Cote, I.M., Gill, J.A., Grant, A. and Watkinson, A.R., 2005, Hurricanes and Caribbean coral reefs: Impacts, recovery patterns, and role in long-term decline, *Ecology*, 86(1), 174-184.

Goldberg, W.M., 1974, Evidence of sclerotized collagen from the skeleton of a gorgonian coral, *Comparative Biochemical Physiology*, B49, 525-529.

Goldberg, W.M., 1976, Comparative study of the chemistry and structure of gorgonian and antipatharian coral skeletons, *Marine Biology*, 35, 253-267.

Goldberg, W.M., 1978. Chemical changes accompanying maturation of the connective tissue skeletons of gorgonian and antipatharian corals, *Marine Biology*, 49, 208-210.

Goldberg, W.M. and Hamilton, R.D., 1974, The sexual cycle in *Plexaura homomalla*, In Bayer, F.M. and Weinheimer, A.J. (eds) Prostaglandins from *Plexaura homomalla*: ecology, utilization and conservation of a medical marine resource a symposium, University of Miami Press, Florida, pp 58-61.

Griffin, S., and Druffel, E.R.M., 1989, Sources of carbon to deep-sea corals, *Radiocarbon* 31, 533-543.

Grigg, R.W., 1974, Growth rings: Annual periodicity in two gorgonian corals, *Ecology*, 55, 876-88.

Grigg, R.W., 1977, Population dynamics of two gorgonian corals, *Ecology*, 58, 278-290.

Hart, S. R. and Cohen, A.L., 1996, An ion probe study of annual cycles of Sr/Ca and other trace elements in corals, *Geochimica et Cosmochimica Acta,* 60(16), 3075-3084.

Heikoop, J.M., Hickmott, D.D., Risk, M.J., Shearer, C.K. and Atudorei, V., 2002, Potential climate signals from the deep-sea gorgonian coral *Primnoa resedaeformis*, *Hydrobiologia*, 471, 117-124.

Hernaman, V., Munday, P.L. and Schläppy, M.L., 2000, Validation of otolith growth-increment periodicity in tropical gobies, *Marine Biology*, 137, 715-726.

Huang, Y. and Fairchild, I.J., 2001, Partitioning of Sr^{2+} and Mg^{2+} into calcite under karst-analogue experimental conditions, *Geochimica et Cosmochimica Acta*, 65(1), 47-62.

Huheey J.E., Keiter, E.A. and Keiter, R.L., 1993, in Inorganic Chemistry: Principles of Structure and Reactivity, 4th edition, HarperCollins, New York, USA.

Humann, P. and Deloach, N., 2002, Reef Coral Identification, (2^{nd} edition), New World Publications Inc. Florida.

Istin, M., 1975. The structure and formation of calcified tissue, *in* Malins, D.C. and Sargent, J.R., eds., Biochemical and biophysical perspectives in marine biology, 2, 23-35.

Jenkins, W.J., 1998, Studying thermocline ventilation and circulation using tritium and ^{3}He, *Journal of Geophysical Research*, 103, 15817-15831.

Jeyasuria, P. and Lewis, J.C., 1987. Mechanical properties of the axial skeleton in gorgonians, *Coral Reefs*, 5, 213-219.

Jouzel, J., Merlivat, L., Mazaudier, D., Pourchet, M. and Lorius, C., 1982, Natural tritium deposition over Antarctica and estimation of the mean global production rate, *Geophysical Research Letters*, 9, 1191-1194.

Kapela, W. and Lasker, H.R., 1999, Size dependent reproduction in the Caribbean gorgonian *Pseudoplexaura porosa*, *Marine Biology*, 135, 107-114.

Knutson, D.W., Buddemeier, R.W. and Smith, S.V., 1972, Coral chronologies: seasonal growth bands in reef corals, *Science*, 177, 270-272.

Lasker, H.R., 1981, A comparison of the particulate feeding abilities of three species of gorgonian soft coral, *Marine Ecology Progress Series*, 5, 61–67.

Lasker, H.R., 1984, Asexual reproduction, fragmentation, and skeletal morphology of a plexaurid gorgonian, *Marine Ecology Progress Series*, 19, 261-268.

Lasker, H.R., 1990, Clonal propagation and population dynamics of a gorgonian coral, *Ecology*, 71, 1578-1589.

Lasker, H.R., Gottfried, M.D. and Coffroth, M.A., 1983, Effects of depth on the feeding capabilities of two octocorals, *Marine Biology*, 73, 73–78.

Lasker, H.R., Kim, K. and Coffroth, M.A., 1996, Reproductive and genetic variation among Caribbean gorgonians: the differentiation of *Plexaura kuna*, new species, *Bulletin of Marine Science*, 58, 277-288.

Lea, D.W., 2003, Elemental and isotopic proxies of past ocean temperatures. In: Elderfield H (ed) The Oceans and Marine Geochemistry, Volume 6. Holland, H.D., Turekian, K.K., Treatise on Geochemistry, Elsevier Pergamon.

Leversee, G.J., 1976, Flow and feeding in fan-shaped colonies of the gorgonian coral, *Leptogorgia*. *Biological Bulletin*, 151, 344–356.

Leversee, G.J., 1980, Incorporation and distribution of labelled proline in collagenous and non-collagenous components of the gorgonian coral Leptogorgia virgulata (Coelenterata, Octocorallia), *Comparative Biochemistry and Physiology*, 67B, 499-503.

Lewis, J.B., 1982, Feeding behaviour and feeding ecology of the Octocorallia (Coelenterata: Anthozoa), *J Zool Lond*, 196, 371–384.

Lewis, J.C., Barnowski, T.F. and Telesnicki, G.J., 1992, Characteristics of carbonates of gorgonian axes (coelenterata, Octocorallia), *Biological Bulletin*, 183, 278-296.

Lide, D.R., 2000, CRC handbook of chemistry and physics, 81st ed., CRC Press, Boca Raton, Florida.

Lofgren, G., 1974, An experimental study of plagioclase crystal morphology: Isothermal crystallization, *American Journal of Science*, 274, 243-273.

Lorens, R.B., 1981, Sr, Cd, Mn and Co distribution coefficients in calcite as a function of calcite precipitation rate, *Geochimica et Cosmochimica Acta*, 45, 553-561.

Lowenstam, H.A. and Weiner, S., 1989, On Biomineralization, Oxford University Press, New York.

Lucas, L.L. and Unterweger, M.P., 2000, Comprehensive review and critical evaluation of the half-life of tritium, *Journal of Research of the National Institute of Standards and Technology*, 105(4), 541-549.

Macintyre, I.G., Bayer, F.M., Logan, M.A.V. and Skinner, H.C.W., 2000, Possible Vestige of early phosphatic biomineralisation in gorgonian octocorals (Coelenterata), *Geology*, 28(5), 455-458.

Marschal, C., Garrabou, J., Harmelin, J.G. and Pichon, M., 2004, A new method for measuring growth and age in the precious red coral *Corallium rubrum*, *Coral Reefs*, 23, 423–432.

Marks, R.E., Bear, R.S. and Blake, G.H., 1949. X ray diffraction evidence of collagen in various phyla, *Journal of Experimental Zoology*, 111, 55-77.

Michel, R.L. and Suess, H.E., 1975, Bomb tritium in the Pacific Ocean, *Journal of Geophysical Research*, 80(30), 4139-4152.

Mucci, A. and Morse J.W., 1983, The incorporation of Mg^{2+} and Sr^{2+} into calcite overgrowths: influences of growth rate and solution composition, *Geochimica et Cosmochimica Acta*, 47, 217-233.

Murdock, G.R., 1978, Digestion, assimilation, and transport of food in the gastrovascular cavity of a gorgonian octocoral (Cnidaria, Anthozoa), *Bull. Mar. Sci.*, 28, 354-362.

Musik, K. and Wainwright, S.A., 1977, Morphology and habitat of five Fijian fans, *Bulletin of Marine Science*, 27, 350-363.

Nozaki, Y., Rye, D.M., Turekian, K.K. and Dodge, R.E., 1978, A 200 year record of carbon-13 and carbon-14 variations in a Bermuda coral, *Geophysical Research Letters*, 5, 825-828.

Ohde, S. and Kitano, Y., 1984, Coprecipitation of strontium with marine Ca-Mg carbonates, *Geochem. J.*, 18, 143-146.

Oomori, T., Kaneshima, H., and Maezato, Y., 1987, Distribution coefficient of Mg^{2+} ions between calcite and solution at 10-50ºC, *Marine Chemistry*, 20, 327-336.

Postlethwaite, C.F., 2002, Developing a tool for evaluating the role of seasonal sea ice in deep-water formation, Ph.D. thesis, University of Southampton, UK.

Ribes, M., Coma, R. and Gili, J.M., 1998a, Seasonal variation of *in situ* feeding rates by the temperate ascidian *Halocynthia papillosa*, *Mar. Ecol. Prog. Ser.*, 175, 201–213.

Ribes, M., Coma, R. and Gili, J.M., 1999b, Heterogeneous feeding in benthic suspension feeders: the natural diet and grazing rate of the temperate gorgonian *Paramuricea clavata* (Cnidaria: Octocorallia) over a year cycle, *Mar. Ecol. Prog. Ser.*, 183, 125–137.

Rickaby, R.E.M., Schrag, D.P., Zondervan, I. and Riebesell, U., 2002, Growth rate dependence of Sr incorporation during calcification of *Emiliania huxleyi*, *Global Biogeochemical Cycles*, 16(1), 1006, 10.1029/2001GB001408.

Risk, M.J., Heikoop, J.M., Snow, M.G. and Beukens, R., 2002, Lifespans and growth patterns of two deep-sea corals: *Primnoa resedaeformis* and *Desmophyllum cristagalli*, *Hydrobiologia*, 471, 125-131.

Roark, E.B., Guilderson, T.P., Flood-Page, S., Dunbar, R.B., Ingram, L., Fallon, S. and McCulloch, M., 2005, Radiocarbon-based ages and growth rates of bamboo corals from the Gulf of Alaska, *Geophysical Research Letters*, 32: L04606. doi: 10.1029/2004GL021919.

Schimmelmann, A., 1991, Determination of the concentration stable Isotope composition of nonexchangeable hydrogen in organic matter, *Analytical Chemistry*, 63, 2456-2459.

Sherwood, O.A., Heikoop, J.M., Scott, D.B., Risk, M.J., Guilderson, T.P., McKinney, R.A., 2005, Stable isotopic composition of deep sea gorgonian corals (*Primnoa* spp.): a new archive of surface processes, *Marine Ecology Progress Series* (in press).

Smith, P.K., Gorham, A.T. and Smith, E.R.B., 1942, Properties of solutions of amino acids and related substances. VII. The ionization of some hydroxy amino acids and proline in aqueous solution from one to fifty degrees, *Journal of Biological Chemistry*, 144, 737-745.

Smith, S.V., Buddemeier R.W., Redalje, R.C. and Houck, J.E., 1979, Strontium-Calcium Thermometry in Coral Skeletons, *Science*, 204(4391), 404-407.

Sorokin, Y.I., 1991, Biomass, metabolic rates and feeding of some common reef zoantharians and octocorals, *Aust. J. Mar. Freshwater Res.*, 42, 729-741.

Sponaugle, S., 1991, Flow patterns and velocities around a suspension-feeding gorgonian polyp: evidence from physical models, *J. Exp. Mar. Biol. Ecol.*, 148, 135-145.

Sponaugle, S. and LaBarbera, M., 1991, Drag-induced deformation: a functional feeding strategy in two species of gorgonians, *J. Exp. Mar. Biol. Ecol.*, 148, 121-134.

Stark, S., 2003, Development of methods to improve knowledge of tritium inputs to the Ocean, Ph.D. thesis, University of Southampton, UK.

Stark, S., Statham, P.J., Stanley, R. and Jenkins, W.J., 2005, Using tree ring cellulose as a tool to estimate past tritium inputs to the ocean, *Earth and Planetary Science Letters*, 237(3-4), 341-353.

Sterrer, W.E., 1986, Marine Flora and Fauna of Bermuda, Wiley, New York, p.742.

Stoll, H.M. and Schrag, D.P., 2000, Coccolith Sr/Ca as a new indicator of coccolithophorid calcification and growth rate, *Geochemistry, Geophysics, Geosystems*, 1, Paper # 1999GC000015.

Stuiver, M. and Polach, H.A., 1977, Discussion: Reporting of ^{14}C data, *Radiocarbon*, 19, 355-363.

Szmant-Froelich, A., 1974, Structure, iodination and growth of the axial skeleton of *Muricea Californica* and *M. Fruticosa* (Coelenterata: Gorgonacea), *Marine Biology*, 27, 299-306.

Tesoriero, A.J. and Pankow, J.F., 1996, Solid solution partitioning of Sr^{2+}, Ba^{2+} and Cd^{2+} to calcite, *Geochemica and Cosmochemica Acta*, 60(6), 1053-1063.

Theodor, J., 1967, Contribution à l'étude des gorgones VII. Ecologie et comportement de la planula, *Vie Milieu*, 18, 291-301.

Thresher, R., Rintoul, S.R., Koslow, J.A., Weidman, C., Adkins, J. and Proctor, C., 2004, Oceanic evidence of climate change in southern Australia over the last three centuries, *Geophysical Research Letters*, 31, L07212, 10.1029/2003GL018869.

Tidball, J.G., 1985, Changes in skeletal chemistry and skeletogenic cell ultrastructure between young and old sites on axial skeletons (*Leptogorgia virgulata*), (Cnidaria: Gorgonacea). *Comparative Biochemical Physiology*, 81B, 827-831.

Toyofuku, T., Kitazato, H., Kawahata, H., Tsuchiya, M. and Nohara, M., 2000, Evaluation of Mg/Ca thermometry in foraminifera: Comparison of experimental results and measurements in nature, *Paleoceanography*, 15(4), 456-464.

Tracy, S.L., François, C.J.P. and Jennings, H.M., 1998, The growth of calcite spherulites from solution I. Experimental design techniques, *Journal of crystal growth*, 193, 374-381.

Voet, D. and Voet, J.G., 1990, Biochemistry, John Wiley and Sons, Inc. 159 p.

Wainwright, S.A., Biggs, W.D., Currey J.D. and Gosline, J.M., 1982, Mechanical design in organisms, Princeton University Press, Princeton.

Walker T.A. and Bull, G.D., 1983 A newly discovered method of reproduction in gorgonian coral, *Marine Ecology Progress Series,* 12, 137-143.

Ward-Paige, C.A., Risk, M.J. and Sherwood, O.A., 2005, Reconstruction of nitrogen sources on coral reefs: δ15N and δ13C in gorgonians from Florida Reef Tract, *Marine Ecology Progress Series*, 296, 155–163.

Weinbauer, M.G. and Velimirov, B., 1995, Calcium, Magnesium and Strontium concentrations in the calcite sclerites of Mediterranean gorgonians (Coelenterata:Octocorallia), *Estuarine, Coastal and Shelf Science*, 40, 87-104.

Weinbauer, M.G., Brandstatter, F. and Velimirov, B., 2000, On the potential use of magnesium and strontium concentrations as ecological indicators in the calcite skeleton of the red coral (*Corallium rubrum*), *Marine Biology*, 137, 801–809.

Weiss, W. and Roether, W., 1980, The rates of tritium input to the world oceans, *Earth and Planetary Science Letters*, 49, 435-446.

Williams, P.M., and E.R.M., Druffel, Radiocarbon in dissolved organic carbon in the central North Pacific Ocean, *Nature,* 330**,** 246-248, 1987.

Wilson, T.R.S., 1975, The major constituents of seawater. In: (J.P. Riley and G. Skirrow, eds.) Chemical Oceanography, 2nd Ed., Vol. 1, p. 365-413. Academic Press

Zeevi Ben-Yosef, D. and Benayahu, Y., 1999, The gorgonian coral *Acabaria biserialis*: life history of a successful colonizer of artificial substrata, *Marine Biology*, 135, 473-481.